FATTY ACID SYNTHASE EXPRESSION AND INHIBITION IN TRIPLE-NEGATIVE BREAST CANCER

Ariadna Giró Perafita

Universitat de Girona

Doctoral Thesis

Fatty Acid Synthase Expression and Inhibition in Triple-Negative Breast Cancer

Ariadna Giró Perafita

2016

Universitat de Girona

Doctoral Thesis

Fatty Acid Synthase Expression and Inhibition in Triple-Negative Breast Cancer

Ariadna Giró Perafita

2016

Doctoral Program in Experimental Sciences and Sustainability

Directed by:

Dra. Teresa Puig Miquel

Tutored by:

Dr. Enric Verdú Navarro

Presented in partial fulfillment of the requirements for a doctoral degree with international recognition from the University of Girona

Universitat de Girona

Dr. Teresa Puig Miquel, professor at the University of Girona and director of the Targets Lab group

Certifies:

That the thesis titled "Fatty Acid Synthase Expression and Inhibition in Triple-Negative Breast Cancer", presented by Ariadna Giró i Perafita to obtain a doctoral degree with recognition as an international doctorate, has been completed under my supervision and meets the requirements to opt for an International Doctorate.

For all intents and purposes, I hereby sign this document.

Signature

Girona, November 2nd of 2016

Al tete

Acknowledgements

Una tesis engloba molt més que el que hi ha escrit en les seves pàgines. L'acompanya tota aquella gent que camina al teu costat: amics de tota la vida, els nous, la parella, els pares, companys, professors, experiències.. i per fi un dia, arriba aquest moment. I per això, vull agrair-vos a tots els que heu fet camí amb mi durant aquests quatre anys.

Primer de tot, volia agrair a la Teresa per confiar amb mi, per brindar-me la oportunitat de començar aquest projecte i per fer-me sentir orgullosa de pertànyer a un petit però que molt gran grup de recerca.

Evidentment voldria agrair també a la Glòria i l'Adriana, l'engranatge que ho va començar tot, amb qui vaig començar al grup, vaig aprendre, i amb qui va ser tant fàcil treballar (tot i que portés el desordre..)

Glòria, gràcies també per aquests últims anys, tant per l'esforç perquè tot tirés endavant com per els cafès entre *array* i *array*.

Adriana, et dec un sopar encara. Has estat el meu amulet en molts moments, a veure com me'n surto a partir d'ara... Gràcies per la teva amistat, empenta, energia i mil coses més.

Sònia, la meitat d'aquesta tesis ens l'hem passat treballat colze a colze, ens hem avingut i ajudat, i no podria estar més orgullosa de tu! De petit *saltamontes* ja no en tens res. Ara ja veus te, vi i vermut. Et trobaré molt a faltar.

A l'Ariadna (àlies AS, amb qui hem compartit molts "reptes"), a en Marc i la Núria. Gràcies a tots per tota la ciència, i per tot el que no és ciència però que tant necessitem. Cafès, dinars a l'alzina, i com no per acompanyar-me de tant en tant en els atacs de ganes de xocolata de després de dinar. Gràcies per deixar-me parlar amb veu alta (ve d'herència de la Glòria), i deixar-me tenir el millor lloc i la millor cadira del lab. No em voldria deixar tampoc a *l'Enrique*, el nostre estudiant d'estiu preferit, que tant ens ha animat les tardes de divendres...

A tots els membres de TargetsLab en general, i a en particular a en Xavi, perquè sempre t'has ofert per ajudar amb el que sigui, i no ens podíem oblidar tampoc de les teves dolces promeses. També a la Gemma, la meva oncòloga de referència.

Francisco, Brian, Irma: Thank you for welcome me and make me feel like one more of the team the months I stayed at the NYU.

I also would like to mention all the other members of the NYU lab: Karin, Lei, Liming, Marion, Marae, Nan and Wenxiang. Thank you for being so nice and helpful. I felt very comfortable since the beginning.

Thank you also to all the other people I met along the way: Sweden, Madrid, Barcelona, New York. A part of you is reflected here as well.

A tots els components del grup NEOMA, amb qui he compartit laboratori en algun moment o altre. I més concretament, Beltrán, Aina, Marc..., aquell estiu va ser una *locura*! Però no em faria res repetir-lo. Beltrán, no m'oblido de la teva promesa (*palabra de honor*).

A tots els companys de l'IDIBGI: hem sigut companys de *poyata*, després de despatx, finalment d'edifici i ara quasi ni de ciutat! Però sempre heu estat allà i sou una part molt important d'aquests quatre anys.

A la Colla, aquesta gran família. M'heu acompanyat aquests anys en tots els aspectes. Sense vosaltres no hauria sigut possible. Gràcies per preguntar-me, escoltar-me o simplement acompanyar-me. Gràcies per fer-me sentir, per part de molts de vosaltres, que tot aquest esforç valia la pena. Us estimo amb bogeria.

A les biòlogues, Adriana, Celia, Judit, Mar, Míriam... què seria sense vosaltres? Tot i el temps i la distància, hem anat creixent. Compartim des de ciència a bèsties, *barbudos* i totes les BBQ que podem. Gràcies per ser-hi!

A la família *Atlètica*: heu omplert els dilluns, divendres i caps de setmana dels últims quatre anys amb futbol (o ho hem intentat). Aquest esport que tant ens enganxa i que només nosaltres entenem, però tant necessari per descarregar i omplir-nos. Us trobaré molt a faltar.

A els meus pares, perquè sempre, sempre, sempre hi sou. Procurant, preguntant i sobretot recolzant-me amb totes les decisions. Sé que m'ho heu donat tot sense haver de demanar res, i per això segurament he pogut arribar fins aquí. Gràcies infinites.

I com no podia ser a en Jordi (en Bahi), amb qui més he compartit i a qui més li dec. Podria escriure gràcies cent vegades i no en faria prou. Gràcies per entendre'm, per compartir, per creure, per la paciència, per esperar-me, per entendre'm novament a mi i a aquesta *feina*, i per aquest dolça creença de que un dia la biologia ens permetrà "viure bé". Gràcies de tot cor.

List of publications resulted from this thesis (see Annex)

ARTICLE 1

Title: Preclinical Evaluation of Fatty Acid Synthase and EGFR Inhibition in Triple Negative Breast Cancer.

Authors: Ariadna Giró-Perafita, Sònia Palomeras, David H. Lum, Adriana Blancafort, Gemma Viñas, Glòria Oliveras, Ferran Pérez-Bueno, Ariadna Sarrats, Alana L. Welm and Teresa Puig

Journal: Clincial Cancer Research (2016) 1-11

Impact factor (2015): 8.738 (Q1, Oncology / Position 12 of 213)

DOI: 10.1158/1078-0432.CCR-15-3133

ARTICLE 2

Title: Fatty Acid Synthase and EGFR Expression in Association with Clinical Outcomes in Triple-Negative Breast Cancer Patients.

Authors: Ariadna Giró-Perafita* and Ariadna Sarrats*, Ferran Pérez-Bueno, Glòria Oliveras, Maria Buxó, Joan Brunet, Gemma Viñas** and Teresa Puig**.

Journal: Sent to Breast Cancer Research 20/09/2016.

Impact factor (2014): 5,221 (Q1, Oncology / Position 32 of 213)

DOI: -

ARTICLE 3

Title: Optimization of Poli(ε-caprolactone) scaffolds suitable for 3D cancer cell culture.

Authors: Ariadna Giró-Perafita, Marc Rabionet, Teresa Puig and Joaquim Ciurana.

Journal: Procedia CIRP 49 (2016) 61 – 66

Impact factor (2015): H index of 15

DOI: 10.1016/j.procir.2015.07.031

Abbreviations

ACP	Acyl carrier protein
ALDH	Aldhyde dehydrogenases
ALDH^{br}	ALDH bright
AmR	Amphiregulin
AR	Androgen receptors
BC	Breast Cancer
BL	Basal-like
BTC	Betacellulin
CIs	Confidence intervals
CK	Cytokeratin
CL	Claudin-low
CSCs	Cancer stem cells
CPI	Cell proliferation inhibition
CPT1	Carnitine palmitoyltransferase 1
DSF	Disease-free survival
DH	Dehydratase
EGFR	Epidermal Growth Factor Receptor
EGCG	Epigallocatechin Gallate
EGF	Epidermal growth factor
EMT	Epithelial-to-Mesenchymal transition
ER	Enoyl reductasa
ER	Estrogens
EPG	Epigen
EPR	Epiregulin
FASN	Fatty acid synthase
FISH	Fluorescence *in situ* hybridization
G28	G28UCM
gpNMB	Glycoprotein non-metastatic melanoma B
HCC	HCC1806
HCCDXR	HCC1806 doxoresistant
HER2	Human epithermal growth factor receptor 2
HG-EGF	Heparin-binding epidermal growth–factor like growth factor
HRs	Hazard ratios
IHC	Immunohistochemistry
Ix	Interaction index
KR	β-ketoacyl reductase
KS	β-ketoacyl synthase
MAT	malonyl-CoA-/acetyl-CoA-ACP transacylase

MFI	Mammosphere forming index
MFIn	Mammospehre forming inhibition
ML	Mesenchymal-like
NCI	National Cancer Institute
NF-Y	Nuclear factor Y
NHI	National Health Institutes
OS	Overall survival
PARP	Poly adenosine diphosphate-ribose polymerase
PDGFR	Platelet-derived growth factor receptor
PR	Progesterone
SERMs	Selective estrogen receptor modulators
Sp1 / 3	Stimulatory proteins 1 or/and 3
SREBP-1	Sterol regulatory element binding protein-1
TE	Thioesterase
TGF-α	Transforming growth factor-alfa
TKIs	Tyrosine kinase inhibitors
TMA	Tissue microarray
TNBC	Triple Negative Breast Cancer
USF	Upstream stimulatory factor
VEGFR	Vascular endothelial growth factor receptor
231	MDA-MB-231
231DXR	MDA-MB-231 doxoresistant

Index of Figures

Index of Tables

RESUM

El càncer de mama triple negatiu (TNBC) no disposa de teràpia dirigida. Tot i la bona resposta inicial a la quimioteràpia, el 30% dels pacients recauen durant els següents 5 anys post-tractament. El receptor de factor de creixement epidèrmic (EGFR) és un marcador que es troba normalment sobreexpresat en TNBC, i la seva expressió s'associa amb mal pronòstic. El creixement incontrolat que presenten les cèl·lules dels tumors, no només implica una desregulació en el control de creixement cel·lular sinó que les cel.lules tumorals també presenten una alteració en la regulació metabòlica. S'ha observat que alguns enzims relacionats amb la lipogènesis, com la Sintasa d'Àcids Grassos (FASN), està sobre expressada en càncer i que la seva inhibició provoca l'entrada en apoptosis de les cèl·lules cancerígenes que sobre expressen aquest enzim. Els àcids grassos sintetitzats *de novo* son els blocs principals per la síntesis de fosfolípids membrana, també estan implicats en la senyalització de proteïnes i s'ha vist que tenen un possible rol en l'adquisició de resistència. Durant els últims anys, la teoria de les Càncer Stem Cells (CSC, que significa cèl·lules mare del càncer) ha sorgit amb força com a nou camp d'estudi en la progressió del càncer. Aquesta teoria creu que una petita població que del tumor amb característiques úniques, té propietats de cèl·lules mare. Per tant presenta resistència intrínseca a la quimioteràpia, i per tant les identifica com a possibles responsables de les recaigudes.

En aquesta tesis, s'ha testat la hipòtesis que FASN està sobre expressat en càncer de mama triple negatiu, i que per tant, la seva inhibició farmacològica, sola o en combinació amb inhibidors d'EGFR, pot ser una estratègia efectiva per el tractament de tumors sensibles o resistents a la quimioteràpia. Amb aquest objectiu, a la primera part de la tesis s'han desenvolupat i caracteritzat línies de TNBC resistents a la quimioteràpia (doxorubicina, **DXR**) dels dos principals subtipus molecular que es troben dins del TNBC, *Basal-like* (BL, cel.lules HCC i HCC**DXR**) i *Mesenchymal-like* (ML, cel.lules 231 i 231**DXR**). Seguidament, s'han testat els compostos anti-FASN (EGCG, C75 i G28), sols o en combinació amb doxorubicina o cetuximab (inhibidor d'EGFR), mitjançant estudis de proliferació com també a nivell d'interacció molecular. Finalment s'ha testat l'efecte anti-tumoral *in vivo* d'EGCG, cetuximab, o la combinació d'ambdós mitjançant orthoxenografts. A més, s'ha avaluat l'expressió de FASN i EGFR en una petita cohort de pacients.

L'objectiu de la segona part de la tesis ha estat avaluar l'expressió de FASN en una cohort més àmplia de pacients triple negatius, per tal d'estudiar la seva correlació amb les característiques clinicopatològiques, subtipus molecular, i el seu potencial com a biomarcador. Mitjançant una

matriu de teixits (TMA) amb mostres de 100 pacients de TNBC obtinguts de l'Hospital Universitari Dr.Josep Trueta de Girona, s'ha avaluat mitjançant immunohistoquímica l'expressió de FASN, EGFR, CK5/6 i Vimentina (els últims dos marcadors han estat utilitzats per la classificació molecular). S'ha recollit la informació clínica i histopatològica de cada pacient.

La última part de la tesis ha consistit en avaluar la població enriquida amb CSC després de l'adquisició de resistència a doxorubicina en un model cel·lular (tant sensible i resistent) del subtipus molecular ML. Aquest subtipus molecular s'ha descrit que estar ja enriquit amb característiques de cèl·lules mare. Seguidament, s'ha evaluat el potencial de la inhibició de FASN en la població enriquida amb CSC utilitzant l'assaig de formació de mamosferes.

Els nostres resultats mostren que tant les línies cel·lulars com els tumors de pacients triple negatiu sobre expressen FASN. *In vitro*, la inhibició per EGCG, C75 o G28 juntament amb cetuximab, mostra un potent sinergisme tant en les línies sensibles com resistents. *In vivo*, la combinació d'EGCG amb cetuximab mostra un potent efecte anti-tumoral en els models animals tant sensibles com resistents, sense signes de toxicitat. L'anàlisi de l'expressió de FASN en l'array de teixit mostra que, tot i que de manera no significativa, els pacients amb alts nivells de FASN presenten una pitjor supervivència (OS) i una taxa de recurrència (DSF) més elevada que els pacients amb baixos nivells de FASN. A més, nivells alts de FASN estan associats amb la positivitat dels nodes sentinella, un dels marcadors més potents per a preveure recaigudes. Els pacients catalogats com a tumors BL (tumors altament proliferatius), presenten nivells de FASN significativament més elevats que aquells que es varen catalogar com a ML (poc proliferatius). A més, FASN també correlaciona negativament amb els nivells de vimentina, un marcador altament lligat al subtipus molecular ML. EGFR, en concordança amb altres estudis, s'expressa en un 45% de les mostres, i els pacients que presenten expressió d'aquest marcador presenten una taxa de recurrència (DFS) més elevada.

Tot i que no s'observen diferències a nivell d'inhibició de FASN entre les cèl·lules parentals o resistents, la suma d'aquests inhibidors als tractaments amb doxorubicina sensibilitza les cèl·lules resistents de nou al tractament, millorant la interacció farmacològica d'ambdós fàrmacs comparat amb les cèl·lules parentals. Per aquesta raó, es va avaluar l'expressió de FASN durant el tractament amb doxorubicina en la cèl.lula 231**DXR** i es va observar un augment significatiu al cap de 24 hores. En el mateix període de temps, també es va observar com la població enriquida amb CSC havia augmentat de manera significativa en el model resistent. Resultats preliminars de la inhibició de FASN en la població enriquida amb CSC mostra resultats interessants per els inhibidors G28 i C75, ja que tenen l'habilitat per inhibir la formació de

mamosferes.

En resum, els nostres resultats mostren que FASN es sobrexpressa en càncer de mama triple negatiu, i que la seva expressió està relacionada amb una pitjor evolució de la malaltia. Els nostres resultats mostren que FASN pot tenir no només un rol en la progressió del càncer, sinó també en l'adquisició de resistència. A més, la inhibició dual de FASN i EGFR es efectiva en models preclinics sensibles i resistents de de càncer de mama triple negatiu. Com a conclusió general, aquests resultats poden servir com a bases de noves estratègies farmacològiques mitjançant la inhibició de FASN (sola o en combinació) en càncer de mama triple negatiu.

RESUMEN

El cáncer de mama triple negativo (TNBC) no dispone de terapia dirigida. A pesar de la buena respuesta inicial a la quimioterapia, el 30% de los pacientes recaen durante los siguientes 5 años post-tratamiento. El receptor del factor de crecimiento epidérmico (EGFR) es un marcador que se encuentra normalmente sobreexpresat en TNBC, y su expresión se asocia con mal pronóstico. El crecimiento incontrolado que presentan las células de los tumores, no sólo implica una desregulación en el control de crecimiento celular, sino que las células tumorals también presentan una alteración en la regulación metabólica. Se ha observado que algunas enzimas relacionadas con la lipogénesis, como la Sintasa de Ácidos Grasos (FASN), está sobreexpresada en cáncer y que su inhibición provoca la entrada en apoptosis de las células cancerígenas que sobreexpresan esta enzima. Los ácidos grasos sintetizados *de novo* son los bloques principales para la síntesis de fosfolípidos de membrana, también están implicados en la señalización de proteinas y se ha visto que tienen un posible rol en la adquisición de resistencia. Por otra parte, durante los últimos años, la teoría de las Cáncer Stem Cells (CSC, que significa células madre del cáncer) ha surgido con fuerza como nuevo campo de estudio en la progresión del cáncer. Esta teoría cree que una pequeña población del tumor, con características únicas, tiene propiedades de células madre, con resisténcia intrínseca a la quimioterapia y por tanto las identifica como posibles responsables de las recaídas.

En esta tesis se ha testado la hipótesis que FASN está sobre expresado en cáncer de mama triple negativo, y que su inhibición farmacológica, sola o en combinación con inhibidores de EGFR puede ser una estrategia efectiva para el tratamiento de tumores sensibles o resistentes a la quimioterapia. Con este objetivo, en la primera parte de la tesis, se han desarrollado y caracterizado líneas de TNBC resistentes a la quimioterapia (doxorubicina, **DXR**) de los dos principales subtipos molecular que se encuentran dentro del TNBC, *Basal-like* (BL, células HCC y HCC**DXR**) y *Mesenchymal-like* (ML, células 231 y 231**DXR**). Seguidamente, se han testado los compuestos anti-FASN (EGCG, C75 y G28), solos o en combinación con doxorrubicina o cetuximab (inhibidor de EGFR), mediante estudios de proliferación y también a nivel de interacción molecular. Finalmente se ha testado el efecto anti-tumoral in vivo de EGCG, cetuximab, o la combinación de ambos mediante orthoxenografts. Además, se ha evaluado la expresión de FASN y EGFR en una pequeña cohorte de pacientes.

El objetivo de la segunda parte de la tesis ha sido evaluar la expresión de FASN en una cohorte más amplia de pacientes tiple negativos, para estudiar su correlación con las características clinicopatológicas, subtipo molecular, y su potencial como biomarcador. Mediante una matriz

de tejidos (TMA) con muestras de 100 pacientes de TNBC obtenidos del Hospital Universitari Dr. Josep Trueta de Girona, se ha evaluado mediante inmunohistoquímica la expresión de FASN, EGFR, CK5/6 y Vimentina (los últimos dos marcadores han sido utilizados para la clasificación molecular). Se ha recogido la información clínica y histopatológica de cada paciente.

La última parte de la tesis ha consistido en evaluar la población enriquecida con CSC después de la adquisición de resistencia a doxorrubicina en un modelo celular (tanto sensible y resistente) del subtipo molecular ML. Este subtipo molecular se ha descrito que está ya enriquecido con características de células madre. Seguidamente, se ha evaluado el potencial de la inhibición de FASN en la población enriquecida con CSC utilizando el ensayo de formación de mamosferes.

Nuestros resultados muestran que tanto las líneas celulares como los tumores de pacientes triple negativo sobreexpresan FASN. *In vitro*, la inhibición por EGCG, C75 o G28 junto con cetuximab, muestra un potente sinergismo tanto en las líneas sensibles como resistentes. *In vivo*, la combinación de EGCG con cetuximab muestra un potente efecto anti-tumoral en los modelos animales con tumores tanto sensibles como resistentes, sin signos de toxicidad. El análisis de la expresión de FASN en el array de tejido muestra que, aunque de forma no significativa, los pacientes con altos niveles de FASN presentan una peor supervivencia (OS) y una tasa de recurrencia (DSF) más elevada que los pacientes con bajos niveles de FASN. Además, niveles altos de FASN están asociados con la positividad de los nodos centinela, uno de los marcadores más potentes para predecir recaídas. Los pacientes catalogados como tumores BL (tumores altamente proliferativos), presentan niveles de FASN significativamente más elevados que los que se catalogó como ML (poco proliferativos). Además, FASN también correlaciona negativamente con los niveles de vimentina, un marcador altamente ligado al subtipo molecular ML. EGFR, en concordancia con otros estudios, se expresa en un 45% de las muestras, y los pacientes expressan de este marcador presentan una tasa de recurrencia (DFS) más elevada.

Aunque no se observan diferencias a nivel de inhibición de FASN entre las células parentales o resistentes, la suma de estos inhibidores a los tratamientos con doxorrubicina sensibiliza las células resistentes de nuevo al tratamiento, mejorando la interacción farmacológica de ambos fármacos comparado con las células parentales. Por esta razón, se evaluó la expresión de FASN en el modelo celular 231**DXR** durante el tratamiento con doxorrubicina y se observó un aumento significativo al cabo de 24 horas. En el mismo período de tiempo, también se observó como la población enriquecida con CSC había aumentado de manera significativa en el modelo resistente. Resultados preliminares de la inhibición de FASN en la población enriquecida con

CSC muestra resultados interesantes para los inhibidores G28 y C75, mostrando la habilidad para inhibir la formación de mamosferas.

En resumen, nuestros resultados muestran que FASN se sobrexpressa en cáncer de mama triple negativo, y que su expresión está relacionada con una peor evolución de la enfermedad. Nuestros resultados muestran que FASN puede tener no sólo un rol en la progresión del cáncer, sino también en la adquisición de resistencia. Además, la inhibición dual de FASN y EGFR es efectiva en modelos preclínicos sensibles y resistentes de de cáncer de mama triple negativo. Como conclusión general, estos resultados pueden servir como base para el desarrollo de nuevas estrategias farmacológicas mediante la inhibición de FASN (sola o en combinación) en cáncer de mama triple negativo.

ABSTRACT

Triple-negative breast cancer (TNBC) lacks an approved targeted therapy. Despite initial good response to chemotherapy, 30% of the patients relapse within 5 years after treatment. Epidermal Growth Factor Receptor (EGFR) overexpression is a common marker in TNBC, and its expression has been associated with poor outcome. The uncontrolled cell proliferation of neoplastic disease involves not only deregulated control of cell growth but also altered metabolic pathways. Lipogenic enzymes, such as Fatty-acid synthase (FASN), are commonly overexpressed in cancer and its inhibition leads to apoptosis of human carcinoma cells overexpressing FASN. In cancer, this newly synthetized fatty acids are the major building-blocks for new membrane synthesis, protein signaling and even have a role in drug resistance. In the last years, the theory of the Cancer Stem Cells (CSCs) has emerged as a new field of study in cancer progression. This theory says that a unique and small niche of cells within the tumor has Stem Cells properties, with high intrinsic resistance to chemotherapy, and therefore they might be responsible of relapse after general therapy.

The main hypothesis of ths thesis is that FASN is expressed in TNBC and, therefore, blocking FASN in combination with anti-EGFR signaling agents would be an effective antitumor strategy in sensitive and chemoresistant TNBC. For that purpose, in the first part of this work, we have developed and characterized TNBC cell lines resistant to chemotherapy (doxorubicin, **DXR**) from the two main moleculars subtypes in TNBC, Basal-like (BL, cells HCC and HCC**DXR**) and Mesenchymal-like (ML, cells 231 and 231**DXR**). Then, we evaluated the cellular and molecular interactions of anti-FASN compounds (EGCG, C75 and G28) with doxorubicin and cetuximab (EGFR inhibitor). Finally, cetuximab, EGCG, or the combination were evaluated in vivo by its capability of tumor growth inhibition using orthoxenograft models. Furthermore, FASN and EGFR expression were evaluated in a small cohort of TNBC tumor samples.

The purpose of the second part of the thesis was to evaluate FASN expression in a large cohort of TNBC samples and study its correlation with clinico-pathological characteristics, intrinsic subtypes and its potential as a prognosis marker. Using tissue microarrays (TMAs), we evaluated by immunohistochemistry the expression of FASN, EGFR, CK5/6 and Vimentin, (the last two markers were used for molecular classification) in 100 TNBC tumor samples obtained from the Hospital Universitari Dr. Josep Trueta de Girona (Spain). The clinical and histopathological features were obtained for each patient.

The last part of the work consisted in the evaluation of the CSC population after doxorubicin resistance acquisition in a ML cells lines (sensitive and resistant), a molecular subtype already identified to be enriched with CSC features. We then evaluated FASN inhibition in this enriched CSC population using the mammosphere forming assay.

Our results showed that both patients and TNBC cell lines overexpress FASN. In vitro, EGCG, C75 or G28 plus cetuximab showed strong synergism in sensitive and chemoresistant cells. In vivo, the combination of EGCG with cetuximab displayed strong antitumor activity against the sensitive and chemoresistant TNBC orthoxenografts, without signs of toxicity. Interestingly, when analyzing FASN in the patient set, our results showed that although no significantly, High FASN expressing patients showed lower Overall-Survival (OS) and Disease-Free Survival (DFS) rates than the Low FASN ones, and were significantly associated with positive node status, one of the most powerful markers to predict relapse. FASN expression was significantly higher in BL (high proliferative subtype) patients than in ML (low proliferative) ones, and it was negatively correlated with Vimentin levels (a marker strongly related to the ML intrinsic subtype). EGFR expression was positive in 45% of the tumors, and those patients showed poorer DFS. While no differences where observed between FASN inhibitors in either parental or resistant cell line, the addition of FASN inhibitors to the doxorubicin treatment resensitized resistant cell lines to doxorubicin, improving the combination interaction index (Ix) compared to the parental ones. For that reason, we evaluated FASN expression under doxorubicin treatment in 231**DXR** cell line, and interestingly its expression levels increased significanitly after 24h. In the same period of time, CSC enriched population was enriched significantly in this doxorubicin-resistant cell line, indicating that CSC play a role in drug resistance in this model of a ML subtype. Preliminary results of FASN inhibition in a CSC population show interesting results for FASN inhibitors G28 and C75, showing the abililty to inhibit mammosphere formation.

In summary, our results show that FASN is overexpressed in TNBC and its expression is related with poorer outcomes in TNBC, suggesting that FASN expression could have a role not only in cancer progression, but also in drug resistance. Furthermore, the simultaneous blockade of FASN and EGFR is effective in preclinical models of sensitive and chemoresistant TNBC. As general conclusion, these resulst may account for the bases of future therapeutic strategies of TNBC using FASN inhibitors (alone or in combination).

INDEX

Introduction

1. Cancer

The number of diagnosed cancer in western countries increased every year until the last decade, due to a combination of factors such as population aging or improvement of the detection tools and protocols. On the other hand, the number of death do to cancer has dropped in the last two decades thanks to prevention, early detection and treatment improvement[1–3]. Still, cancer is the second cause of death in Europe (the third worldwide), after cardiovascular disease[4].

Cancer can be defined as a disease in which abnormal cells divide without control and, eventually, invade nearby tissues. Cancer cells can also spread to other parts of the body, a process called metastasis, which is the main responsible for cancer death[5].

Cancer is a very complex disease. In a way to summarize the complexity, Hanahan and Weinberg *et al.* described the hallmarks of cancer, which are the biological capabilities acquired by cancer cells during the development of human tumors that provide them advantage to survive, proliferate and disseminate[6,7]. In their first work published in 2000, they first described six main biological processes, which are: sustaining proliferative signaling, evading growth suppressors, resisting cell death, enabling replicative immortality, inducing angiogenesis, and activating invasion and metastasis[6]. In their revised work from 2011, they included genome instability and inflammation as an underlying process that fuel cells to acquire the characteristics above mentioned. In the same review, they also included two new emerging hallmarks: energy metabolism deregulation and evading immune system destruction[7].

Depending on the type of cell it is originate, cancer can be grouped in five main categories: **Carcinomas**, that are cancers that have their origin in the in the skin or in tissues that line or cover internal organs; **Sarcomas**, that refers to those cancers that begin in the connective or supportive tissues such as bone, cartilage, fat or muscle; **Leukemia**, which starts in the bone marrow, causing a large number of immature lymphocytes unable to defeat infections; **Lymphomas and myelomas** are cancers that begin in the cells of the immune system, that divide uncontrollably resulting in abnormal cells unable to fight infections and **Central nervous system cancers,** that are originated in the brain or spinal [5].

Types of cancer are usually named after the organs or tissues where the cancer form, such as lung, colon or breast cancer.

2. Breast Cancer

Breast Cancer (BC) is the leading cause of cancer dead affecting women worldwide[8], and represents 41% of cancers diagnosed in women in western countries [1,2]. The median age at diagnose for breast cancer is 61, earlier than in other common cancer types. Survivorship for patients diagnosed with more than 60 years old is about 70% while barely reaches 10% for women diagnosed before 50 years old[1].

Patients with breast cancer show a wide range of clinical, pathologic, and molecular characteristics [9,10]. Ongoing improvements in the understanding of the biology of breast cancer have led to a more specific classification of tumors according to their therapeutic options. **Hormone Positive Breast Cancer** accounts for 60-70% of breast cancers, and women with this type of BC have a better prognosis among other cancer types[9]. These tumors are characterized by the overexpression of the estrogens (ER) and/or progesterone (PR) receptors, responsible for permanent activation of proliferation pathway that triggers cell division and proliferation. Selective estrogen receptor modulators (SERMs), such as tamoxifen and raloxifene, selective estrogen receptor downregulator (SERDs) and aromatase inhibitors are currently used to treat ER-positive breast cancer[11,12]. **HER2 Positive Breast Cancers** are characterized by the overexpression of the human epithermal growth factor receptor 2 (HER2) due to ErbB2 gene overexpression[13]. These tumors represent approximately 20-30% of breast cancer, and patients diagnosed with HER2 positive breast cancer have poor prognosis and high risk of metastasis[14,15]. Principal treatment options are the anti-HER2 therapies, which block the proliferative signaling pathway driven by the HER2 receptor, leading to apoptosis of cancer cells[16,17].**Triple-negative breast cancer (TNBC)** represents 15%-20% of the patients diagnosed with breast carcinomas and is characterized by the lack of expression of estrogen and progesterone receptors (ER/PR) and no amplification of the HER2 oncogene [18]. TNBC runs an aggressive course and has a poor prognosis. As TNBC lacks a validated targeted therapy, patients are treated mainly with cytotoxic chemotherapy (anthracyclines and taxanes). Even though TNBC patients show a good initial response to chemotherapy, the recurrence rate within 5 years following diagnosis is about 30% [19,20], the highest relapse rate compared to other breast cancer types.

2.1. Prognosis Factors and Treatment Options of Breast Cancer

The prognostic factors are established at the time of the diagnosis and might determine the natural evolution of the disease in the absence of treatment and are associated with outcome[21]. Staging of breast cancer allow grouping patients according to the extent of their disease, and helps in determining the choice of treatment and estimate their prognosis. There are several prognosis factors, here are described the most currently used in the clinic[21].

Tumor size **(T),** lymph Node involvement **(N)** and Metastasis **(M)**, known as the **TNM** classification, are one of the most used methods for clinical and pathological staging system.

Tumor size (T): Refers to the size of the primary tumor, and can be classified manly in six different groups: **TX** (when primary tumor cannot be assessed), **T0** (no evidence of primary tumor), **Tis** (*in situ*, no healthy tissues are involved), **T1** (Tumor 2 cm or less in greatest dimensions), **T2** (Tumor more than 2 cm but less than 5cm in greatest dimensions), **T3** (Tumor more than 5cm in greatest dimensions) and **T4** (tumor of any size with any direct extension to **a)** chest wall, **b)** skin, **c)** both or **d)** Inflammatory carcinoma).

Lymph node involvement: Lymph nodes are small, bean-shaped masses of tissue scattered along the lymphatic system that act as filters and immune monitors, removing fluids, bacteria, or even cancer cells that travel through the lymph system. If cancer cells can be detected in the regional lymph nodes to the mammary gland (also called axillary lymph nodes), increases the risk of cancer spreading**.** The sentinel lymph node is the first in receive the lymphatic drainage from a primary tumor, and the first one tested to content cancer cells. If sentinel node is free of metastatic cells, the other lymph node dissection is not recommended[22]. Node involvement can be classified in five different groups: **NX** (Regional nodes cannot be assessed), **N0** (No regional lymph node metastasis), **N1**, **N2**, **N3** (Lymph node involvement. The higher the N number, the greater the extent of the lymph node involvement).

Metastasis: Metastasis is when cells escape from the primary tumor through the circulatory system and generates a new tumor in a distant site from the original tumor.

All distant visceral sites are potential sites of metastasis, the four major sites of involvement are bone, lung brain and liver. Distant metastasis can be classified as **MX** (when metastasis cannot be assessed), **M0** (no distant metastasis) and **M1** (distant metastasis).

Stadium: Stadium of the tumor give information about the size, localization and invasiveness of the tumor as well. It can go from **0** (local and non-invasive) to **IV** (cancer that have spread in distant sides of the body). The stage of a tumor can be determined by the **TNM** values (See Table 1).

Histological grade: The histological grade gives information of how differentiated are the cells within the tumor. It can be classified from **G1** to **G4**, being **G1** cells that barely look different from normal cells, while **G3-4** are tumors formed by cells that look very different from normal cells. They grow quickly in disorganized, irregular patterns, and are high proliferative.

Table 1: Stage according to the TNM classification[21]

Stage grouping			
Stage 0	T*is*	N0	M0
Stage I	T1	N0	M0
Stage IIA	T0	N1	M0
	T1	N1	M0
	T2	N0	M0
Stage IIB	T2	N1	M0
	T3	N0	M0
Stage IIIA	T0	N2	M0
	T1	N2	M0
	T2	N2	M0
	T3	N1	M0
	T3	N2	M0
Stage IIIB	T4	Any N	M0
	Any T	N3	M0
Stage IV	Any T	Any N	M1

Proliferation rate: The most widely marker used to assess the proliferation rate is the evaluation by IHC of the Ki-67 antigen[23]. Ki-67 is highly expressed during mitosis. High values of Ki-67 are associated poor prognosis but at the same time they show good response to chemotherapy.

As mentioned beforehand, breast cancer can be divided in three different groups depending their treatment options. In order to assess this classification, immunohistochemistry (IHC) of the biopsy from the primary tumor is performed in

order to determinate the levels of expression of the **Hormonal** or **HER2 receptors.**

The presence of at least >1% of cells positives for **ER/PR** is enough to consider tumors as hormone positive and benefit for hormonal therapy, such as tamoxifen. This type of cancer is considered to have good prognostic[24,25].

HER2 blocking therapies (e.g. trastuzumab, lapatinib, pertuzumab) are effective for those tumors that overexpress the HER2 receptor[26]. IHC results of 3+ are considered positive. For 2+ results otherwise, the confirmation of the amplification of the HER2 gene is assesses using the Fluorescence *in situ* hybridization (FISH).

2.2. Molecular Classification of Breast Cancer

Breast tumors are very heterogeneous regarding its phenotype, response to drug therapy, dissemination patterns and patient outcomes[27]. The current parameters used by clinicians to predict prognosis and decide treatment strategies do not provide a complete understanding of the disease. *Perou et al.* thought that this diversity could be accompanied or explained by the diversity in gene expression, and that molecular intrinsic subtypes could help to explain heterogeneity. Using cDNA microarray, they analyzed the expression of more than 8000 gene of 78 tumors from 42 patients. By gene-clustering analysis, they identify a set of 496 gene that were able to differentiate four different molecular subtypes within breast cancer tumors, defined as ER+/Luminal, basal-like, Erb-B2+ and normal-like[28]. In a posterior study, they were able to divide the Luminal subgroup into two groups, later called Luminal A and Luminal B[25]. Years later, a major comprehensive analysis pointed out the existence of a new molecular subgroup, the so-called claudin-low[29–31]. This rare molecular subtype has poor prognosis, and is linked to a unique biologic properties such as mammary stem cells and EMT[29,32]. The five intrinsic molecular subgroups (Luminal A, Luminal B, Her2-enriched, basal-like and Claudin-low) also presented diverse clinically implications respect to overall survival (OS) and disease-Free survival (DFS, Figure 1). Patients with Luminal A tumors had the better prognosis among the five molecular subgroups, and basal-like together with HER2-enriched classified tumors showed the poorest one[9,25].

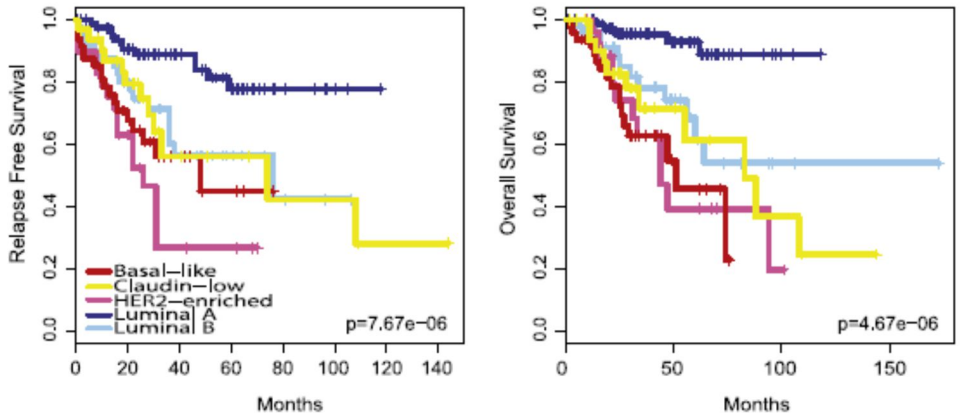

Figure 1. Kaplan-Meier relapse-free survival and overall survival curves for molecular subtypes of breast cancer. Taken from Prat *et al.*, 2011.

The molecular portraits revealed in the pattern of gene expression, not only uncovered

similarities and differences among the tumors, but in many cases pointed to a biological interpretation. Variations in growth rate, in signaling pathways specific activation (ER and ERBB2), and in the cellular composition of the tumors (luminal – basal/myoepithelial) were all reflected in the corresponding variation in the expression of specific subset of genes, providing new insights in the biology of the disease.

In 2009, Parker *et al.* derived a minimal gene set (PAM50) for classifying intrinsic subtypes of breast cancer[33]. This algorithm uses 50 genes to identify the four major intrinsic subtypes (luminal A, luminal B, basal-like, HER2-enriched) and the normal breast-like group.

Luminal A and B subtypes depict the majority of breast cancer tumors (they represent 40% and 10% respectively[9]). They are characterized for positively expressing ER and PR receptor. Usually these tumors are classified as low-grade. Luminal A tumors generally have high expression of ER and PR regulated genes, low expression of the HER2 receptor cluster (which is variable in luminal B tumors), and low expression of proliferation-associated genes, including Ki-67[10,25] (Figure 2). Conversely, luminal B tumors tend to be highly proliferative, TP53 mutant, and in general show lower expression of ER and ER-regulated genes[10,25].

HER2-enriched represent about 10% of breast cancer. Generally, tumors that classify in this group show Her2 loci amplification or HER2 receptor overexpression. Other common features of this subtype are low expression of the luminal, hormone receptor-regulated gene cluster and low expression of basal-like genes (Figure 2). Usually, these tumors are classified as high-grade, and over 40% show p53 mutations[34].

Basal-like was the intrinsic subtype that caused the greatest impact, as triple-negative breast cancer weren't identified as a unique disease, contrary to the ER+ or HER2+ breast cancers. Many studies used the term basal-like to refer to TNBC, as this intrinsic subtype represented the majority of TNBC(~75%) [27,35] until the claudin-low intrinsic subtype was identified[29]. Basal-like molecular subtype is characterized by low expression of the luminal genes, low expression of the HER2 gene cluster, high expression of the proliferation cluster, and high expression of a unique cluster of genes called the basal cluster (that includes cytokeratin CK5, CK6, CK14, CK17 and the Epidermal Growth Factor Receptor, EGFR) (Figure 2). Basal-like subtype show the poorest prognosis compared to other subtypes[9,25,35] (Figure 1).

Claudin-low (CL) was the latest intrinsic subtype to be identified. These tumors share gene expression features with basal-like breast cancer, such as low HER2 expression

and luminal cytokeratin. However, these tumors show two unique clusters: low expression of genes related to cell-cell adhesion proteins (claudin genes), and highly enriched with immune system response genes[27,29] (Figure 2). Furthermore, they also show low proliferation phenotype and are enriched with mesenchymal genes, such highest expression of vimentin, N-cadherin and TWIST, features linked to the induction of epithelial-to-mesenchymal transition (EMT). This molecular subtype is also known as **Mesenchymal-like (ML)**[31], and during this thesis we will refer to the claudin-low subtype as Mesenchymal-like.

Claudin-low or **Mesenchymal-like** are the least frequent subtype (~15%), are mostly high-grade an ER-\PR-\HER2- (TNBC). In terms of patient outcomes, these tumors show poor outcome compared to Luminal A, but no difference is observed in terms of survival compared to other poor prognosis subtypes[27,29] (Figure 1).

The **Normal-like** group is composed of normal breast samples from reduction mammoplasties, and also some tumor samples that after H&E examination showed less than 50% of malignant cells, or tumors with high stromal content or lymphocyte infiltration. This intrinsic subgroup cluster close to the Luminal A due to their common low proliferation rates and high expression of the luminal cluster[34] (Figure 2). It is controversial if it's a real subtype of breast cancer.

Table 2. Main characteristic of breast cancer intrinsic subtypes[10,27–29,36] .

	Tumor features					
Breast cancer intrinsic subtype	**Cellular composition**	**Proliferative rate**	**Outcome**	**Tumor grade**	**Classical IHC classification**	**Common mutations**
Luminal A	Luminal	low	good	low	ER+/HER2-	
Luminal B	luminal	high	poor	low	ER+/HER2+ or HER2-	TP53
HER2- enriched	luminal /basal	high	poor	high	ER-/HER2+	TP53
Basal-like	basal	high	poor	high	ER-/HER2-	BRCA1
Claudin-low	basal	low	poor	high	ER-/HER2-	

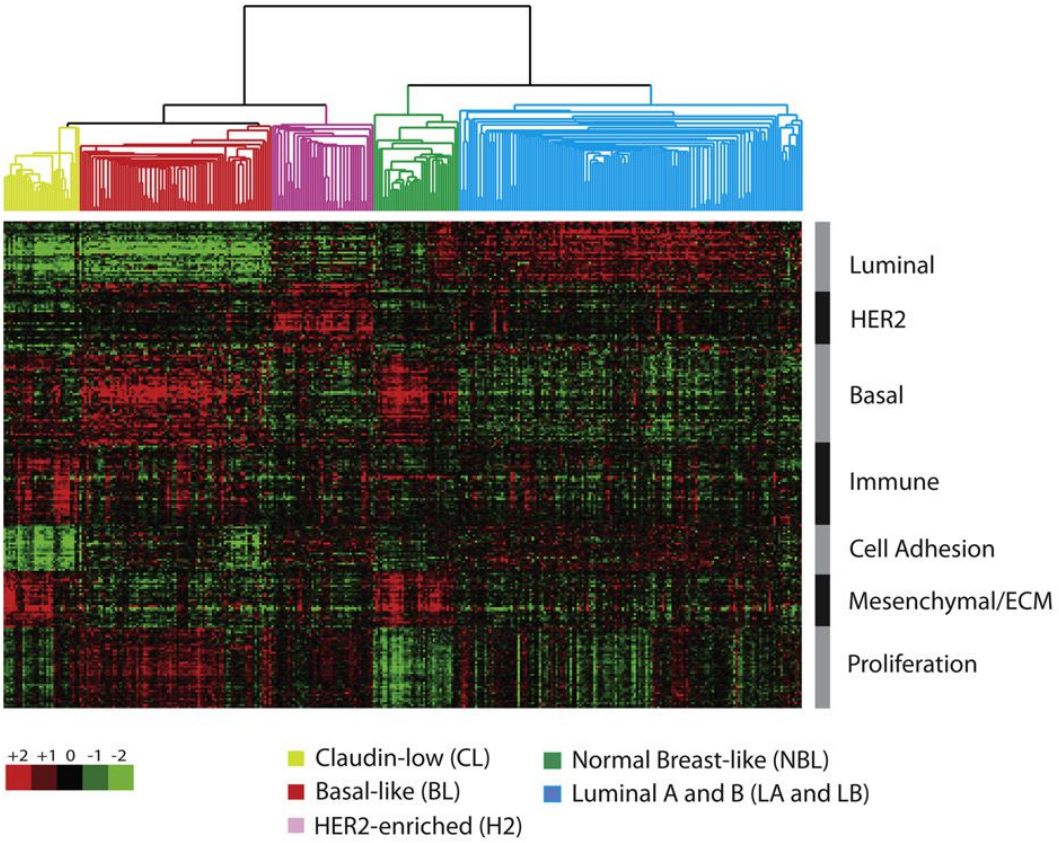

Figure 2. Hierarchical clustering of molecular subtypes of breast cancer. The 5 major intrinsic subtypes (Luminal A and B, basal-like, claudin-low) plus the normal-like were identified. The gene clusters that better define each subtype are shown. Modified from Prat A *et al*., 2011 [27].

2.3. Triple-Negative Breast Cancer and Molecular Classification

BL and CL or ML molecular subtypes are the major groups within the TNBC, representing 49% and 30% respectively (Figure 3A)[27,31]. It is important to notice that the clinic classifications of the tumors (ER, PR and HER2) do not overlap completely with the intrinsic subtypes (Figure 3B)[27,31,35].

The use of the molecular classification using cDNA microarrays is not still a common technique in the clinic. For that reason, efforts have been done to improve the IHC to better identify the BL and CL/ML molecular subtype because both share negativity for the common biomarkers (ER/PR/HER2). Studies comparing molecular classification

and IHC markers of basal-like subtype showed that the addition of the specific markers CK5/6 and EGFR to the classical ones have more prognostic value to identify BL cancer[37–39]. On the other hand, immunohistochemically features such are high levels of vimentin, low expression of E-Cadherin and claudin proteins are common markers among the CL/ML subtype[40,41].

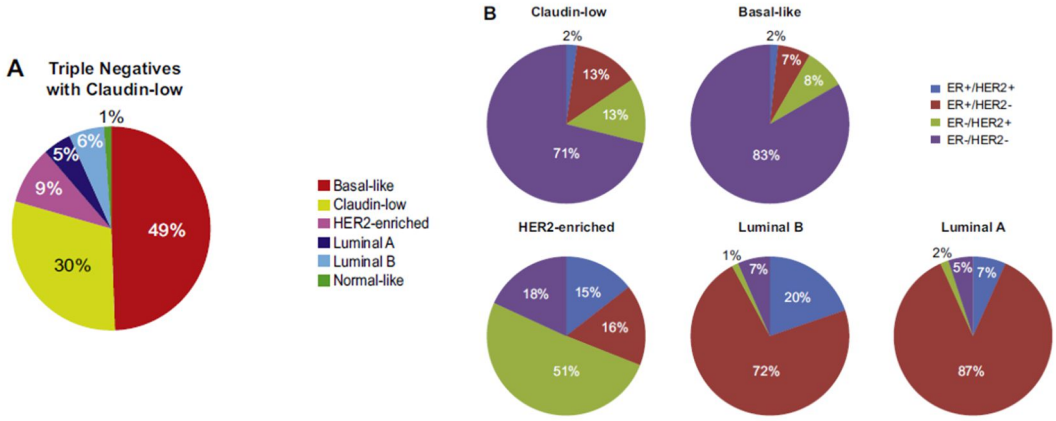

Figure 3. Distribution of clinical-pathological categories relative to the intrinsic subtypes of breast cancer. (**A**) Intrinsic subtype distribution within the triple-negative tumor category (**B**) Distribution of ER+/HER2+, ER+/HER2-, ER-/HER+, ER-/HER2- clinical groups in the claudin-low, Basal-like, HER2-enriched, Luminal B, and Luminal A within each subtype. Modified from Prat *et al*., 2011.

2.4. Targeted Therapies in Development for TNBC Treatment

Patients with TNBC have higher chemosensitivity than non-TNBC. Actually, patients who achieved pathological complete response is higher in TNBC, showing these patients higher relapse-free survival compared to patients with residual disease[42]. On the other hand, TNBC have the highest relapse rates compared to other subtypes[19,20]. The need to identify TNBC biomarkers to find and develop targeted therapies for this subtype of cancer has become a priority.

In order to identify those therapies that achieved the last steps in the clinical trials (Phase III and II), the U.S. National Cancer Institute (NCI) and National Health Institutes (NHI) clinical trials search tools were used. The focus was in targeted therapies, so new systemic treatments in development are not here described (**Table 3**).

There are three clinical trials being conducted in phase III with the drugs Olaparib (PARP inhibitor), Atezolizumab and Pembrolizumab (anti-PD-1 therapies).

PARP (poly adenosine diphosphate-ribose polymerase) is leading to cell recovery from DNA damage. Basal-like breast cancer, that represent ~50% of TNBC, have shown a prevalence in BRCA mutation[35,43]. BRCA plays also a role in DNA repair, and for that

reason PARP inhibitors in BRCA-mutated breast cancers were proposed as a good strategy. **Oliparib** is a FDA-approved PARP inhibitor for the treatment of ovarian cancer deficient in BRCA1 or BRCA 2. **Iniparib** was the first PARP inhibitor to reach phase III in clinical trials, but the addition of this compound to chemotherapy did not improve neither disease free survival (DFS) or overall survival (OS) significantly[44].

The two other drugs (**Atezolizumab** and **Pembrolizumab**) recruiting for phase III studies are based on immunotherapy against the PD-1 pathway. Some TNBC cells and tumor infiltrating immune cells express high levels of PD-L1, a ligand that binds the PD-1 receptor that inactivates T cells, allowing cancer cells to escape immune surveillance. By upregulating ligands for PD-1, cancer cells block antitumor immune responses in the tumor microenvironment. PD-1 and PD-L1 inhibitors specifically disrupts the interaction between the ligand and the receptor, and restoring T-cell function[45,46]. Two different compounds, from two different investigators, with clinical trials performed in different hospital are having similar outcomes and showing promising results using immunotherapy for the first time in TNBC.

There are other compounds in Phase II study for TNBC. Here, the principal mechanism of action will be described.

The PI3K/AKT/mTOR pathway is over activated in many cancers, leading to cell proliferation and apoptosis inhibition. **Ipatasertib** and **GSK2141795** are inhibitors of the serine/threonine kinase AKT currently in phase II studies. The mTOR inhibitor **AZD2014** is also in a phase II study for the treatment of TNBC.

Sorafenib is an oral, multitarget tyrosine kinase inhibitor that blocks vascular endothelial growth factor receptor (VEGFR), platelet-derived growth factor receptor (PDGFR), and Raf family kinases. **PLX3397** is also an inhibitor of several tyrosine kinase in phase II studies for the treatment of TNBC.

Glembatumumab vedotin, is a monoclonal anti-body against the protein membrane gpNMB (glycoprotein Non-Metastatic Melanoma B), conjugated with a cytotoxic agent. gpNMB is overexpressed in 40% of TNBC, and promotes angiogenesis, migration, invasion and metastasis[47]. First studies showed good overall response rate (40% vs 0%) in those patients overexpressing gpNMB (>25% in IHC analysis)[48].

Targeting the Androgen receptor seemed to have good response for those advanced TNBC that overexpress this receptor (about 20-40% of the tumors[49]). **Enzalutamide** is in a phase II study, and the first results showed a clinical benefit for patients overexpressing AR.

Table 3. Targeted therapies in clinical trials Phase II or III for the treatment of TNBC

Clinical trials in development for the treatment of TNBC							
	Drug	**Code**	**Administration**	**Clinical trial phase**	**Biomarker**	**FDA-aproved**	**Commercial name**
PARP- inhibitors	Oliparib	AZD-2281	orally	Phase III	BRCA1-2 mutation	for ovarian cancer	Lynparza
	Talazeparib	BMN 673	orally	Phase III	BRCA1-2 mutation	-	-
	Veliparib	ABT-888	orally	Phase III	BRCA1-2 mutation	-	-
PD-1/L1 - inhibitors	Atezolizumab	MPDL3280A	IV	Phase III	PD-L1 overexpression	for urothelial carcinoma	Tecentriq
	Pembrolizumab	MK-3475	IV	Phase III	PD-L1 overexpression	for metastatic melanoma	Keytruda
	Durvalumab	MEDI4736	IV	Phase II	PD-L1 overexpression	-	-
Multiple tyrosin-kinase inhibitors	Sorafenib	BAY43-9006	orally	Phase II	-	for hepatic, renal and thyroid cancer	Nexavar
	Pexidartinib	PLX3397	orally	Phase II	-	-	-
AKT/PI3K/mTOR inhibitors	GSK2141795	GSK2141795	orally	Phase II	-	-	-
	Vistusertib	AZD2014	orally	Phase II	-	-	-
	Ipatasertib	GDC-0068	orally	Phase II	-	-	-
OTHERS	Glembatumumab vedotin	CDX-011	IV	Phase II	gpNMB overexpression	-	-
	Enzatulamide	MDV3100	orally	Phase I/II	AR overexpression	for prostate cancer	Xtandi

*IV (Intravenous therapy)

3. Fatty Acid Metabolism and Cancer

Metabolism deregulation in cancer cells was firstly observed by Warburg in 1924[50,51], and recently has been considered a *hallmark of cancer*[7]. Warburg described the process now known as the *Warburg effect*, in which tumor cells convert the majority of their glucose to lactose, a process called aerobic glycolysis [52]. While 38 ATP molecules are derived from the oxidative glycolysis, only two are obtained from anaerobic conditions[51]. Contrary to the original Warburg hypothesis, the aerobic glycolysis activation was not due to mitochondrial defects in cancer. Instead, in proliferating cells, mitochondrial metabolism is reprogrammed to fulfil the needs of macro-molecular synthesis by cancer cells[52]. Uncontrollable cell growth and proliferation of cancer cells is a high demanding process of cellular building blocks, such as nucleic acids, proteins, and lipids. Perturbed metabolism, allows them to accumulate metabolic intermediates as sources of these building blocks and provide advantage in the tumor environment [53,54].

Long-chain fatty acids are essential constituents of membrane lipids and are important substrates for energy metabolism of the cell. Palmitate, the most abundant acid, is synthesized de novo from acetyl-coA, malonyl-CoA, in a NADPH dependent manner by the Fatty Acid Synthase (FASN)[55].

FASN has been described to be overexpressed in several carcinomas such as breast, prostate, lung and colon among others[56–59]. This enzyme is not expressed in normal tissue, except in lipogenic tissues (liver, adipose tissue[60,61] and lactating mammary glands[62,63]), where its expression is tightly regulated by diet. In cancer, however, cells overexpress FASN enzyme to synthesize almost all their fatty-acids de novo[54]. In normal tissue, fatty acid synthesis occurs when there is an excess of calories, and the carbohydrates are stored as triglyceride. In cancer cells however, most of the fatty acid are synthetize *de novo* mainly as phospholipids, acting as structural or functional blocks for membrane biosynthesis, protein modification, or signaling molecules[64–66].

3.1. FASN Regulation in Normal Tissues and Cancer

FASN is low expressed in most of the tissues, as cells preferably acquire all the fatty acids from exogenous supplies[67].

Lipogenic tissues, hormone-sensitive tissues such as endometrium during menstrual cycle, mammary gland during lactation or hypothalamus (as a mechanism for food

intake regulation) are the exceptions in which the novo synthesis pathways are activated in normal tissues[60–63,67,68].

In normal tissues, the regulation of FASN expression can be mediated both metabolically and hormonally. This hormonal and nutritional regulation converges, at least in part, on PI3K/AKT and MAPK signal transduction cascades that modify the expression or maturation of transcription factors that regulates the expression of FASN [64]. Stimulatory proteins 1 and 3 (Sp1 and Sp3), nuclear factor Y (NF-Y), upstream stimulatory factor (USF) and the sterol regulatory element binding protein-1 (SREBP-1) have cognate binding sites on the promoter of the FASN gene[69]. Interestingly, the activation of the SREBP-1 play an important role in FASN regulation in cancer[64]. On the other hand, leptin (the hormone made by adipose cells that inhibit hunger), decrease SREBP-1 gene expression inhibiting the expression of lipogenic enzymes such us FASN[70].

In Cancer, the main regulatory elements for FASN overexpression change from diet aspects to regulatory elements such as **growth factor and their receptors** (Figure 4).

The HER family receptors have been linked with FASN overexpression in several cancers[71–73], as they share the downstream pathways that leads to the activation of the SERBP-1 transcription factor. Deregulation or alterations in the HER-downstream pathways (PI3K/AKT and MAPK) have also been related to FASN, in cancer such as breast, prostate or ovarian among others[72,74,75]. **Over-activation of hormonal pathways** (including ER, PR and androgen receptors (AR)) also converges to the hyper-activation of PI3K/AKT and MAPK cascades that stimulates FASN expression through the SREBP-1 transcription factor[76]. **Disturbance in post-translational regulations** have also been described in cancer. The Ubiquitin-specific protease USP2a stabilizes FASN avoiding proteasome-degradation and contributing to FASN overexpression[77].

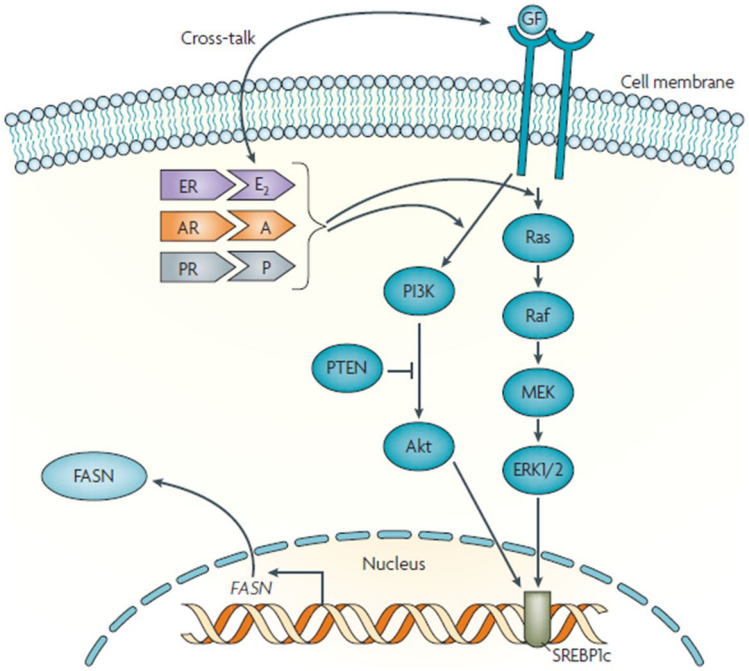

Figure 4. Regulation of Fatty Acid Synthase expression in cancer cells. Contrary to normal cells, cancer cells regulate FASN expression through membrane receptors (HER family as an example) and/or hormone receptors (ER,PR,AR) that activate the PI3K/AKT or MAPK pathway. The activation of this pathways leads to the activation of the SERBP1c transcription factor of the FASN gene. Taken from Menendez *et al.*, 2007 [64]).

3.2. FASN Structure and Function

FASN is a sophisticated multifunctional enzyme, with a molecular weight of 260KDa, that contains seven catalytic subunits divided in three different domains[55,78]. Structurally, the functional enzyme is composed of two identical peptide sequences, in which three N-terminus domains (β-ketoacyl synthase (**KS**), malonyl-CoA-/acetyl-CoA-ACP transacylase (**MAT**), dehydratase (**DH**)) are separated by 600aa from the four domains located in the C-terminus (enoyl reductasa (**ER**), β-ketoacyl reductase (**KR**), acyl carrier protein (**ACP**), thioesterase (**TE**))[78]. The conventional model for peptide organization proposed that the two monomers were arranged in a fully extended head-to-tail conformation. New studies based on high resolution crystallographic maps, catalytic domain mutations, chemical crosslinking and monomer interaction studies proposes that FASN monomers adopt an X-shape with a central body extended at the upper and lower ends by ‘‘arms’’ and ‘‘legs,’’ that allows for a variety of intra- and

intermonomer functional domain interactions[78,79].

As cancer cells fervently consume glucose, pyruvate is made via the glycolytic pathway. Pyruvate is subsequently fed into the Krebs cycle in the mitochondria to yield ATP, releasing acetyl-coenzyme A as one of the by-products of this reaction[80].

Palmitate is synthesized de novo from acetyl-coA, malonyl-CoA, in a NADPH dependent manner by FASN[55]. The synthesis basically consists of elongating the acetyl group by C_2 units derived from malonyl-CoA in a stepwise and sequential manner. For instance, in the synthesis of palmitate there are over 40 steps [55,78].

The reaction can be divided in three different steps (Figure 5). The first one, is initiated by the transfer of the acyl moiety of the starter substrate acetyl-CoA to the ACP catalyzed by MAT which also transacylates the malonyl group of the elongation substrate malonyl-CoA to ACP. Then, the elongation is a repetition of cycles of reduction and rehydration that add two carbons in each cycle of elongation to the fatty acid chain, until a length of C_{16} or C_{18} is reached. These reactions are catalyzed by KS, DH, ER and KR. Finally, the product is released from the ACP by TE.

To synthetize one molecule of palmitate FASN needs 1 Acetyl-CoA, 7 Malonyl-CoA, 14 NADPH and 7 ATP[55].

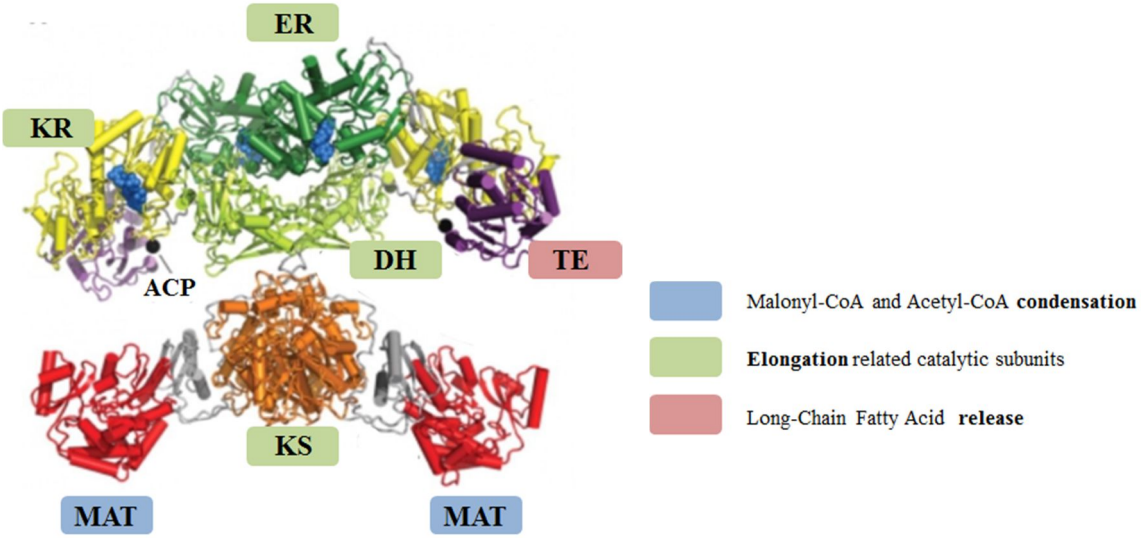

Figure 5. Fatty Acid Synthase structure. Modified from Maier *et al.,* 2006 [78].

3.3. Fatty Acid Inhibition in Cancer

Fatty Acid Synthase has been described to be over-expressed specifically in cancer

tissues. Cancer cells are dependent on the generation of lipids to keep its demanding proliferation ratio, and consequently, FASN has emerged as a unique oncologic target. Since the first FASN inhibitor described to be cytotoxic in cancer cells in 1960, several FASN inhibitors have been developed (Table 4). Unfortunately, some limitation were observed in the early generation of FASN inhibitors (Cerulenin[81], Cerulenin-derived C75[82,83] and C93[84], Orlistat[85], Triclosan[86] or EGCG[87]), by significant off-target toxicity, bioavailability or stability of the compound. In the last years, a new generation of FASN inhibitors are in development (G28UCM[88,89], GSK 2194069[90,91] , JNJ- 54302833 [92], IPI-9119 [93], and TVB-2640[94]), being the TVB-2460 the first FASN inhibitor to reach the clinic (reviewed in Jones *et al.,* 2015 [66]).

FASN inhibition in cancer cells have been shown to prompt cytotoxicity and inhibit tumor progression[95–100], block angiogenesis[101,102] and even overcome drug-resistance to chemotherapy[103,104]. FASN inhibition have also shown to accentuate the cytotoxic effect of common chemotherapies, such are taxans or anthracyclines[105,106].

Several mechanisms that trigger anti-tumoral effect by FASN inhibition have been identified (reviewed in Menendez *et al.* 2007 [64]):

End-product starvation. Highly proliferating tumor cells require the activity of FASN to produce the phospholipids that will form the newly synthesized membrane. As a consequence of FASN inhibition there is a lack on phospholipids, which induces apoptosis in cancer cells[107,108].

Disturbance of membrane and protein localization function. Lipid rafts are localized regions that contain high concentrations of lipids such as palmitate, cholesterol, and sphingosine, and also are rich in lipid-modified membrane-associated proteins that function in receiving, localizing, and transmitting cell growth signals[109,110]. Several receptors, such are the HER family, are localized in the lipid raft of the membrane. The lack of phospholipids disrupts lipid raft assembling, impairing the correct localization or function of these receptors. Furthermore, they serve as substrates for post-translational protein modification that affect protein localization and activity[65].

Inhibition of DNA replication. The lack of phospholipids, important for the preparation of cell division, blocks the cell cycle before G1 and impedes cell division[78].

p53-regulated non-genotoxic metabolic stress. FASN inhibitors are more effective at initiating apoptosis in tumor cells with non-functioning p53, whereas cells with intact p53 function tend to exhibit cytostatic responses[96]

Toxic accumulation of substrates. FASN inhibition causes toxic accumulation of its

substrate, malonyl-CoA. Malonyl-CoA inhibits carnitine palmitoyltransferase 1 (CPT1), which in turn inhibits the β-oxidation promoting the accumulation of the sphingolipid ceramide. The accumulation of ceramide is followed by the induction of the pro-apoptotic genes involved in the ceramide-mediated apoptotic pathway[111].

Inhibition of proliferative pathways. Inhibition of FASN results in the downregulation of AKT, which precedes the induction of tumor cell apoptosis[112,113].

The first FASN inhibitor that showed cytotoxicity in cell lines *in vitro* and *in vivo* was a molecule isolated from *Cephalosporium cearulens*, called **cerulenin**[81,114]. Clinical application were limited because the chemical instability caused by its very reactive epoxy group[82]. To overcome chemical instability, **C75** cerulenin-derived was designed lacking the epoxy group. **C75** showed tumor growth inhibition in xenograft prostate, breast, mesothelioma, lung and ovarian cancer models[83,95,115]. Clinical application is limited because induces rapid weight loss and affects food intake[116]. Weight loss occurs through activation of fatty acid oxidation in the mitochondria via stimulation of CPT1 (even in the presence of inhibitory concentrations of malonyl-CoA), and through the inducement of anorexia via inhibition of neuropeptide Y production within the hypothalamus[116].

EGCG is the main catechin found in green tea. It is a powerful antioxidant, and has been described to have preventive effect and anti-proliferative activity through the induction of apoptosis[167-172]. Although **EGCG** is a non-specific inhibitor targeting multiple signaling pathways[174], its apoptosis-inducing effect seems to correlate with FASN inhibition[167]. **EGCG** induces apoptosis and inhibit HER1-HER2, MAPK and AKT activity in cancer cells[83,175-179]. The high concentrations needed and its poor oral bioavailability and relative instability in physiological conditions limit its clinic application.

Based on the chemical structure of **EGCG**, our group have developed a new series of polyphenolic derivatives, which resulted in the identification of a new potent inhibitor named **G28UCM**[88,113] (in this thesis G28). This compound showed strong FASN activity inhibition (90%) and cancer cell cytotoxicity in a panel of human breast cancer cells. In vivo, showed marked tumor volume reduction without weight loss or anorexia[88]. **G28UCM** showed to induce apoptosis and tumor reduction in HER2+ breast cancer xenograft and in HER2+ resistant cell lines[89,99].

3.4. Fatty Acid Synthase in Breast Cancer

Fatty acid synthase expression and inhibition has been widely studied in several cancers, including breast cancer. A link between HER2+ breast cancer and FASN overexpression have been described[72], and its inhibition have been demonstrated to be effective to overcome HER2 therapies resistance[99]. On the other hand, FASN expression is not limited to this type of cancer as its activity has also been described in various cell lines, including hormone-dependent and hormone-independent[100,108,117,118]. Some of the FASN inhibitors mentioned beforehand have been tested in different models of breast cancer.

The study of FASN expression and its potential as a feasible target in TNBC has become a field of interest in the last years, and few studies have been published[119–123].

Table 4. Summary of the FASN inhibitors and their principal characteristics[81–94]

		Origin - type of inhibitor	Inhibition mechanisms	Limitations
Early Generation	**Cerulenin**	*Cephalosporium caerulens*	Covalent binding to KS domain	Limited biodisponabilty - chemical inestability
	C75	cerulenin-derived	Inhibition of KS, ER and TE domains	The off-target timulation of CPT-1 induces anorexia
	C93	cerulenin-derived	KS inhibition, malonil CoA analogy	*not described*
	Orlistat	β-lactone	irreversible inhibition of the TE domain	Poor solubility and cell permeability, low bioavailability and poor metabolic stability
	Triclosan	antibiotic - synthetic inhibitor	Blocks the ER domain	*not described*
	EGCG	Natural component of the green tea	Blocks the KS domain	Poor oral bioavailability and low stability in physiological conditions

		Origin - type of inhibitor	Inhibition mechanisms	anti-cancer activity
New Generation	**G28UCM**	EGCG -derived	*not described*	Strong *in vitro* inhibition in cancer cells. Preliminar in vivo studies show a decrease in tumor growth and no side-effects
	GSK 2194069	*not described*	KS domain inhibition	- *In vitro* and *in vivo* studies show strong inhibition and no side effects in mice
	JNJ- 54302833	Spirocyclic imidazolinone analog	KR domain inhibition	- Strong proliferation inhibition *in vitro* in ovarian and prostate cell lines. Shows good bioavailabilty and selectivity in lung xenografts *in vivo* .
	IPI-9119	β-lactone analog	irreversible inhibition of the TE domain	- Strong biochemical inhibition *in vitro* .Orally bioavailable and show pharmacokinetic propierties suitable for *in vivo* studies. Preliminar studies *in vivo* and *in vitro* show no anti-proliferative effect in cancer models.
	TVB-2640	Small-molecule reversible inhibitor	*not described*	- The first FASN inhibitor tested in patients. Stable disease progression has been observed in monotherapy, and in combination with paclitaxel in lung and breast cancer patients.

4. Epidermal Growth Factor Receptor

Receptor tyrosine kinases determine various cell cellular functions such are growth, differentiation, cell motility or survival (reviewed in Van der Geer *et al.,* 1994 [124]). The ErbB/HER family of the tyrosine kinase receptors is ubiquitously expressed in epithelial, mesenchymal, neuronal cells and their cellular progenitors[125].The deregulation of this tightly controlled system by overexpression, amplification, mutation on critical pathway elements can lead to a hiperproliferative disease such as cancer[126].

The epidermal growth factor receptor (EGFR, also known as ERBB, ERBB1 or HER1) belongs the he ErbB/HER family protein-tyrosin kinases. This 170 kDa receptor consist of a glycosylated extracellular domain, a single transmembrane segment, and an intracellular portion that have a juxtamembrane segment, a protein kinase domain and a carboxyterminal tail. Seven ligands haven been described to bind EGFR: Epidermal growth factor (EGF), epigen (EPG), transforming growth factor-alfa (TGF-α), amphiregulin (AmR), betacellulin (BTC), heparin-binding epidermal growth–factor like growth factor (HG-EGF) and epiregulin (EPR). Like all the protein-tyrosine kinase receptors, ErbB family function mainly as dimers. EGFR can form homodimers or heterodimers with all the other members of the ErbB family[127]. In the general mechanism for the activation of receptor protein-tyrosine kinases, activating ligands or growth factors bind to the extracellular domains of two receptors and induce the formation of an activated dimerization state[16]. Once activated, the signal transduction cascades of these receptors promote cellular proliferation and survival through a highly diverse repertoire of cellular signalling pathways, such as the RAS-MAPK pathway or PI3K/AKT/mTOR pathway[128] (Figure 6).

4.1. Epidermal Growth Factor Receptor Inhibition

EGFR over-expression has been linked to tumour initiation and progression in cancer. For that reason, several strategies have been developed to target HER receptors. Those strategies can be divided in antibody-based therapies using monoclonal antibodies against the extracellular domain of these receptors, and small molecule tyrosine kinase inhibitors (TKIs) against the intracellular kinase domain[129] (Figure 6).

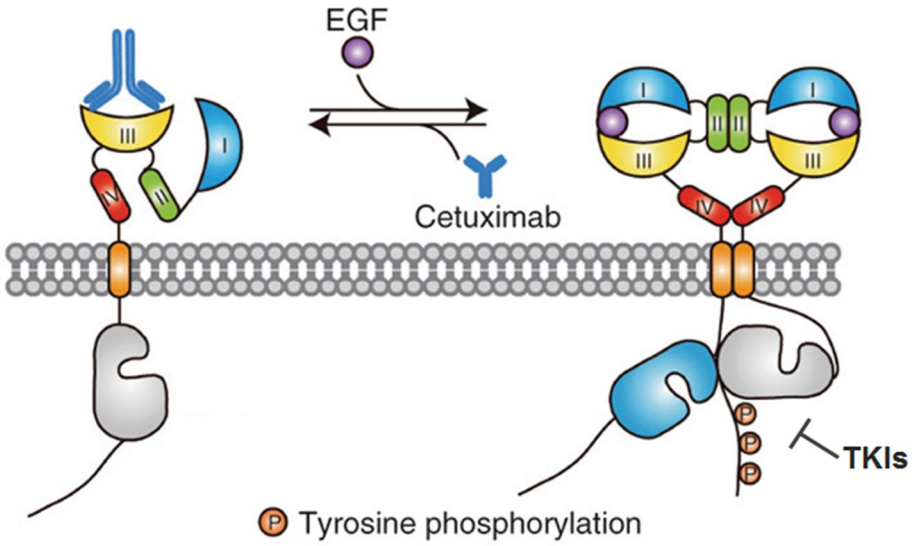

Figure 6. Activation and inhibition mechanisms for the Epidermal Growth Factor Receptor (EGFR). EGF binding to the extracellular domain initiates formation of a specific receptor-mediated dimer and activation of the intracellular kinase domain through formation of an asymmetric dimer. Cetuximab binding impedes EGF activation of the receptor keeping it at tis inactive conformation. Tirosin Kinsase Inhibitors (TKIs) compete with the ATP binding site and avoid consequent signal transduction activation. Modified from Wang, Z *et al.*, 2011[130].

Cetuximab, is a chimeric (human/mouse) immunoglobulin monoclonal antibody that targets the ligand-binding domain of the EGFR, blocking receptor activation and subsequent signal-transduction events that lead to cell proliferation or angiogenesis and inducing apoptosis[131,132]. Furthermore, cetuximab induces receptor downregulation through its initial dimerization and internalisation [132]. Cetuximab is currently used in the treatment of colon, lung, and head and neck cancers[127,132].

Lapatinib is a small molecule that binds at the tyrosine kinase domain of the EGFR and HER2 receptors competing with ATP and avoiding consequent signal transduction activation[133]. It is approved for the treatment of breast cancer with HER2 overexpression.

Erlotinib and **Gefitinib**, are also TKIs that bind in the tyrosine kinase domain of the EGFR receptor and are used for the treatment of breast and lung cancer.

4.2. Epidermal Growth Factor Receptor in Breast Cancer

The EGFR was the first tyrosine-kinase receptor to be linked directly to human tumors[127]. This receptor plays an important role in the pathogenesis of many lung cancers (60% of cancer express EGFR)[134], colon cancers and head and neck cancer[127]. In breast cancer, between 50-70% of TNBC have been shown to express the epidermal growth factor receptor[39,49] and it expression has been associated with poor prognosis[135,136]. More accurately, EGFR expression is linked to the basal-like intrinsic subtype[39]. While EGFR inhibition has been considered a promising approach for TNBC, minimum benefit has been observed in the clinical settings alone or in combination with chemotherapy. Two completed trials investigated the addition of the monoclonal anti-EGFR antibody cetuximab to a platinum-crosslinking agent in metastatic TNBC[49]. In TBCRC001, the response rates of patients treated with cetuximab alone or in combination with carboplatin were relatively low at 6% and 17%, respectively[137]. The BALI-1 trial demonstrated that the addition of cetuximab to cisplatin increased overall response rate of TNBC patients from 10% to 20%[138]. However, the combinations minimally increased DFS or OS. These results prompted for the investigation of other therapeutic strategies for TNBC patients.

5. Cancer Stem Cells

Stem cells are defined as cells that have the ability to perpetuate themselves through self-renewal and to generate mature cells of a particular tissue through differentiation[139]. These cells are a rare population within the tissue.

The classical model to explain tumorigenesis was based on the intrinsic heterogeneity of the tumor, in which each of these cells has the potential to form new tumors (Figure 7A). However, in solid tumors, only a small proportion of cells are able to form colonies *in vitro*, and able to trigger tumorigenesis *in vivo*[140]. These small populations of cells, identified as Cancer Stem Cells (CSCs), are a rare, phenotypically distinct subset of cells that have the ability to proliferate forming solid tumors whereas most cells are depleted of this ability (Figure 7B).

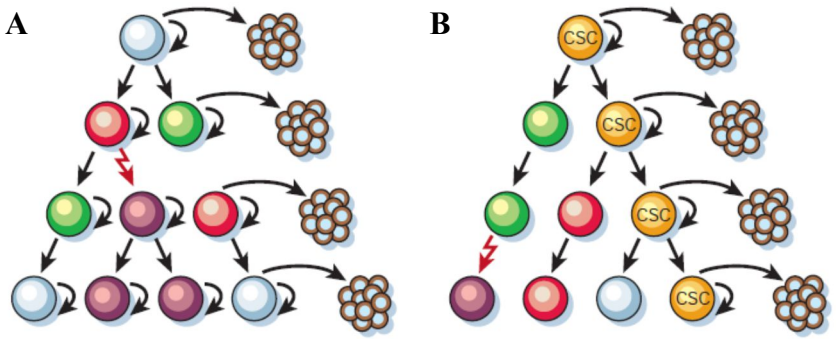

Figure 7. Two general models of heterogeneity in solid cancer cells. **A.** Cancer cells of many different phenotypes have the potential to proliferate extensively, but any one cell would have a low probability of exhibiting this potential in an assay of clonogenicity or tumorigenicity. **B.** Most cancer cells have only limited proliferative potential, but a subset of cancer cells consistently proliferate extensively in clonogenic assays and can form new tumours on transplantation. Taken from *Reya et al. 2001*[139].

In vitro, CSC enriched population exhibit specific properties: cell-surface specific marker profiles ($CD44^{high}/CD24^{low}$)[140], the ability to grow in non-adherent conditions forming mammospheres[141], activation of the ALDH enzyme [142,143] and also increased resistance to general chemotherapy[144,145].

In vivo, the most common way to determine the frequency of self-renewing cells within a tumor is a limiting dilution cell transplantation assay, in which tumor cells are transplanted into recipient animals at increasing doses; the proportion of animals that develop tumors is used the calculate the number of self-renewing cells within the original tumor sample. Those tumors recapitulate the morphologic heterogeneity of the

original tumor [146,147].

Al-Hajj *et al.* were the first to describe the tumorigenic properties of the population isolated using the cell surface markers $CD44^{high}/CD24^{low}$ from breast cancer patients. While only 100 cells with this phenotype were able to form tumors in mice, tens of thousands failed to grow tumors *in vivo*[140]. Although the use of this phenotype is widely used to identify stem cell enriched population, some studies show controversial results(reviewed in [148,149]). Therefore, additional markers are now been taken into account, such as CD15 (SSEA-1, Lewis X), CD133 (prominin- 1), and CD166 (ALCAM) to better identify CSC enriched population [150],

Dontu *et al.* were the first in developing an *in vitro* method that allowed the propagation of human mammary epithelial cells in an undifferentiated state, based on their ability to proliferate in suspension. This cells were able to grow in nonadherent conditions, forming mammospheres[141]. They also demonstrated that this population was enriched in stem cells, as this cells were able to differentiate in different mammary lineages and form complex and functional 3D structures[141]. Not all cells lines show the ability to form mammosphere, and different shapes and ratios differ widely among them[151–153].

Aldehyde dehydrogenases (ALDH) belong to the oxidoreductase family enzymes, which catalyze the conversion of aldehydes to their corresponding acids. ALDH1 oxidizes retinoil to retinoic acid, which is a modulator of cell proliferation. For that reason, ALDH1 might have a role in early differentiation and stem cell proliferation[154,155]. Several studies have shown that ALDH1 activity works as a marker for the identification of non-neoplastic stem cells and CSCs, including breast cancer[143,150,155].The most universal kit to detect ALDH1 activity is the ALDEFLUOR kit. This kit uses the BODIPY aminoacetaldehyde, which is converted to the fluorescent product BODIPY aminoacetate by ALDH activity. These cell populations, which are known as ALDH bright ($ALDH^{br}$) cells can be isolated from adult tissues or cell lines by flow cytometry.

5.1. Cancer Stem Cells and Chemoresitance

The standard care for tumor treatment is based in conventional and targeted therapies. Even their application sometimes succeeds in reducing tumor volume and improve survival, many patients relapse within few years. Tumor heterogeneity plays an important role in relapse afther therapy, because while many cells perish during the treatment, some survive to chemotherapy exposure and contribute to disease progression. Recent studies showed that chemo-resistance –and so recurrence- can be achieved by a unique cell niche with higher resistance to chemotherapeutic agents and with stemness features [32,156,157] (Figure 8). For instance, higher mammosphere-forming index and $CD44^{high}/CD24^{low}$ frequencies were observed in tumor patients treated with chemotherapy compared to the untreated ones[158,159]. ALDH-positive cells in axillary lymph-node metastases after chemotherapy has also been associated with disease recurrence[160]. In addition, *Creighton et al*., defined a gene expression signature common to both $CD44^{high}/CD24^{low}$ and Mammospehre-forming cells. In their study, they determined that tumor cells surviving after conventional treatments were enriched for this specific gene-signature[32].

Preclinical models also showed an increase of CSC phenotype after therapy in both cell lines[159,161] and xenograft models[162].

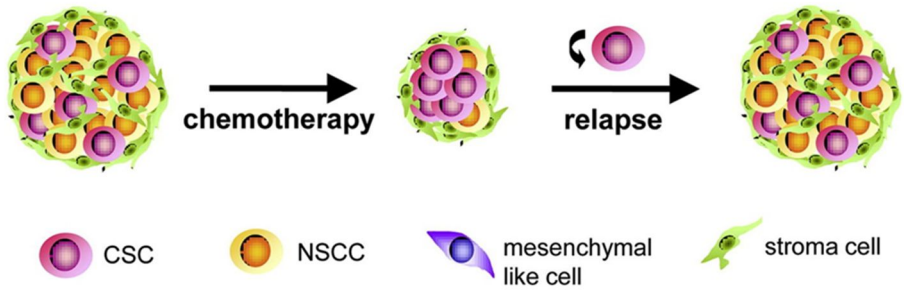

Figure 8. Cancer Stem Cells intrinsic chemo-resistance might be the responsible of relapse after therapy treatment. Modified from Muñoz *et al.,* 2012[163].

5.2. Epithelial-Mesenchymal Transition and Cancer Stem Cells

Epithelial-to-Mesenchymal Transition (EMT) is an evolutionarily conserved developmental process[164]. Conventionally, epithelial cells are defined as surface barrier

that display distinct apical versus basolateral polarity established by adherent and tight junctions. Mesenchymal cells serve scaffolding or anchoring functions and have multifunctional roles in tissue repair and wound healing. During embryonic development, certain differentiated cells undergo profound morphogenetic changes, resulting in the formation of migratory mesenchymal cells with invasive properties[165]. This process is referred as EMT. Then, these mesenchymal cells are recruited to specific sites in the developing embryo where they can differentiate.

EMT is characterized by cellular and molecular changes such as (1) loss of cell-cell adhesion and apical-basal polarity involving E-cadherin, occludins and claudins in cell-cell junctions; (2) downregulation of epithelial cytokeratins (CK8, CK18, and CK19); (3) upregulation of mesenchymal proteins such as vimentin; (4) reorganization of cytoskeleton to acquire more spindle-like morphology; (5) increased motility and invasiveness and (6) resistance to apoptosis.

The process of EMT involves the coordination of a complex network. EMT can be induced *in vitro* under the influence of extracellular matrix components and growth factors, such as TGF-β growth factor[166,167]. Wnt, Hedgehog and Notch are also signal transduction pathways that can also coordinate EMT programs[168]. A number of transcription factors induce EMT through transcriptional control of E-cadherin, including snail, slug zeb1, zeb2, and twist among others[169].

The EMT process is also reactivated in a variety of diseases including tumor progression[166]. In summary, cell plasticity plays a crucial role in resistance acquisition to chemotherapy, as cells undergoing EMT acquire stem cells features[170–173]. The reversion of some cells to a CSC-like phenotype provides an association between EMT, CSCs and drug resistance[165].

Targeting CSCs constitute a new challenge and a unique therapeutic opportunity to improve the efficacy of chemotherapy and suppress acquired resistance (reviewed in Vidal SJ *et al.*, 2013 [157]).

5.3. Triple-Negative Breast Cancer and Cancer Stem Cells

The two main molecular subtypes represented in the TNBC are basal-like and claudin-low (also refered as ML in this thesis) in that order. Prat *et al.* described claudin-low molecular subtype to have specific characteristics such as low expression of genes related to cell-cell adhesion proteins (claudin genes) and enrichment with mesenchymal genes (vimentin, N-cadherin and TWIST for example), features linked to the induction of EMT[29]. In addition, the gene signature obtained from the $CD44^{high}/CD24^{low}$ and Mammosphere was found mainly in this subtype of cancer[32].

Hypothesis and Objectives

Hypothesis

De novo lipogenesis is a mechanism activated in Triple-Negative Breast Cancer (TNBC) and therefore its inhibition through Fatty Acid Synthase (FASN) blockade activity may be a feasible new strategy (alone or in combination) for the treatment of patients with primary triple-negative breast cancer or for those who progressed after therapy.

Objectives

The main objective of this thesis was to determine the role of Fatty Acid Synthase in TNBC assessed by expression and inhibition analysis in sensitive and resistant TNBC pre-clinical models (cellular and animal models) and a large cohort of tumor patient samples.

In order to accomplish the main objective, three specific objectives were described:

1. **Pre-Clinical Evaluation of Fatty Acid Synthase Expression and Inhibition in combination with EGFR inhibitors in sensitive and resistant TNBC.**

    - Develop and characterize TNBC cell lines resistant to chemotherapy (doxorubicin) representing the two major molecular subtypes in TNBC (Basal-like and Mesenchyma-like).
    - Evaluate the implications of FASN blockade assessed by cell proliferation inhibition alone or in combination with doxorubicin or cetuximab (an EGFR inhibitor) in TNBC cell lines sensible or resistant to general chemotherapy.
    - Analyze the antitumor activity of FASN inhibitor (EGCG) in combination with EGFR inhibitor (cetuximab) in different orthoxenograft models using sensitive and resistant cell lines (231, 231**DXR**, HCC, HCC**DXR**).
    - Study the molecular interactions of FASN inhibition, alone and in combination with cetuximab.
    - Determine FASN and EGFR expression in a small cohort of TNBC patient tumor tissue samples.

2. **FASN and EGFR expression in TNBC patients and its correlation with Clinical and histological characteristics.**

- Evaluate FASN expression in a large cohort of TNBC tumor samples (n=100) by IHC.
- Determine the association of FASN tumor tissue expression with clinicopathological features in TNBC.
- Determine the association of FASN tumor tissue expression with molecular subtypes of TNBC assessed by IHC.
- Study the association of FASN expression with overall survival and disease free survival.
- Evaluate EGFR expression and its relationship to DFS and OS in our cohort of TNBC patients in order to compare with other studies.

3. **Cancer stem cells and FASN implication in chemoresitance acquisition in a mesenchymal-like cell line sensitive and resistant to chemotherapy**

- Evaluate CSCs implication in resistance acquisition to chemotherapy in a sensitive and a resistant triple-negative breast cancer cell line with Mesenchymal-like molecular subtype.
- Study FASN inhibition implication in the CSC enriched population in a sensitive and a resistant Mesenchymal-like cell line.

Materials and Methods

1. Cell culture and development of doxorubicin-resistant triple-negative breast cancer cells

All triple-negative breast cancer cells were obtained from ATCC (Manassas, VA, USA). MDA-MB-231, MDA-MB-468 and MDA-MB-157 were routinely grown in DMEM (Gibco). HCC1806, DU4475 and BT549 were maintained with RPMI. Cell culture media were supplemented with 10% FBS (HyClone Laboratories) 1% L-glutamine (Gibco), 1% Sodium pyruvate (Gibco), 50 U/ml Pen/Strep (Linus). RPMI was additionally supplemented with 0.023 IU/ml insulin for BT549 culture. Cell lines were kept at 37ºC and 5%CO_2 atmosphere. Doxorubicin-resistant cells MDA-MB-231 (231**DXR**) and HCC1806 (HCC**DXR**) were developed using a stepwise selection method (Figure 9). Increasing doses of doxorubicin (TEDEC-Meiji Farma) were performed until their corresponding IC_{50} was reached. Briefly, initially cells were treated with a concentration of doxorubicin of 0,1xIC_{50}. After 48h, the treatment medium was replaced for fresh medium. When the cells were capable of growing and reached appropriate confluence, they were treated with double the previous doxorubicin concentration for 48h. The stepwise selection method was subsequently performed until the final concentration of doxorubicin achieved the parental IC_{50}. It took around 6 month for each cell line. Resistance was confirmed by cell viability assay.

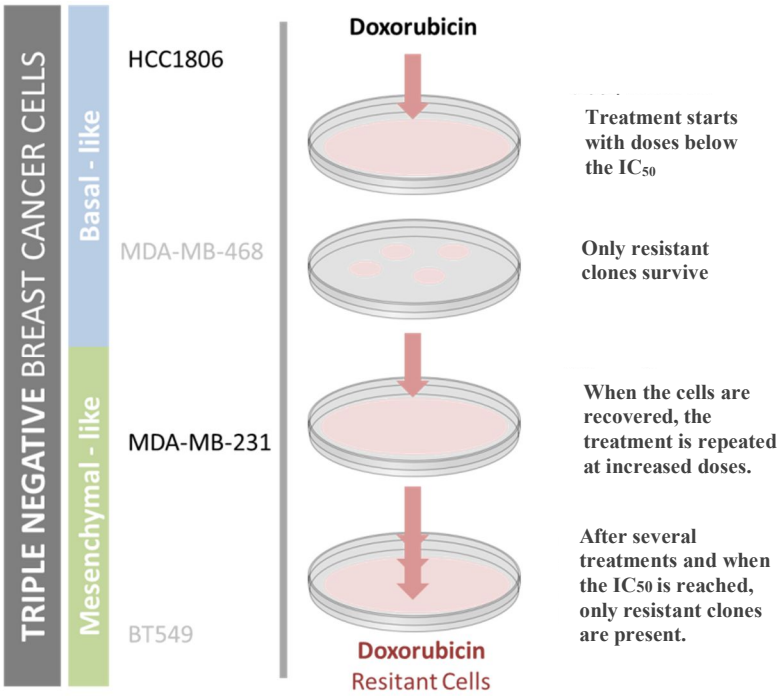

Figure 9. Development of doxorubicin-resistant cell lines.

2. Western blot analysis of cell and tumor lysates

Parental and resistant TNBC cells were synchronized by starvation in serum-deprived medium (0.5% FBS) for 24 hours. Cells were lysed in ice-cold lysis buffer (Cell Signaling Technology, Inc.) with 100 µg/mL PMSF by vortexing every 5min for 30 min. Frozen tumors were first ground (Dounce) in ice-cold lysis buffer and then vortexed as described above. Equal amounts of protein were heated in LDS Sample Buffer with Sample Reducing Agent (Invitrogen) for 10 min at 70°C, electrophoresed on SDS-polyacrylamide gel (SDS-PAGE), and transferred onto nitrocellulose membranes. Blots were incubated for 1h in blocking buffer (5% powdered-skim milk in Phosphate-buffered saline 0.05% Tween (PBS-T)) and incubated overnight at 4°C with the appropriate primary antibodies (Table 5) diluted in blocking buffer. Specific horseradish peroxidase (HRP)-conjugated secondary antibodies were incubated for 1h at room temperature. The immune complexes were detected using a chemiluminescent HPR substrate [Super Signal West Femto (Thermo Scientific Inc.) or Immobilon Western (Millipore)]. β-actin (Santa Cruz Biotechnology Inc.) was used as a control of protein loading. Western blot analyses were repeated at least three times and representative results are shown.

Table 5. Antibody description

Antibody	# Ref	Supplier	Dilution	Source
FASN	ADI-905-069-100	EnzoLife Sciences	1:1500	rabbit
EGFR	2231	CellSignaling	1:1000	rabbit
p-EGFR	2234	CellSignaling	1:500	rabbit
AKT	9272	CellSignaling	1:1000	rabbit
p-AKT	4058	CellSignaling	1:500	rabbit
ERK1/2	9102	CellSignaling	1:1000	rabbit
p-ERK1/2	9106	CellSignaling	1:500	mouse
mTOR	2983	CellSignaling	1:1000	rabbit
p-mTOR	2971	CellSignaling	1:1000	rabbit
p-S6	2211	CellSignaling	1:1000	rabbit
Pi3K	4249	CellSignaling	1:1000	rabbit
p-Pi3K	4228	CellSignaling	1:1000	rabbit
PTEN	5384	CellSignaling	1:1000	rabbit
β-actin	Sc-47778	Santa Cruz Inc	1:1000	mouse

3. Cell viability assays

Parental and resistant cells were plated in 96-well plates at a cell density of 4 x 10^3 cells per well in their corresponding growth medium. After 24 hours, growth medium was removed and 100 µL of fresh medium containing the corresponding concentration of doxorubicin(TEDEC-Meiji Farma), EGFR inhibitor [cetuximab (erbitux®, Merck)], or FASN inhibitors [EGCG (Sigma) or C75 (Sigma)] were added to each well. For drug-combination experiments cells were treated with a fixed FASN inhibitor concentration in combination with a serial of concentrations of (i) doxorubicin for 48 h or (ii) cetuximab for 4 days. Same treatments were assessed in monotherapy. Following treatment, cell viability was measured using the standard colorimetric MTT assay as previously described[99]. Combinatorial effects were evaluated using the Interaction index (Ix) = ∑(% CPI drug alone) / % CPI combination. Ix <1, synergism; Ix =1, additivism and Ix >1, antagonism.

4. Quantitative real-time PCR analysis

Cells were PBS washed, and then 1mL of Qiazol (Qiagen) was added. Total-RNA was isolated using RNeasy mini kit (Qiagen) following the instructions provided by the manufacturer. RNA was reverse-transcribed into complementary DNA (cDNA) using High Capacity cDNA Archive Kit (Applied Biosystems). Gene expression levels of EGFR and FASN were assessed using LightCycler® 480 Real-time PCR System (Roche) with LightCycler® 480 SYBR Green I Master (Roche). Primers used are described in Table 6. RT-PCR analyses were performed at least three times and each gene was run in triplicate. β-actin or PP1A was used for normalization.

Table 6. Primer design

EGFR	Fw	CATGTCGATGGACTTCCAGA
	Rv	GGGACAGCTTGGATCACACT
FASN	Fw	CAGGCACACACGATGGAC
	Rv	CGGAGTGAATCTGGGTTGAT
Snail	Fw	GCTGCAGGACTCTAATCCAGA
	Rv	ATCTCCGGAGGTGGGATG
Vimentin	Fw	TGGTCTAACGGTTTCCCCTA
	Rv	GACCTCGGAGCGAGAGTG
β-actin	Fw	ATTGGCAATGAGCGGTTC
	Rv	CGTGGATGCCACAGGACT

5. *In vivo* studies: orthoxenografts experiments

TNBC cell lines HCC1806 and MDA-MB-231 and their doxorubicin-resistant derivatives 231**DXR** and HCC**DXR** were orthotopically implanted ($2x10^6$ cells in 25µl matrigel) into both inguinal cleared mammary fat pads of NRG (NOD-Rag1<null> IL2rg<null>) mice (The Jackson Laboratory). When tumors reached 15 mm^3, animals were randomized into four different treatment groups. Each group received intraperitoneal (i.p.) injection of control (vehicle alone, 3d/wk), 30 mg/kg EGCG 3d/wk, 0.5mg/mice cetuximab 1d/w, or combination of EGCG + cetuximab. Tumor xenografts were measured with calipers and tumor volumes were determined using the formula: (π/6 x (v1 x v2 x v2)), where v1 represents the largest tumor diameter, and v2 the smallest one. Body weight was registered every two days. At the end of the experiment or when tumors reached 1 cm in diameter, animals were weighed and then euthanized using CO_2 inhalation. Tumors were stored at -80ºC. Apoptosis in control and treated tumors was analyzed by Western-blot (PARP). *In vivo* mouse experiments were performed in Dr. A. Welm's laboratory at the Huntsman Cancer Institute (University of Utah, Salt Lake City, Utah, USA) and at the Oklahoma Medial Research Foundation (ORMF, Oklahoma, USA). All protocols and experiments involving animals, including care and handling, were conducted in accordance with guidelines on animal care and use established by institutional guidelines. All mice were maintained in a specific pathogen-free facility with controlled light/dark cycle, temperature, and humidity. All surgery was performed under inhaled isoflurane anesthesia; burprenorphine was administered as analgesic to mice after surgery. All efforts were made to minimize pain and distress.

6. Patients and tissue samples

Core-biopsy study

FASN and EGFR tumor expression levels were retrospectively evaluated in paraffin-embedded core-biopsies of 29 patients with TNBC diagnosed in the Hospital Josep Trueta of Girona between 2007 and 2012.

Tissue microarray study

The study group consisted of 100 patients with primary triple-negative breast cancer (TNBC) diagnosed between 1990 and 2012 at Hospital Universitari Dr.Josep Trueta (Girona, Spain). For each patient clinical and histopathological feature were obtained from medical records: age, stage, surgery, chemotherapy, relapse, histological grade, lymph node involvement and Ki-67 grade. Stage was determined according TNM classification (7th edition of AJCC cancer staging manual[174]). Histological grade was defined using Bloom-Richarson grading system. FASN, Cytokeratins 5/6, EGFR and Vimentin expression were evaluated on tissue microarrays (TMA) containing tissue sections of patients' primary tumour obtained by surgery. Analysis was carried out by two board-certified pathologists. The protocol was approved by the Institutional Review Board of Dr. Josep Trueta Hospital and an informed written consent was obtained from the patients included in the study.

7. Construction of Tissue Microarrays (TMA)

A representative tumor area was selected from an H&E section. Then, the corresponding area was precisely punched out from the donor block into a recipient block using Galileo TMA CK3500 Platform and IseTMA software (Integrated System Engineering). From each patient's tissue block, four tumoral cores and one non-tumoral peripherical core of 1mm were extracted and placed into an 8×5 recipient block. Each TMA contained 8 blocks, each one from a diferent patient (Figure 10). All samples were histologically reassessed by the pathologist to verify tumoral and non-tumoral spots before IMC analysis. All tumor spots included in the study contained more than 50% tumor cells.

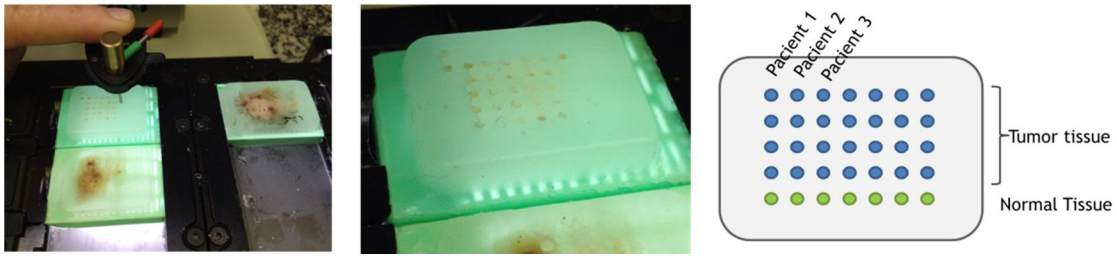

Figure 10. Tissue microarray construction and design.

8. Immunohistochemistry on core-biopsies and TMA

Immunohistochemical staining was performed on formalin-fixed, paraffin-embedded tissue TMA sections. Briefly, 3 µm-thick TMA tissue sections were placed onto adhesive slides and treated with the PT link (DAKO) solution at high pH as a deparaffination and antigen retrieval steps. Immunohistochemical staining was performed using the following primary antibodies : anti-Fatty Acid Synthase polyclonal antibody (dilution 1:100, Enzo Life Sciences), anti-EGFR monoclonal antibody (dilution 1:100, clone D38B1CellSignaling), anti-Cytokeratin 5/6 monoclonal antibody (dilution 1:50/100, Clone D5/16 B4, DAKO) anti Monoclonal Mouse Anti-Vimentin (dilution 1:100/200, Clone Vim 3B4, DAKO). Negative control, using mouse or rabbit IgG at a comparable concentration in place of the primary antibody was also carried out. Sections were washed with PBS and sequentially incubated at room temperature for 45 minutes with antirabbit or antimouse IgG. Immunodetection was performed with the kit EnVision™ (DAKO, Glostrup, Denmark) using the AutostainerPlus Link (DAKO).

9. Interpretation of immunohistochemical staining

FASN staining was scaled from 0 to 3: 0, no staining; 1, low staining; 2, moderate staining; and 3, high staining and was determined both in tumoral spots and non-tumoral, peripherical tissue. For analytical purposes patients with 0-1 FASN staining were grouped as low-FASN expression and patients with 2-3 FASN staining were grouped as high-FASN expression. EGFR staining was classified as positive when staining of >1% of the cells (membrane stained or both membrane and cytoplasm) or negative (only cytoplasm stained)[175]. When positive, EGFR expression was scaled from 1+ to 3+. Cytokeratin 5/6 expression was classified as positive when staining of >1% of the cells (cytoplasmic and/or membranous staining)[175]. Vimentin expression was classified as positive when >50% of the tumoral cells were stained. Focal positive staining was also recorded when positivity was restricted to certain areas of the tissue.

10. Classification of TNBC patients in intrinsic subtypes

TNBC patients were stratified in Basal-Like (BL), Mesenchymal- Like (ML) and Non-BL/Non-ML (NonBLML). The classification of intrinsic subtypes was done according the expression of EGFR, Cytokeratin 5/6 and Vimentin by IHC. Patients with any degree of positive expression (even focal) for EGFR and/or Cytokeratin 5/6 were classified as Basal-Like as proposed by Nielsen and coworkers[39]. Patients with negative EGFR and Cytokeratin 5/6 expression and positive expression of Vimentin were classified as Mesenchymal-Like. Vimentin is regarded as a major and conventional canonical marker of EMT[166] and Mesenchymal-like tumors have been described to show higher Vimentin expression levels compared to Basal-like and other tumor subtypes[27,40,41]. Therefore, positive Vimentin expression was used to classify Non-Basal TNBC patients as Mesenchymal-like. If negative expression was obtained for these three proteins, patients were classified as Non-BL/Non-ML.

11. Mammosphere-forming assay

In order to evaluate CSC population, the mammosphere-forming technique was performed (Figure 11). After tripsinisation, cells were counted and seeded into a 6-well cell culture microplate coated with pHEMA using DMEM/F12 medium supplemented with B27, EGF and FGF (20ng/mL), 1% L-glutamine, 1% sodium pyruvate and 25U/mL penicillin and 25µg/mL streptomycin. Finally, cells were incubated for 5 or 7 days and mammospheres bigger than 50µm were counted using an inverted opical microscope. Mammosphere Forming Index (MFI) was calculated using the formula described in Figure 12A. For the mammosphere treatment experiments, doxorubicin was added in the seeding process. Mammosphere Forming Inhibition (MFIn) was calculated, as shown in the Figure 12B.

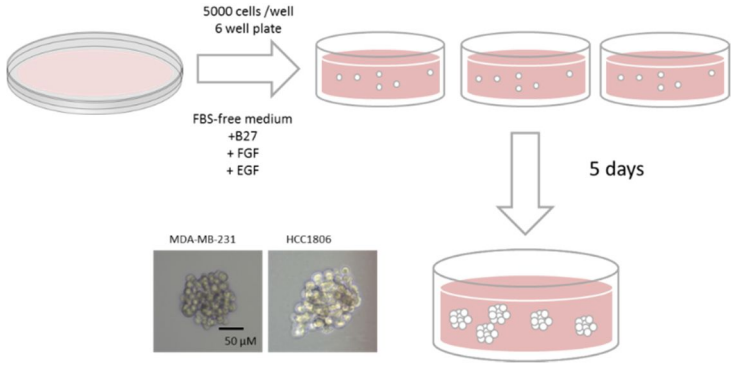

Figure 11. Mammosphere-forming assay protocol

A **B**

$$MFI = \frac{Nº\ mammosphere}{Nº\ cells\ plated} \cdot 100 \qquad MFIn = 100 - \frac{Nº\ mammospheres_{treatment}}{Nº\ mammospheres_{control}} \cdot 100$$

Figure 12. Formula used to obtain **A)** the Mammosphere Forming Index (MFI) and **B)** Mammosphere Forming Inhibition (MFIn)

12. Aldefluor assay

ALDH enzyme activity was determined using the Aldefluor™ kit (STEMCELL technology, France), according to the manufacturer instructions. Briefly, cells were tripsinized, counted, and 2.10^5 cells were separated for each condition to test. After washing them with PBS, 500mL of the buffer provided was added to each sample. Then 2.5µL of the reagent was added and immediately 250mL of the resuspension was moved to a new Eppendorf containing 2.5µl of the ALDH inhibitor DEAB. All samples were kept at 37ºC for 40 min. After a wash step, samples were ready to perform cytometry (FACSCalibur II, BD Bioscience). Images were obtained with FlowJo software.

13. Statistical analysis

Treatments and in vivo studies

Data were analyzed by Student's t-test when comparing two groups or ANOVA using a Bonferrony post-hoc test when comparing more than 2 groups. Non-Parametric analysis by Kruskal Wallis was used when data did not follow normal distribution. Statistical significant levels were $p < 0.05$ (denoted as *), $p < 0.01$ (denoted as **) and $p < 0.001$ (denoted as ***). P-value is shown in results when significance is reached ($p < 0.05$). All data are means ± standard error of the mean (SEM). All observations were confirmed by at least three independent experiments.

Patient related studies

Continuous variables were expressed as mean ± standard and compared using unpaired t-test or Mann-Whitney U-test according to the data distribution with or without normality. Categorical variables were presented as the number and percentage in each category and were compared as needed using χ^2 test or Fisher exact test. When

appropriate, Bonferroni test was used as a post hoc comparison test. Mantel-Haenszel test for linear trend was used to examine the relationship for ordinal variables.

Patients without available information on post-diagnosis relapse or survival status within at least 5-years after diagnosis were not included in the survival analysis. Relapse information was obtained from clinical records. Survival status was obtained from the Hospital Dr. Josep Trueta Cancer Register. The cut-off point for defining survival status was set at 30th September 2015. Overall survival (OS) was defined as the interval between the date of diagnosis and the date of patient death. Disease-free survival (DFS) was defined as the interval between the date of diagnosis and the date of patient's first local or distant relapse. Survival curves were estimated by the Kaplan–Meier method and survival differences between groups were determined via the log-rank test. Cox proportional hazard model was used to examine the effect of several clinical and histological variables on survival outcomes. Results are shown with estimated hazards ratios (HRs) and their 95% confidence intervals (CI). A p-value of <0.05 was considered statistically significant. All statistical analyses were performed with SPSS version 23.0 data analysis [176] and R software [177].

Results

1. Pre-Clinical Evaluation of Fatty Acid Synthase and EGFR Inhibition in TNBC

1.1. Triple-negative breast cancer cell lines express Fatty Acid Synthase (FASN) and are sensitive to FASN inhibitors

We screened several TNBC cell lines for FASN, EGFR and downstream protein expression and activation status (Figure 13A). Molecular classification of TNBC cells was assessed based on Lehman *et al.* [31]. Interestingly, FASN was detected in all TNBC cells examined, and showed higher protein expression levels in the basal-like than in the mesenchymal-like molecular subtype. Basal-like cell lines Du4475 and MDA-MB-468 showed the higher mRNA levels, while the other cell lines showed lower and similar FASN mRNA levels (Figure 13B upper pannel). Activation of the EGFR (as assessed by phosphorylation) was also observed in almost all cell lines. The EGFR mRNA and protein expression showed that MDA-MB-468 had the highest levels and Du4475 the lowest (Figure 13B lower pannel).

To further investigate the role of FASN as a target in TNBC, a cell proliferation inhibition (CPI) assay was performed using C75, EGCG and G28 as FASN inhibitors (Figure 13C). The most sensitive cell lines to C75 were the BL HCC1806 (IC_{50}: 29.4 ± 1.4μM) and MDA-MB-468 (IC_{50}: 31.38 ± 2.5 μM). Higher values of IC_{50} were obtained in the ML subgroup for the lines MDA-MB-231(IC_{50}: 46.6 ± 2.2 μM) and MDA-MB-157 (IC_{50}: 58.3 ± 2.75μM). EGCG showed IC_{50} values ranging from 149 ± 6.7 in MDA-MB-231 to 222 ± 6.7 in BT549. G28, the EGCG derived FASN-inhibitor, showed lower IC50 values compared to EGCG and C75, being the ML cell lines MDA-MB-231 (IC_{50}: 117 ± 11.6 μM) and MDA-MD-157 (IC_{50}: 62.5 ± 2.5 μM) the ones with higher IC_{50} values.

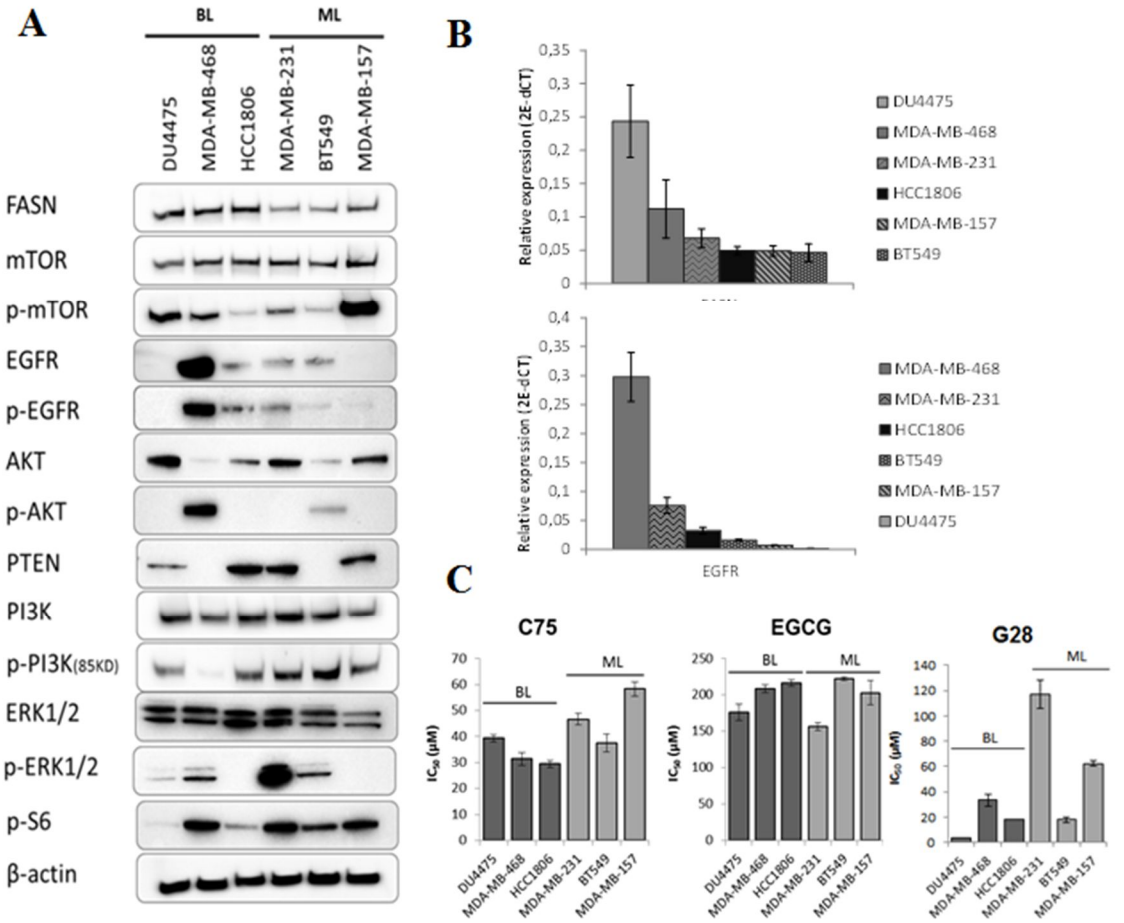

Figure 13. Characterization of different TNBC subtypes and doxorubicin-resistant TNBC cell models. (A) FASN, EGFR and downstream proteins expression and its activation status where analyzed by western-blot. Results shown are representative of those obtained from 3 independent experiments. **(B)** FASN (upper panel) and EGFR (lower panel) mRNA levels in a panel of TNBC cell lines. mRNA levels were obtained by Real-Time PCR and normalized against the β-actin gene. Results shown are mean ± SEM from 3 independent experiments. **(C)** IC_{50} values for the FASN inhibitors C75, EGCG and G28. Results shown are mean ± SEM from 3 independent experiments.

1.2. Doxorubicin-resistant TNBC cellular models are sensitive to FASN inhibitors

As preclinical models of acquired resistance to chemotherapy, we developed two TNBC cell lines resistant to doxorubicin. MDA-MB-231 (231) from the ML subgroup and the BL cell line HCC1806 (HCC) were chosen as two different models for FASN expression levels. 231 doxorubicin-resistant (231**DXR**) and HCC doxorubicin-resistant (HCC**DXR**) cells were developed in our laboratory by dose-increasing treatments of doxorubicin as described in 'Material and Methods' section. 231 and HCC were significantly more sensitive to doxorubicin for doses ranging from 10nM to 350nM compared to the resistant models 231**DXR** and HCC**DXR** respectively (Figure 14A). As shown in Figure 14B, 231**DXR** cells showed no apparent changes in either total protein or activation level in any of the proteins we examined related to the EGFR pathway. HCC**DXR,** however, showed increased expression levels of total EGFR, and the downstream proteins p-AKT and p-ERK1/2. On the other hand, p-EGFR levels decreased compared to the parental, consistent with previous findings showing doxorubicin directly decreases EGF expression[178]. FASN showed similar levels between the parental and resistant cells. Gene expression for FASN and EGFR proteins did not show any significant differences in 231 or HCC versus 231**DXR** and HCC**DXR,** respectively (Figure 14C,D). Interestingly, no changes in sensitivity to FASN inhibitors alone (C75, EGCG or G28) were observed between parental and doxorubicin resistant cell lines (Figure 15).

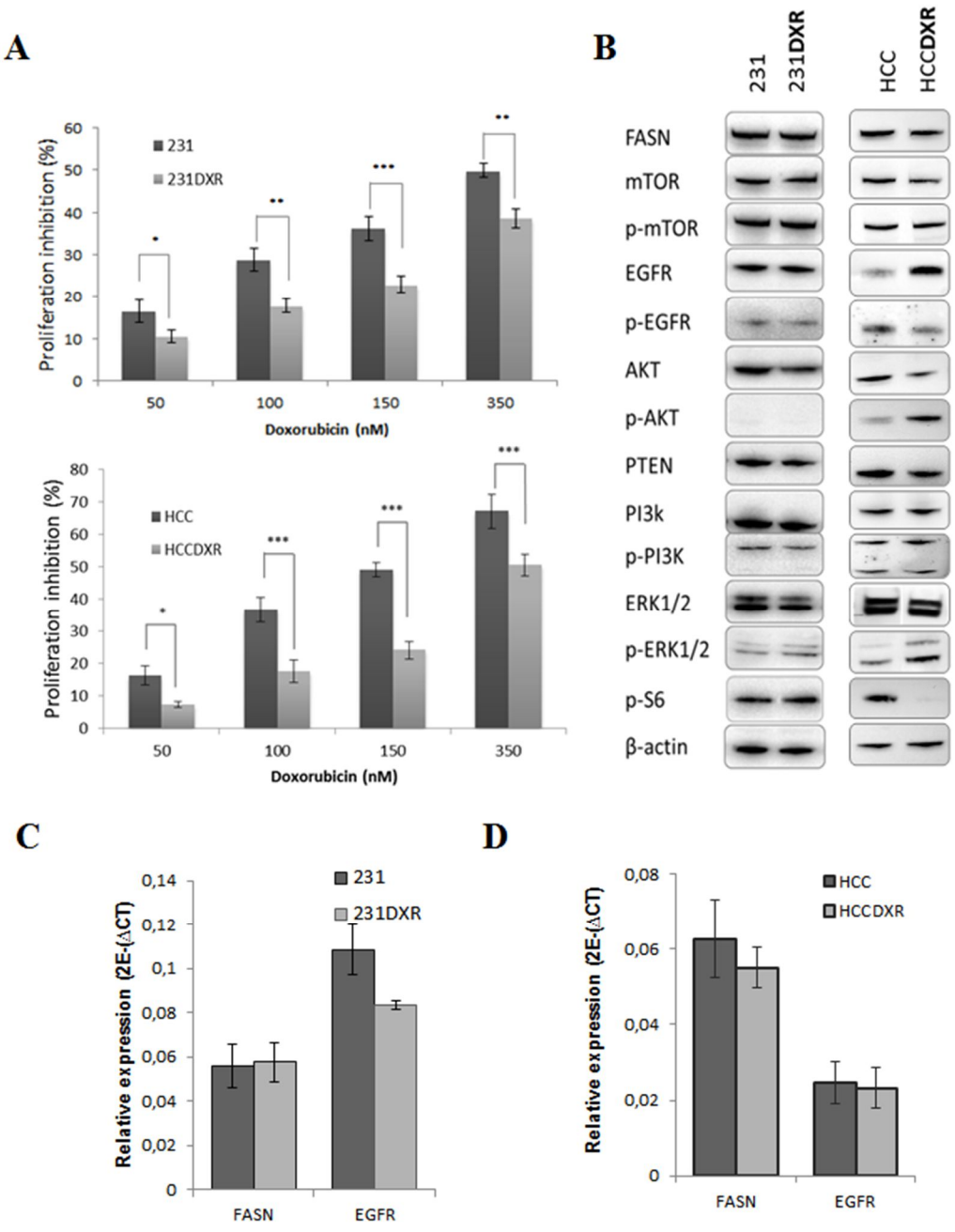

Figure 14. Characterization doxorubicin-resistant TNBC cell models. (A) Cell proliferation inhibition in parental and doxorubicin resistant derivate. 231 and 231**DXR** (upper panel) and HCC and HCC**DXR** cells (lower panel) were treated with increasing concentrations of doxorubicin (50 – 350 nM) for 48h. Experiments were performed at least three times in triplicate. **(B)** Characterization of MDA-MB-231 and HCC1806 doxoresistant models (231**DXR,** HCC**DXR**) and their corresponding parental cells (231, HCC) for FASN, EGFR and downstream proteins expression and its activation status by western-blot. Results shown are representative of those obtained from 3 independent experiments. FASN and EGFR mRNA levels for **(C)** 231 and 231**DXR** and **(D)** HCC and HCC**DXR**. Expressions levels were obtained by Real-Time PCR and normalized against the β-actin gene. Results shown are mean ± SEM from 3 independent experiments. *($p < 0.05$), **($p < 0.01$) and ***($p < 0.001$) indicate levels of statistically significance.

1.3. FASN inhibition resensitizes doxorubicin resistant models to chemotherapy

Resistant cell lines 231**DXR** and HCC**DXR** showed similar FASN expression levels and FASN inhibitor sensitivity when compared to parental cells (Figure 14B, Figure 15). Therefore, we tested the effects of EGCG and C75 in combination with doxorubicin in parental and doxorubicin-resistant models. The results of CPI ratios induced by the mono treatments versus the dual treatments are shown in Table 7. For MTT results see Figure 16 and 16B.

Table 7. Interaction index between doxorubicin and C75, EGCG and G28 in TNBC cells sensitive or doxo-resistant.

	doxorubicin			
plus	MDA-MB-231	231**DXR**	HCC1806	HCC**DXR**
C75	0,84 ± 0,066 synergism*	0,67 ± 0,04 synergism***	1,23 ± 0,12 antagonism*	0,77 ± 0,047 synergism*
EGCG	1,03±0,053 additivism	0,99±0,086 additivism	1,36 ±0,16 antagonism**	0,93 ±0,083 additivism
G28	1,12 ±0,123 additivism	1,06 ±0,113 additivism	0,95 ±0,050 additivism	0,98 ±0,057 additivism

Cells were treated with doxorubicin and C75 (20µM for HCC, HCC**DXR**; 40µM for 231, 231**DXR**) or EGCG (100µM for 231, 231**DXR**; 120µM for HCC, HCC**DXR**) or G28 (30µM for 231, 231**DXR**; 10µM for HCC, HCC**DXR)** for 48h. Results were determined using an MTT assay and are expressed as the Ix obtained from the inhibition of cell proliferation induced for both treatments separately *versus* inhibition for the co-treatment. Experiments were performed at least three times in triplicate. *($p < 0.05$), **($p < 0.01$) and ***($p < 0.001$) indicate levels of statistically significance.

Doxorubicin (50-100-150nM) combined with C75 (40µM) exhibited synergic interaction index (Ix) in 231 and 231**DXR**. Furthermore, resistant cells 231**DXR** showed increased synergic interaction compared to 231. Similar results were observed in HCC**DXR**, because the addition of C75 (20µM) to the doxorubicin (50-100-150nM) treatment improved the effect of the combination compared to the parental cell line. The

combination of doxorubicin (50-100-150nM) and EGCG (100µM) in 231 and 231**DXR** showed an additive effect in both cell lines. Interestingly, EGCG (120µM) combined with doxorubicin (50-100-150nM) also showed a major benefit in HCC**DXR** when compared to the parental. The results obtained with G28 were similar to those from the EGCG. The combination of doxorubicin (10-50-100 nM) with G28 (30µM) in 231 and 231**DXR** showed an additive effect in both cell lines, the same observed with HCC and HCCDXR with the combination of doxorubicin (20-50-100) and G28 (10µM).

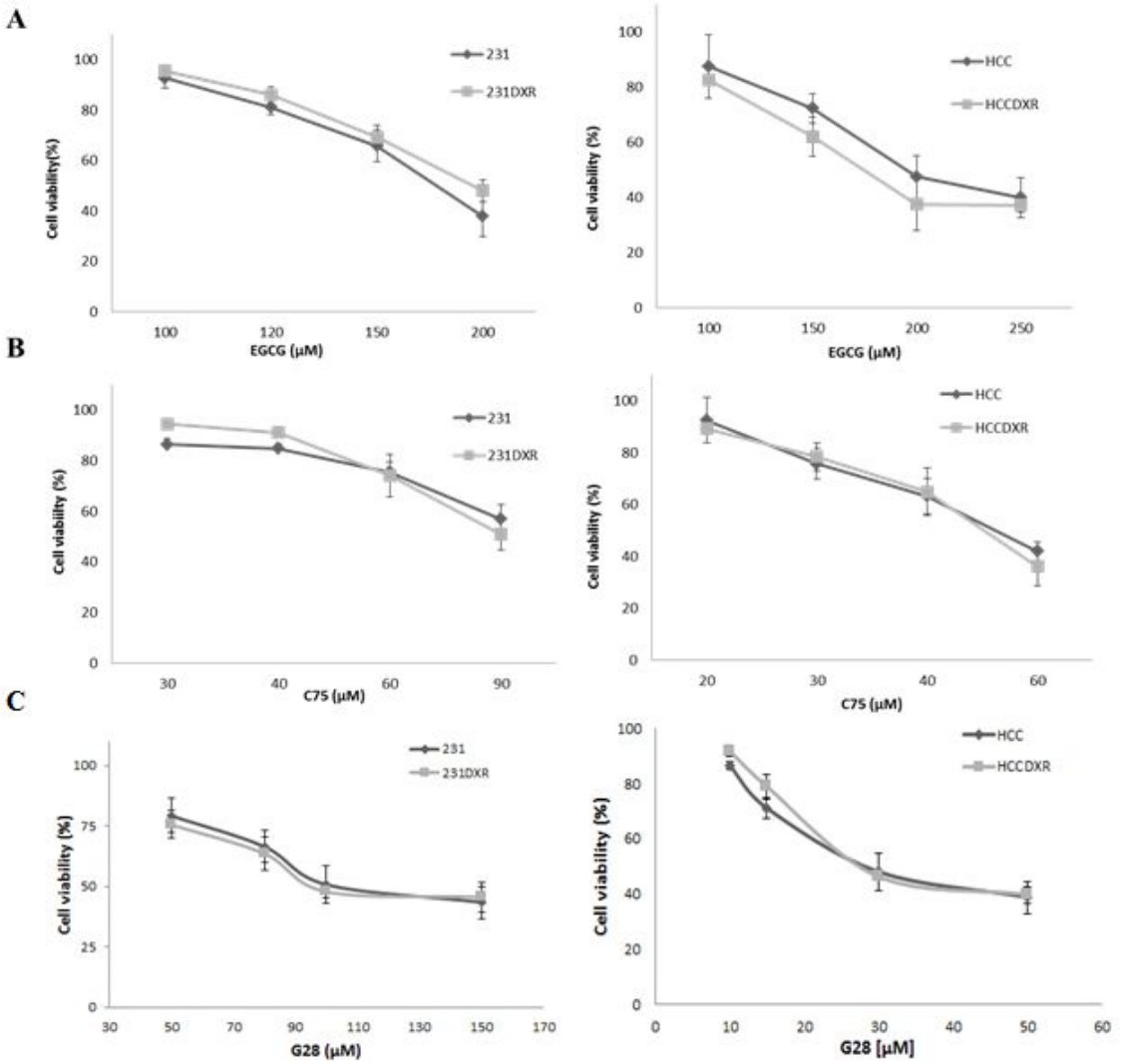

Figure 15. Cell proliferation inhibition of FASN inhibitors EGCG, C75 or G28 in doxorubicin resistant cells. 231, 231**DXR,** HCC and HCC**DXR c**ells were treated with increasing concentrations of **(A)** EGCG (100 – 250 µM) **(B)** C75 (20 – 90 µM) or **(C)** G28 (10 – 150 µM). Results are expressed as mean ± SEM. Experiments were performed at least three times in triplicate.

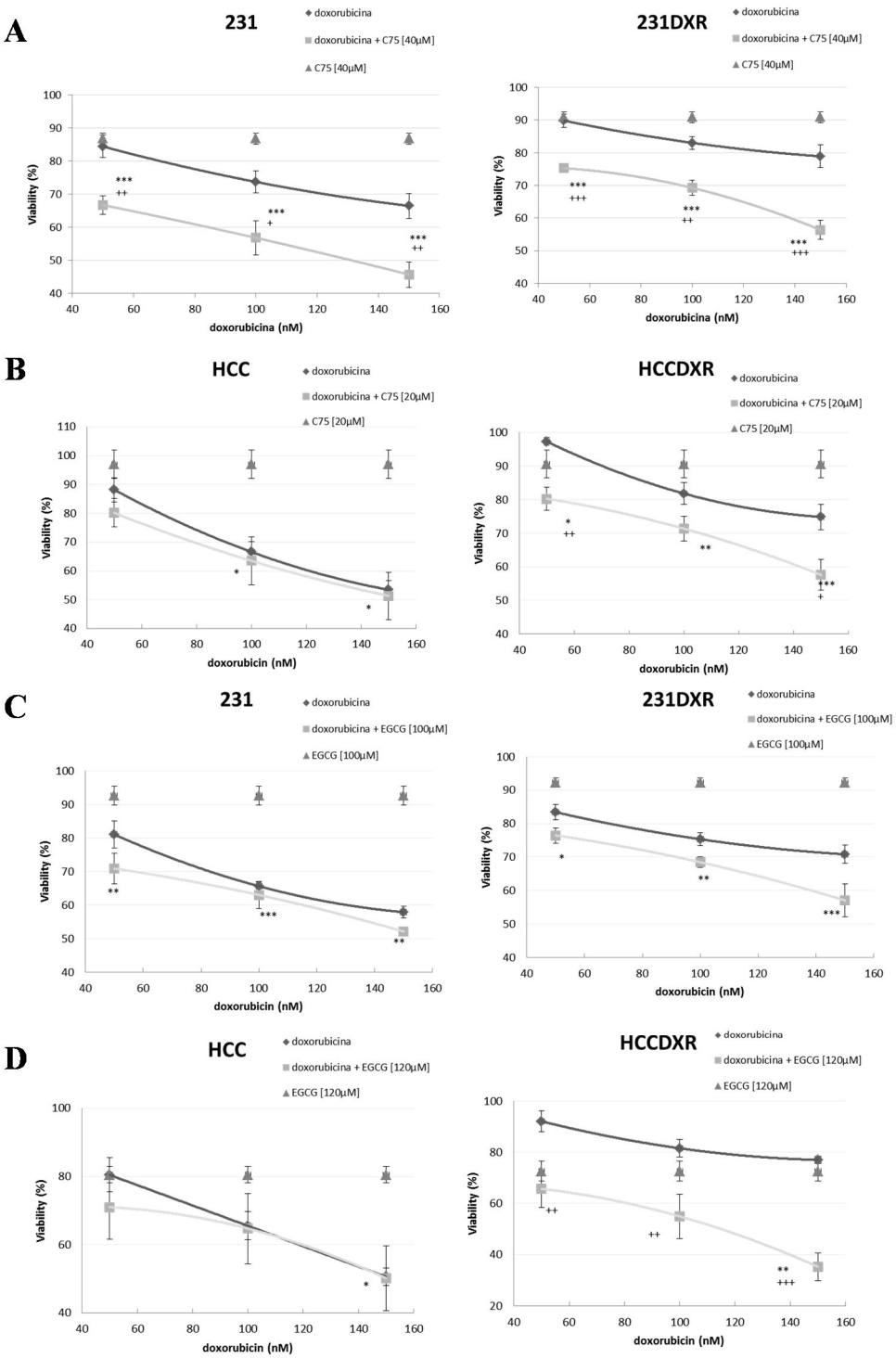

Figure 16. Cell proliferation inhibition of doxorubicin, FASN inhibitor (EGCG or C75) and the combination. (A) 231 and 231**DXR** and **(B)** HCC and HCC**DXR** cells were treated with doxorubicin (50-100-150nM) and C75 (20µM for HCC, HCC**DXR**; 40µM for 231, 231**DXR**) or the combination for 48h. **(C)** 231 and 231**DXR** and **(D)** HCC and HCC**DXR** cells were treated with doxorubicin (50-100-150nM), EGCG (100µM for 231, 231**DXR**; 120µM for HCC, HCC**DXR**) or the combination of both for 48h. Results shown are mean ± SEM. *($p < 0.05$), **($p < 0.01$) and ***($p < 0.001$) indicate levels of statistically significance.

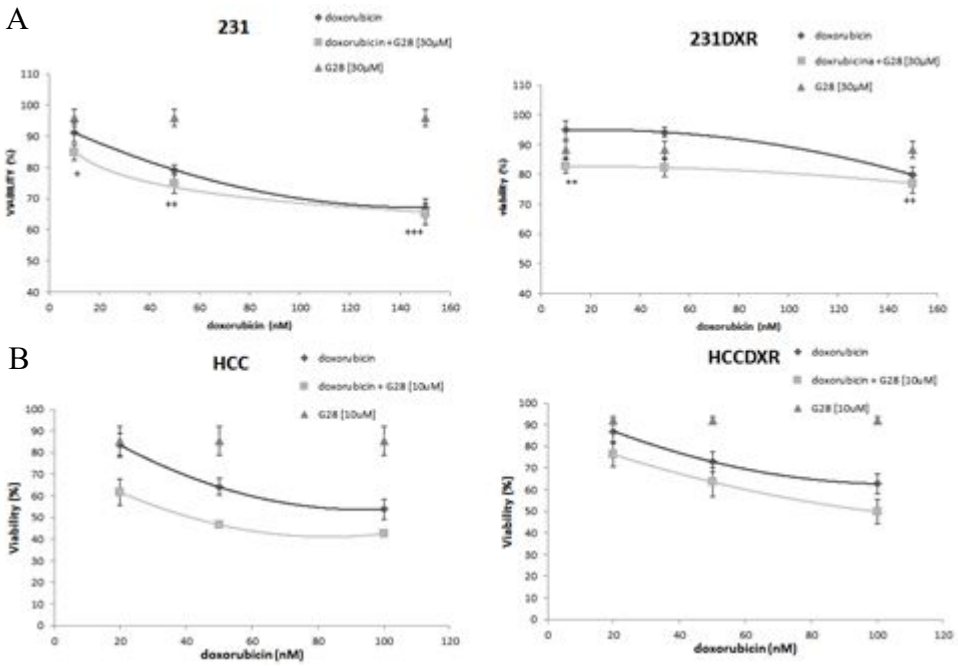

Figure 16B. Cell proliferation inhibition of doxorubicin and the FASN inhibitor G28 and the combination. (A) 231 and 231**DXR** cells were treated with doxorubicin (10-50-150nM), G28 (30µM) or the combination for 48h. **(B)** HCC and HCC**DXR** cells were treated with doxorubicin (20-50-100 nM) or G28 (10 µM) or the combination for 48h. Results shown are mean ± SEM. *($p < 0.05$), **($p < 0.01$) and ***($p < 0.001$) indicate levels of statistically significance.

1.4. FASN inhibitors shows strong synergism with cetuximab in sensitive and resistant cell lines

Several studies reported that EGFR is a common receptor expressed in TNBC[178,179]. *In vitro*, EGFR activation is observed in almost all TNBC cell lines (Figure 13A). Furthermore, we have shown that the expression of EGFR is either maintained or increased in our doxorubicin-resistant models (Figure 14B). Therefore, the effect of combining cetuximab and the FASN inhibitors C75 and EGCG was studied.

Table 8. Interaction index between C75 and EGCG and cetuximab in TNBC cells sensitive or doxo-resistant.

	cetuximab			
plus	MDA-MB-231	231**DXR**	HCC1806	HCC**DXR**
C75	0,69± 0,079 synergism**	0,52±0,037 synergism***	0,78±0,076 synergism*	0,79±0,088 synergism*
EGCG	0,71± 0,055 synergism**	0,56±0,066 synergism***	0,69±0,081 synergism**	0,74±0,035 synergism***
G28	0,78± 0,292 additivism	0,43±0,140 synergism***	0,54±0,103 synergism***	0,73±0,007 synergism*

Cells were treated with cetuximab (0.5-1-2 µM) and C75 (20µM for HCC, HCC**DXR**; 30µM for 231, 231**DXR**), EGCG (50µM for 231, 231**DXR**; 25µM for HCC, HCC**DXR**) or G28 (10µM for 231, 231**DXR**; 5µM for HCC, HCC**DXR**) for 4 days. Results were determined using an MTT assay and are expressed as the Ix obtained as the ratio from the inhibition of cell proliferation induced for both treatments separately *versus* inhibition for the co-treatment. Experiments were performed at least three times in triplicate. *($p < 0.05$), **($p < 0.01$) and ***($p < 0.001$) indicate levels of statistical significance.

The combination of cetuximab (0.5-1-2 µM) with EGCG, C75 and G28 showed a strong synergistic effect in all sensitive and resistant cells (Table 8), unless for the 231 cell line. In this cell line,even the interaccion index is below 0,728, the interaccion was not significative maybe due to high deviation. 231**DXR** showed lower Ix with all C75 (30 µM), EGCG (50 µM) and G28 (10 µM) compared to parental 231 cells. However, HCC and HCC**DXR** showed similar ratio values for both C75 (20 µM) or EGCG (25 µM) when combined with cetuximab, while increased for G28 (µM) . Interestingly, parental and resistant cells showed no significative differences in cell proliferation inhibition

when treated with anti-FASN compounds alone. Even no significantly, G28 treatment after 4 days semeed to be more effective in 231**DXR** cell line. Cetuximab otherwise significantly increased CPI *in vitro* in the HCC**DXR** cell line (Figure 17).

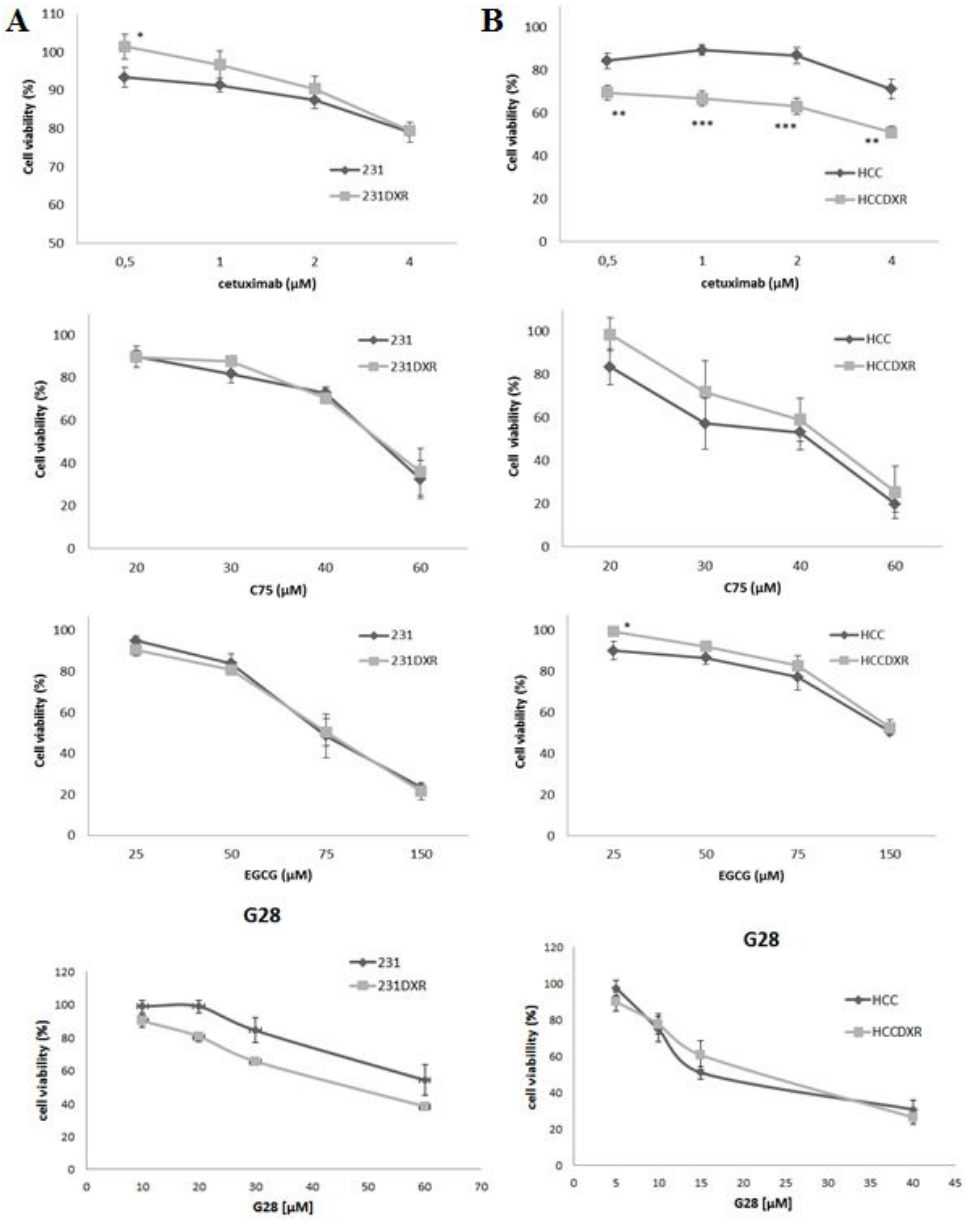

Figure 17. Cell proliferation inhibition of cetuximab and FASN inhibitors EGCG and C75 in doxorubicin resistant cells (A) 231 and 231**DXR** and **(B)** HCC and HCC**DXR** cells were treated with increasing concentrations of cetuximab (0,5 – 4 µM), C75 (20 – 60 µM), EGCG (25 – 150 µM) or G28 (5-60 µM) for 4 days. Results are expressed as mean ± SEM. Experiments were performed at least three times in triplicate. *($p < 0.05$), **($p < 0.01$) and ***($p < 0.001$) indicate levels of statistically significance.

1.5. Synergistic antitumor activity of EGCG in combination with cetuximab in sensitive and doxorubicin resistant TNBC xenografts

To validate our *in vitro* findings, we then tested the antitumor activity of EGCG, cetuximab and the combination treatment *in vivo*. We developed orthotopic xenograft models for 231, its chemoresistant derivative 231**DXR,** HCC and its resistant derivative HCC**DXR.** EGCG (30mg/Kg for 3d/w) and cetuximab (0.5mg/mice 1d/w) as single agents reduced tumor growth in 231 xenografts over 12 days of treatment (Figure 17A). Control animals achieved a relative volume growth of 3.3±0.33, whereas EGCG reduced it to 3.0±0.27 and cetuximab to 2.5±0.29. Interestingly, dual FASN and EGFR blockade showed significantly higher tumor growth inhibition (2.0±0.07) compared to the control (*p-value* <0.01) or EGCG alone (*p-value*<0.05, Figure 18A). Under the same schedule, 231**DXR** xenograft showed a similar relative volume growth as the sensitive model (3.41±0.4, Figure 18B). EGCG showed tumor growth inhibition by day 12 with a relative volume growth of 2.66±0.33, but cetuximab treatment did not inhibit growth. By 12 days of treatment, the relative volume growth for cetuximab was 3.52±0.48, similar to the control group. Again, the combination of EGCG and cetuximab induced significant tumor growth inhibtion (1.98±0.17) compared to control (*p-value* <0.01) and to cetuximab alone (*p-value* <0.05). Despite the absence of tumor shrinkage, the combination treatment (EGCG plus cetuximab) significantly reduced tumor growth in both 231 and 231**DXR** orthotopic xenografts.

In the basal-like HCC xenograft model, EGCG (30mg/Kg for 3d/w) and cetuximab (0.5mg/mice 1d/w) as single agents reduced tumor growth after 10 days of treatment (Figure 18C). Compared to the tumor volume increase observed in the control group (17.79±2.76), EGCG treatment achieved a relative volume growth of 13.03±2.58, while cetuximab significantly reduced the ratio to 6.33±1.25 (*p-value*<0.05). The combination treatment significantly reduced the tumor growth compared to the control (*p-value* 0.001) and to EGCG alone (*p-value* <0.01), with a relative volume growth of 4.87±1.06. In the HCC**DXR** xenograft model, control animals reached a relative volume growth of 5.02±1.38 over the same period of time, significantly lower compared to the parental model (*p-value*<0.05, Figure 18D). EGCG and cetuximab as single agents had higher activity in the HCC**DXR** model compared to HCC, with a relative volume growth of 3.04±0.76 and 0.14±0.04, respectively (cetuximab vs control *p-value* <0.01; cetuximab

vs EGCG *p-value* <0.01). The relative volume growth in the combination setting decreased up to 0.19 ± 0.1 compared to control (p-value<0.05) and EGCG alone (*p-value* <0.05). In the HCC**DXR** model, cetuximab used as a single agent quickly (day 4) displayed strong antitumor activity, leading to effective tumor regression (0.76±0.12). Thus, the combination of EGCG plus cetuximab was not synergic at these treatment doses in the HCC**DXR** xenograft.

Tumor samples from the *in vivo* TNBC models were collected to evaluate drug response signaling mechanisms. 231 and 231**DXR** tumor samples were collected after 12 days of treatment. For HCC and HCC**DXR**, samples were collected after 1 cycle (4 days) because in cetuximab and EGCG plus cetuximab groups total tumor shrinkage was observed after 10 days of treatment. 231, HCC and HCC**DXR** tumor samples showed increased apoptosis (assessed by cleavage of PARP) in the combination treatment settings compared to single treatments and control groups (Figure 18E).

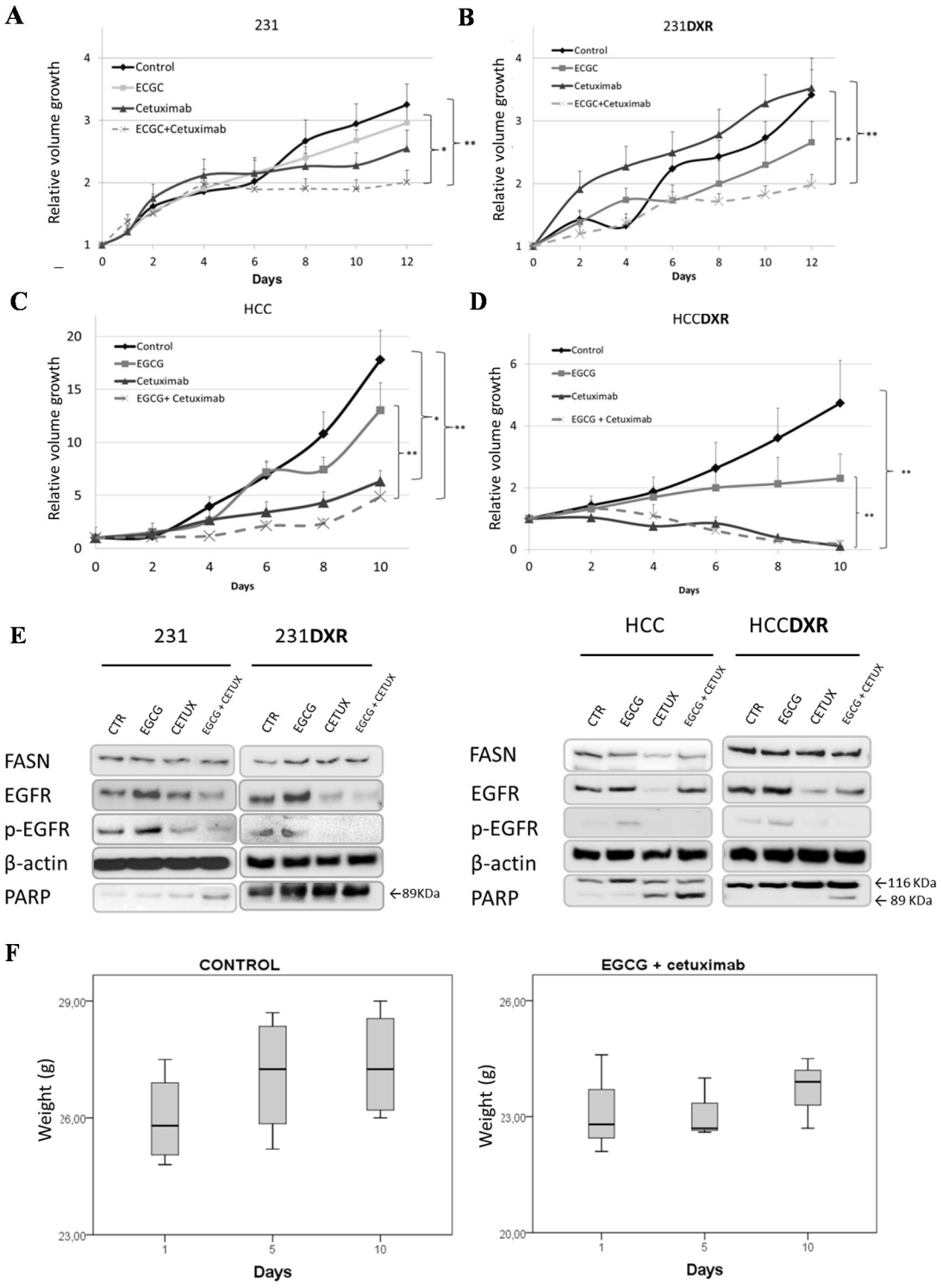

Figure 18. EGCG plus cetuximab in sensitive and resistant TNBC ortoxenograft. (A) Mice bearing 231 and **(B)** 231**DXR** xenografts were treated with saline (Control), EGCG (30mg/Kg, 3 days a week), cetuximab (0.5mg/mice 1 day a week) or the combination (EGCG plus cetuximab) for 12 days. **(C)** Mice bearing HCC and **(D)** HCC**DXR** xenografts were treated with saline (Control), EGCG (30mg/Kg, 3 days a week), cetuximab (100uL/mice 1 day a week) or the combination (EGCG plus cetuximab) for 10 days. **(E)** Western-blot analysis for FASN, EGFR, p-EGFR and PARP in 231, 231**DXR** after 12 days of treatment. HCC and HCC**DXR** tumor samples were collected after one cycle of treatment (4 days). **(F)**

Body weight from NGR mice treated with the combination of EGCG (30mg/Kg, 3 days a week) and cetuximab (100uL/mice 1 day a week) for 10 days. Relative volume growth is expressed as (Final Volume / Initial Volume). Dots are mean of each experimental group and bars, SEM. *($p < 0.05$), **($p < 0.01$) and ***($p < 0.001$) indicate levels of statistically significance.

231**DXR** however showed increased apoptosis in both single and combination treatments compared to control. Total EGFR and p-EGFR levels decreased in 231, 231**DXR** and HCC**DXR** after cetuximab and EGCG plus cetuximab co-treatment. HCC, however, showed a decrease in p-EGFR after cetuximab and combination treatment, but total EGFR levels decreased only after cetuximab treatment. No changes in FASN protein levels were observed among mono- and co-treatments in 231, 231**DXR**, HCC and HCC**DXR** tumors**.**

NRG mice treated with EGCG (30mg/Kg for 3d/w) plus cetuximab (0.5mg/mice 1d/w) were weighed daily to evaluate *in vivo* body weight effect. With respect to initial weight, no significant changes on food and fluid intake or body weight after treatment were identified (Figure 18F).

1.6. Dual blockade of FASN and EGFR changes EGFR downstream activated proteins

We have shown that EGCG combined with cetuximab was synergic in several cellular and animal models of TNBC. Therefore, we planned to study the effect of the EGCG plus cetuximab on FASN, EGFR, and downstream protein expression and activation, alone or in combination, in sensitive (231 and HCC) and resistant (231**DXR** and HCC**DXR**) cells (Figure 19).

Cetuximab as a single agent induced a decrease in total EGFR in 231, 231**DXR** and HCC**DXR** cellular models. On the other hand, the same treatment increased total EGFR in HCC. While cetuximab treatment decreased p-EGFR levels in HCC and HCC**DXR**, 231 and 231**DXR** showed overactivation of p-EGFR after 72h of treatment. Previously described studies suggest that this activation may be likely to receptor homodimerization and autophosphorylation, and does not activate downstream proteins[180]. Protein levels of AKT, ERK1/2 were maintained after cetuximab treatment in all cellular models. Regarding p-AKT activation levels, lower levels were observed compared to control in 231**DXR** and HCC**DXR** after 72h of treatment. 231 and HCC,

however, showed similar or increased p-AKT levels compared to control after 72h of treatment respectively. Cetuximab treatment induced apoptosis in 231 and 231**DXR** after 72h, while cleaved PARP is observed already after 48h in HCC**DXR.** Total PARP increases after cetuximab treatment in HCC, but cleaved PARP was not observed.

EGCG reduced the expression and activation of EGFR and slightly decreased FASN levels after 24h of treatment in all cellular models studied. Downstream proteins AKT and ERK1/2 showed similar levels at 24h of treatment respect to the control. While p-AKT decreased after 24h of treatment, p-ERK1/2 increased considerably after both 12h and 24h in all cellular models. PARP cleavage is observed in all cell lines after EGCG treatment.

The combination of both drugs led to the down regulation after 24h of total EGFR and p-EGFR in 231, 231**DXR** and HCC**DXR**. Otherwise, p-EGFR levels decreased in HCC while total EGFR did not change during the treatment. Regarding to FASN levels, a slight decrease is observed in HCC**DXR**, while the expression level is maintained in the other cell lines. Total ERK1/2 and AKT levels were maintained during the treatment in all cell lines, except for HCC**DXR,** which showed decreased levels of total AKT after 48h of treatment. p-ERK1/2 activation status increased in 231 and 231**DXR** after 48h, while decreased in HCC and HCC**DXR**. Truncated PARP was observed in all cell lines at 24h and 48h for the combination treatment.

In summary, the combination of cetuximab and EGCG enhances the inhibitory effect observed in the EGFR pathway by single treatments, with a general decreasing of EGFR, p-EGFR and p-AKT levels in all cellular models. The activation of ERK1/2 observed after EGCG treatment was decreased or inhibited after combination treatment.

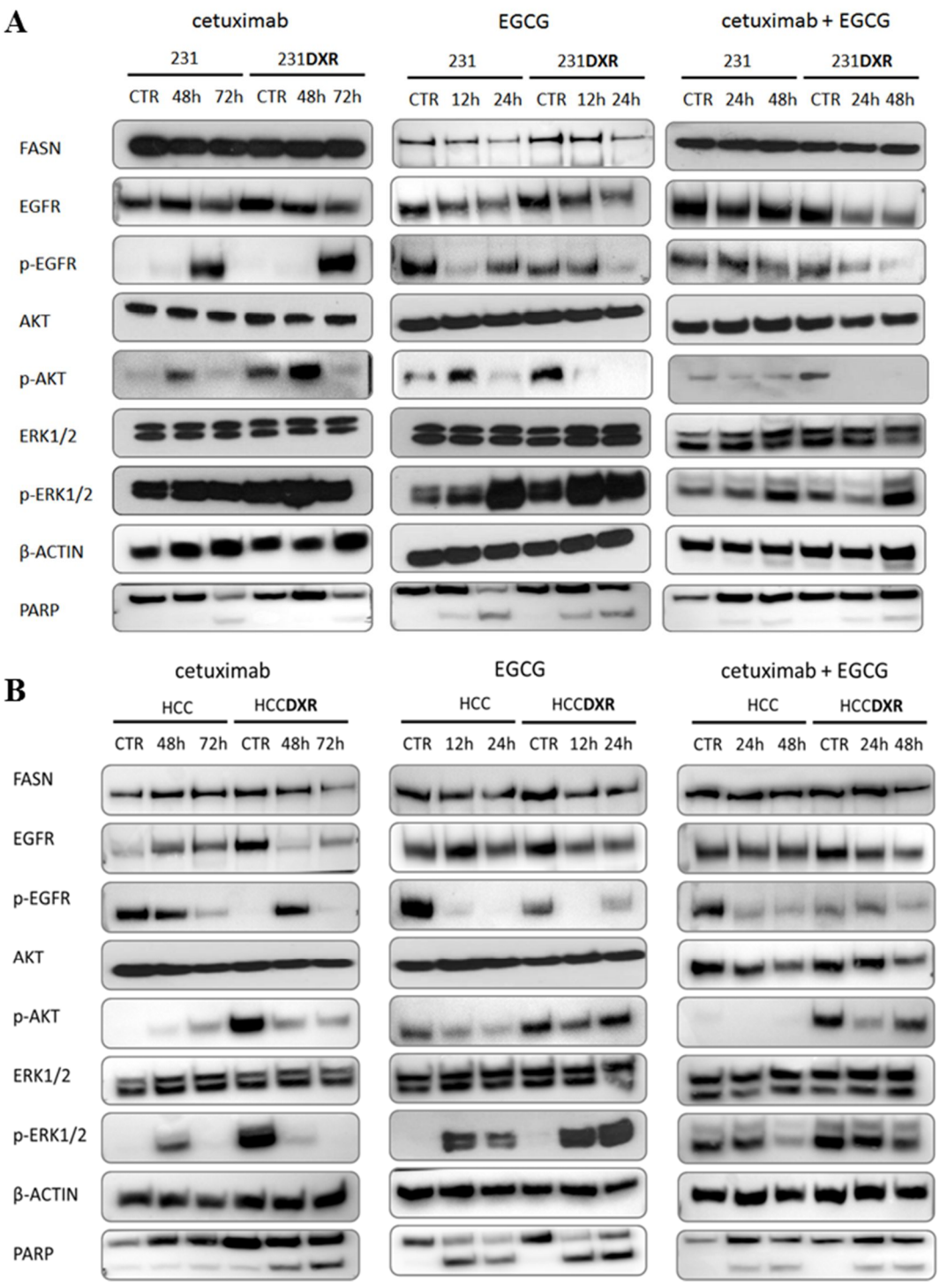

Figure 19. ***In vitro*** **interactions between EGCG and cetuximab in** 231, 231**DXR,** HCC and HCC**DXR**. FASN, EGFR, p-EGFR, AKT, p-AKT, ERK1/2, p-ERK1/2 and PARP expression where analyzed by western-blot at different times after treatments of EGCG (200µM for 12h and 24h), cetuximab (1µM at 48h and 72h), and the combination of both (for 24h and 48h) in **(A)** 231and 231**DXR** and **(B)** HCC and HCC**DXR**.

1.7. FASN and EGFR are expressed in TNBC primary tumor samples

To further validate FASN as a potential target in TNBC, FASN expression was evaluated by Immunohistochemistry (IHC) in paraffin-embedded core-biopsies from 29 TNBC tumour samples. The clinicopathological characteristics of the patients included in the study are shown in Supplementary Table S3. FASN staining was positive in all 29 TNBC samples with tumor specific staining (Figure 20). FASN expression positivity was graded from 0-2+ and scored into three categories, as described in 'Material and Methods' section. Staining was observed in all 29 tumor samples and 31% of them with high positivity (2+). Cellular positivity within the tumor was between 66-100% in 26 (89.7%) of the samples, and between 33-66% in 3 of them (10.3%). The EGFR receptor was also evaluated in the same 29 TNBC core-biopsies with a positivity of 75.9%.

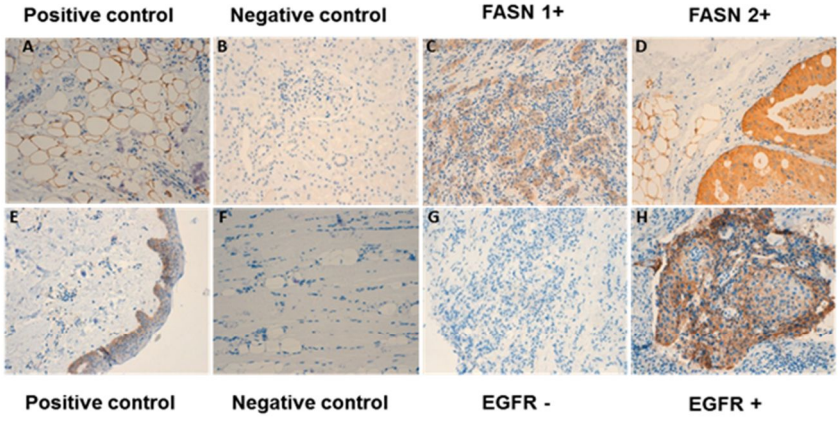

	Total (n=29)(%)		Total (n=29)(%)		Cellular rank (n=29) (%)		
	Positive	Negative	1+	2+	0-33%	33-66%	66-100%
FASN	29(100)	0 (0)	20(68,9)	9(30,1)	0(0)	3(10,3)	26(89,7)
EGFR	22 (75,9)	7(24,1)	-	-	-	-	-

Figure 20. **Immunohistochemistry (IHC) staining of FASN and EGFR in paraffin-embedded core-biopsies from TNBC patients**. **(A)** Adipocytes. **(B)** Renal tissue. **(C)** Ductal carcinoma. **(D)** Ductal carcinoma. **(E)** Skin. (**F**) Muscular tissue (**G**) Ductal carcinoma. (**H**) Ductal carcinoma

2. FASN Expression in TNBC Patients and its Correlation with Clinical and Histological Characteristics.

2.1. FASN expression and clinico-histopathological features of TNBC patients

A total of 100 women with primary triple-negative breast cancer (TNBC) diagnosed between 1990 and 2012 at Hospital Universitari Dr.Josep Trueta (Girona, Spain) were included in the study. Clinico-histopathological characteristics of the study group are shown in Table 9. FASN expression was determined by immunohistochemistry (IHC) in Tissue Microarray (TMA) of paraffin blocks of patients' tumors sections. FASN expression was positive in almost all TNBC samples (92%). As described in methods section, patients were classified in low or high FASN expression according to staining intensity (Figure 21). High FASN expression was observed in 45% of TNBC samples. Interestingly, non-tumoral tissues showed significantly lower level of FASN expression (p-value<0.005), being only detected in 22% of the patients.

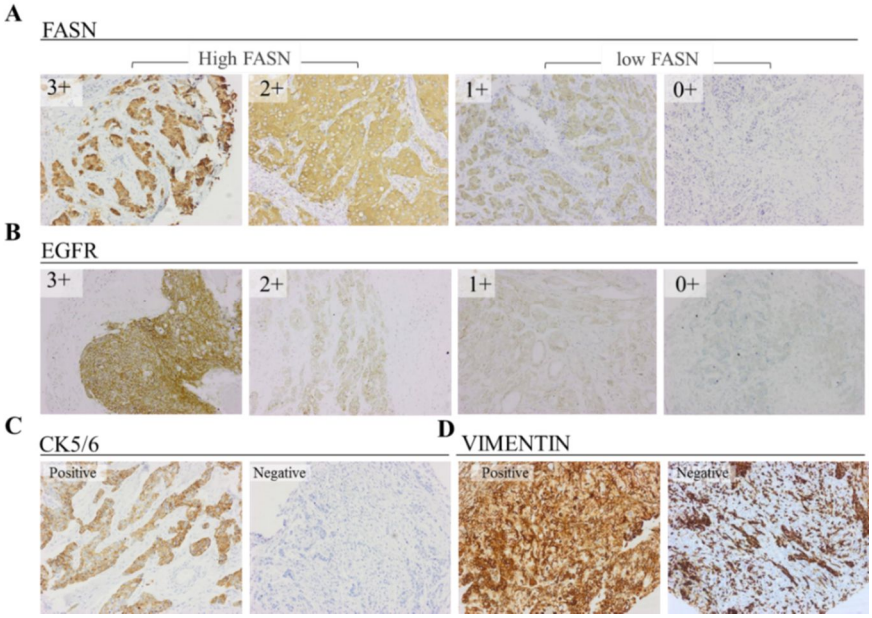

Figure 21. Representative immunostaining results of TNBC tissues for **(A)** FASN, with cytoplasmic localization, and **(B)** EGFR, showing specific membrane staining **(C)** Cytokeratin 5/6 with membrane and/or cytoplasmic localization **(D)** Vimentin, with cytoplasmic staining.

There was no significant difference in patients' mean age between Low and High FASN expression groups, which was 57.3 and 59.0 years old respectively. There was a positive node involvement in 46.9% of the patients and it was significantly more frequent in the High

expressing FASN group (59.5%) when compared to the Low FASN one (36.4%) ($p<0.038$). Approximately half of the patients (48.8%) were stage II, followed by stage III (31.4%) and stage I (19.8%). No association with FASN expression levels and stage was found. The most frequent tumor grade was III (82.5%) and a negative association between tumor grade and FASN levels was observed. Ki-67 was found to be > 20% in most of the patients (97%) therefore no association with High and Low FASN expressing groups was observed.

Table 9. Clinico-histopathological characteristics according to FASN expression in TNBC

Characteristics	**Total**		**Low FASN expression**		**High FASN expression**		**p-value***
	Value	**%**	**Value**	**%**	**Value**	**%**	
Number of patients	100		55	55.0%	45	45.0%	
Mean Age (yrs.) ±SD	58.1	± 16.3	57.3	± 17.0	59.0	± 15.7	0.602*[1]
Node Status							**0.038**
Negative	43	53.1%	28	63.6%	15	40.5%	
Positive	38	46.9%	16	36.4%	22	59.5%	
Unknown	19	-	11	-	8	-	
Stage							0.380
I	17	19.8%	11	23.4%	6	15.4%	
II	42	48.8%	24	51.1%	18	46.2%	
III	27	31.4%	12	25.5%	15	38.5%	
Unknown	14	-	8	-	6	-	
Tumor grade							0.050*[2]
I	0	0%	0	0.0%	0	0.0%	
II	11	17.5%	3	8.6%	8	28.6%	
III	52	82.5%	32	91.4%	20	71.4%	
Unknown	37	-	20	-	17	-	
Ki67							1.000*[2]
≤ 20%	1	2.7%	1	5.0%	0	0.0%	
> 20%	36	97.3%	19	95.0%	17	100.0%	
Unknown	63	-	35	-	28	-	
Ki67 (median; IQR)	(61.0	; 51.0)	(59.5	; 44.0)	(61.0	; 50.0)	0.460*[3]
Surgery							0.224
Lumpectomy	40	49.4%	19	43.2%	21	56.8%	
Mastectomy	41	50.6%	25	56.8%	16	43.2%	
Unknown	19	-	11	-	8	-	
Adjuvant treatment							0.168*[2]
Anthracyclines	6	11.1%	4	13.8%	2	8.0%	
Anthracy.+Taxanes	43	79.6%	22	75.9%	21	84.0%	
Taxanes	3	5.6%	3	10.3%	0	0.0%	
Other	2	3.7%	0	0.0%	2	8.0%	
No treatment	12	-	5	-	7	-	
Unknown	34	-	21	-	13	-	

* Pearson's Chi-Square Test. *[2] Fisher's Exact Test
*[1] Unpaired t-Test *[3] Mann-Whitney U-Test

2.2. FASN expression and intrinsic subtypes of TNBC patients

We have recently reported that TNBC cellular models show different FASN expression levels[106]. In order to verify whether different levels of FASN were also observed in TNBC patients' intrinsic subtypes, we stratified our study group in basal-like (BL), mesenchymal-like (ML) and Non-BL/Non-ML(NonBLML) as described in the Methods section according the expression of EGFR, Cytokeratin 5/6 and Vimentin (Figure 21). The frequencies of each TNBC subtype in our cohort of TNBC were BL (56,1%), ML (31.7%) and NonBLML (12.2%) (Table 10).

Regarding FASN expression, BL patients showed similar percentages of low and high expression (47.8% vs 52.2%), while ML patients showed a marked predominant prevalence of low FASN expression (80.8%). In addition, most patients classified as neither Basal nor Mesenchymal demonstrate to express FASN at high levels (90.0%). The frequencies of low and high FASN populations were significantly different between BL and ML patients and also when comparing ML and NonBLML.

Table 10. FASN expression in Intrinsic subtypes of TNBC patients

	Total		**Low FASN Expression**		**High FASN expression**		**p-value**
	Frequency	**%[1]**	**Frequency**	***%*[2]**	**Frequency**	***%*[2]**	
Intrinsic Subtypes							**<0.001***
Basal-Like	46	56.1%	22	*47.8%*	24	*52.2%*	] **0.020*[1]**
Mesenchymal-like	26	31.7%	21	*80.8%*	5	*19.2%*	] **<0.001*[1]**
Non-BL/Non-ML	10	12.2%	1	*10.0%*	9	*90.0%*	
Unknown	18		11	-	7	-	
TOTAL	**100**						

[1] percentatge within the whole TNBC group
[2] percentatge within each TNBC intrinsic subtype
* Fisher's Exact Test
*[1] Adjusted p-values by Multiple comparisons Bonferroni method

2.3. EGFR, Cytokeratin 5/6 and Vimentin association with FASN expression in TNBC

EGFR, Cytokeratins 5/6 and Vimentin are markers commonly expressed in TNBC which its expression has been correlated with poor outcome [39,175,181–183]. Here, we studied their individual association with FASN expression (Table 11).

EGFR staining was positive in 45% of the samples, being 1+ the most abundant group of positivity (30%). Higher percentages and intensities of EGFR positive tissue samples were observed in the High FASN group compared to the Low one. However, a significant linear trend could not be determined. Only 27% of the patients of this study expressed Cytokeratin 5/6. This biomarker expression was not associated with FASN expression. Vimentin was found to be positive or focal positive in about 72% of the patients, and its expression was significantly inversely associated with the expression of FASN. Therefore, the percentage of patients with low FASN expression increased as Vimentin was more expressed.

Table 11. FASN association with other IHC markers in TNBC

	Total		**Low FASN Expression**		**High FASN expression**		**p-value***
	Frequency	**%**	**Frequency**	**%**	**Frequency**	**%**	
EGFR							0.095
Negative	44	**55.0**%	28	**62.2**%	16	**45.7**%	
Focal positive	2	**2.5**%	0	**0.0**%	2	**5.7**%	
1+	24	**30.0**%	14	**31.1**%	10	**28.6**%	
2+	3	**3.8**%	1	**2.2**%	2	**5.7**%	
3+	7	**8.8**%	2	**4.4**%	5	**14.3**%	
(Total Positives)	*(36)*	***(45%)***	*(17)*	***(37.8%)***	*19*	***(54.3%)***	
Unknown	20		10		10		
Cytokeratin 5/6							0.694
Negative	73	**73.0**%	41	**74.5**%	32	**71.1**%	
Focal positive	21	**21.0**%	11	**20.0**%	10	**22.2**%	
Positive	6	**6.0**%	3	**5.5**%	3	**6.7**%	
(Total Positives)	*(27)*	***(27.0%)***	*(14)*	***(25.5%)***	*(13)*	***(28.9%)***	
Unknown	0		0		0		
Vimentin							**<0.001**
Negative	23	**28.0**%	2	**4.5**%	21	**55.3**%	
Focal positive	23	**28.0**%	15	**34.1**%	8	**21.1**%	
Positive	36	**43.9**%	27	**61.4**%	9	**23.7**%	
(Total Positives)	*(59)*	***(72.0%)***	*(42)*	***(95.5%)***	*(17)*	***(44.7%)***	
Unknown	18		11		7		

* Mantel-Haenszel Test for linear Trend

2.4. Survival analysis

2.4.1. Survival analyses

The log-rank test showed no differences in OS (N=90) or DFS (N=64) between the low and high FASN expressing groups (Figure 22A,B). However, survival rates were usually lower in the high FASN group. For example, OS 3-year probability was 80% (95% CI: 69-91%) for patients with low FASN levels and 70% (95% CI: 57-85%) for patients with high FASN. For DFS, 3-year probability was 83% (95% CI: 73-96%) for patients with low FASN levels and 70% (95% CI: 55-90%) for patients with high FASN.

Survival analysis for EGFR showed a link between tumor EGFR expression and poor outcome, although no significant differences were observed for OS or DFS (Figure 22C,D).

Regarding intrinsic subtype classification, no differences were observed in OS outcome neither in DFS between subtypes (Figure 22E,F), although for this last parameter BL patients showed a 5-year probability of 71% (CI: 56-90%) while the probability for ML was 81% (CI: 64-100%). The NonBLML subtype showed the poorest OS and DSF, with values of 5-year probability of 60% (CI:53-89%) and 57% (CI:30-100%) respectively.

2.4.2. Cox analysis

In the Cox univariate regression analysis, age>49 years, advanced stage (III), and positive expression of CK5/6 were significantly associated with poor OS and DFS (Table 4 and 5). Additionally, Positive node status and high EGFR expression (3+) were significantly associated with poor DFS. In contrast, FASN expression and Intrinsic TNBC Subtypes showed neither a significant association with OS nor with DFS. However, DFS HR was slightly higher for the High FASN expressing group (HR=1.69) when compared to Low FASN one.

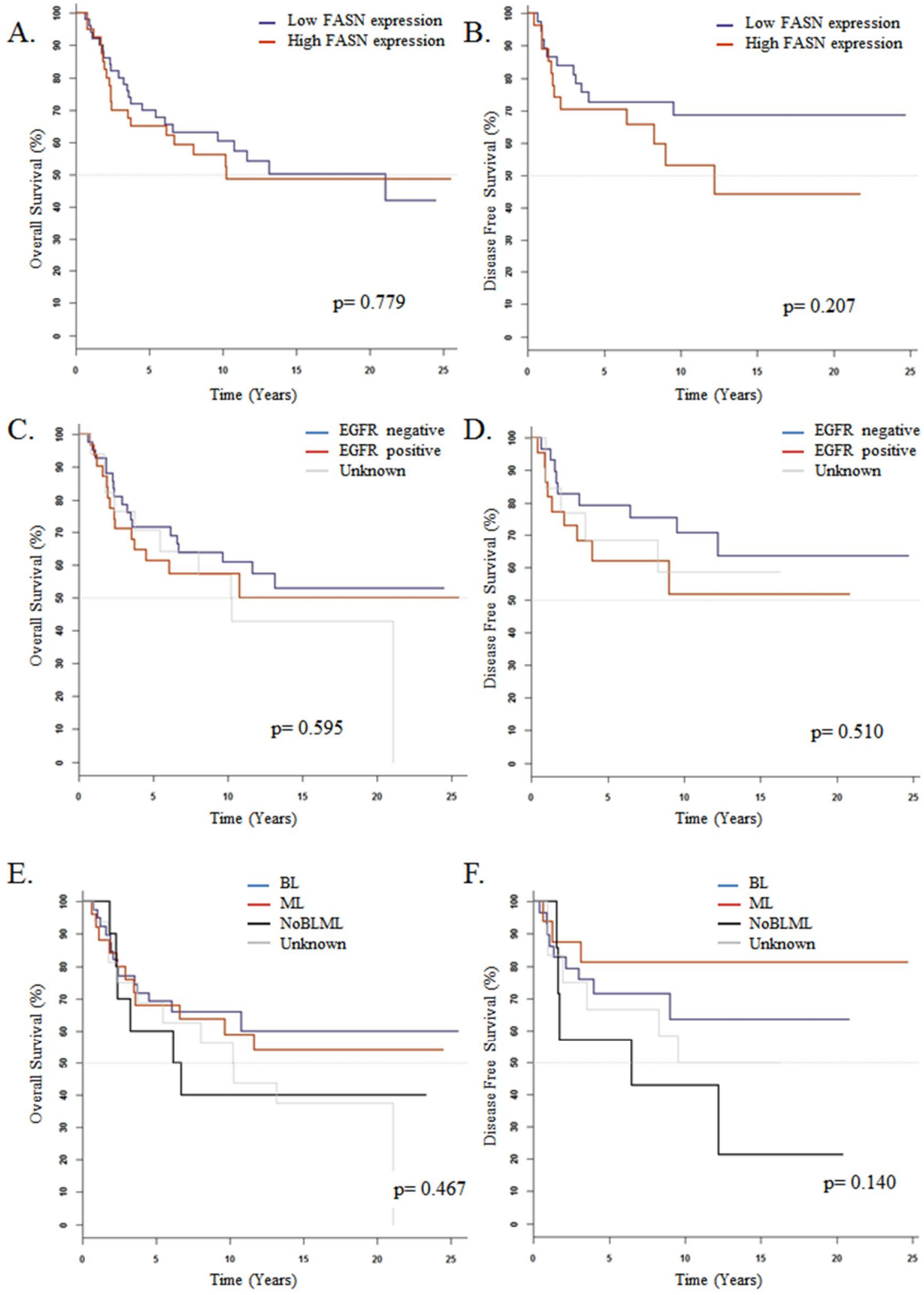

Figure 22. Kaplan-Meier estimate curves of Overall Survival (N=90) **and Disease-Free Survival** (N=64) for **(A)** and **(B)** FASN, **(C)** and **(D)** EGFR and **(E)** and **(F)** Molecular subtypes in TNBC patients.

Table 12. Cox univariate analysis of Overall survival

OVERALL SURVIVAL (N=90)				
Factor	**N (n)[a]**	**HR[b]**	**(95% CI)[c]**	**p-value**
Fasn_2g				
Low	50 (23)	1		
High	40 (19)	1.09	(0.59 -2.00)	0.780
Stage				
I	17 (3)	1		
II	38 (16)	2.55	(0.74 – 8.74)	0.138
III	25 (18)	8.75	(2.56 – 29.91)	**<0.001**
Unknown	10 (5)	3.30	(0.78 – 13.91)	0.104
Age				
≤ 49 years	29(6)	1		
> 49 years	61(36)	3.73	(1.56 – 8.90)	**0.003**
Intrinsic subtype				
Basal-like	39 (14)	1		
Mesenchymal-like	25 (11)	1.09	(0.49 – 2.41)	0.829
Non-BL non-ML	10 (6)	1.65	(0.63 – 4.30)	0.305
Unknown	16 (11)	1.73	(0.78 – 3.82)	0.177
Node Status				
Negative	41 (17)	1		
Positive	34 (18)	1.80	(0.92 – 3.51)	0.085
Unknown	15 (7)	1.25	(0.52 – 3.01)	0.624
EGFR				
Negative	42 (18)	1		
Focal positive	2 (1)	1.36	(0.18 – 10.23)	0.768
1+	21 (8)	0.98	(0.43 – 2.27)	0.967
2+	2 (1)	2.16	(0.28 – 16.42)	0.458
3+	6 (4)	2.56	(0.86 – 7.63)	0.092
Unknown	17 (10)	1.46	(0.67 – 3.17)	0.337
Vimentin				
Negative	22 (12)	1		
Focal positive	22 (7)	0.52	(0.21 – 1.33)	0.175
Positive	30 (12)	0.58	(0.26 – 1.30)	0.186
Unknown	16 (11)	1.04	(0.46 – 2.37)	0.928
Cytokeratin 5/6				
Negative	70 (35)	1		
Focal positive	15 (3)	0.36	(0.11 – 1.16)	0.088
Positive	5 (4)	3.52	(1.21 – 10.28)	**0.021**

[a] N= number of patients at risk; n= number of events
[b] Hazard ratio
[c] 95% confidence interval

Table 13. Cox univariate analysis of Disease Free-Survival

DISEASE FREE SURVIVAL (N=64)				
Factor	**N (n)[a]**	**HR[b]**	**(95% CI)[c]**	**p-value**
Fasn_2g				
Low	37 (11)	1		
High	27 (12)	1.69	(0.74 – 3.83)	0.212
Stage				
I	17 (3)	1		
II	25 (7)	1.61	(0.42 – 6.22)	0.491
III	19 (13)	8.21	(2.28 – 29.54)	**0.001**
Age				
≤ 49 years	28 (8)	1		
> 49 years	36 (15)	1.63	(0.69 – 3.85)	0.266
Intrinsic subtype				
Basal-like	29 (9)	1		
Mesenchimal-like	16 (3)	0.48	(0.13 – 1.78)	0.273
Non-BL non-ML	7 (5)	2.27	(0.76 – 6.82)	0.143
Unknown	12 (6)	1.38	(0.49 – 3.90)	0.547
Node Status (N=61)				
Negative	35 (10)	1		
Positive	26 (13)	2.59	(1.12 – 5.99)	**0.026**
EGFR (N=63)				
Negative	29 (9)	1		
Focal positive	1 (1)	3.01	(0.38 – 24.01)	0.280
1+	16 (4)	0.96	(0.29 – 3.13)	0.945
3+	4 (4)	11.05	(3.05 – 40.00)	< **0.001**
Unknown	13 (5)	1.35	(0.45 – 4.04)	0.589
Vimentin				
Negative	12 (7)	1		
Focal positive	17 (4)	0.39	(0.11 – 1.34)	0.135
Positive	23 (6)	0.33	(0.11 – 1.00)	0.050
Unknown	12 (6)	0.68	(0.23 – 2.04)	0.493
Cytokeratin 5/6				
Negative	47 (18)	1		
Focal positive	13 (2)	0.41	(0.09 – 1.75)	0.227
Positive	4 (3)	4.54	(1.28 – 16.10)	**0.019**

[a] N= number of patients at risk. n= number of events
[b] Hazard ratio
[c] 95% confidence interval

3. Stem Cells and FASN Implication in Chemoresitance Acquisition in a Mesenchymal-like Cell Line Sensitive and Resistant to Chemotherapy

3.1. Doxorubicin treatment and FASN protein expression in 231 and 231DXR cell lines

Recent studies pointed out that FASN activity plays an important role in drug resistance because allows fast synthesis of new phospholipids for membrane remodeling and plasticity, and inhibits apoptosis via PARP activation by decreasing ceramide levels [104,184–187].We and others have previously shown that FASN inhibition could re-sensitize cell lines to doxorubicin treatment[106,188](Figure 16). Here, we observed that FASN protein levels increased significantly, almost 2 folds, after 24h of treatment in the resistant model compared to parental (Figure 23). 231 cell line treated at same time and conditions showed no significant increased levels. Cleavage PARP was increased in the sensitive model after 12h of treatment, while less differences were observed after 24h of doxorubicin treatment.

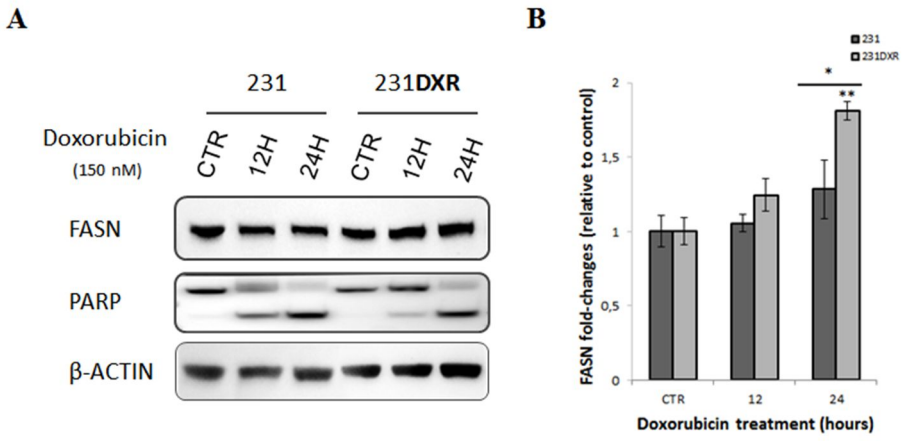

Figure 23. FASN expression after doxorubicin treatment in 231 and 231DXR. (A) Western blot analysis of FASN, EGFR and PARP expression after 12h or 24h of doxorubicin treatment (150nM). **(B)** FASN expression expressed as fold changes relative to control after 12h and 24h of doxorubicin treatment. Results are expressed as mean ± SEM. *($p < 0.05$), **($p < 0.01$) and ***($p < 0.001$) indicate levels of statistically significance.

3.2. Cancer-Stem cells enriched population in sensible and resistant cell lines to doxorubicin

Cancer Stem Cells (CSCs) are a very rare population within the tumor. Relapse after chemotherapy can result as a selection or enrichment of these cells, due to its intrinsic resistance to chemotherapy and its ability to regenerate the tumor[32,156,157]. *In vitro*, these cells have been demonstrated to have the ability to survive and propagate in a non-adherent way forming spheres called mammospheres [141,152], to be enriched in the $CD44^{high}/CD24^{low}$ population[140], and to show increased activity of the ALDH1 enzyme[189]. Here, we pursuit to evaluate the CSC population in our sensible and resistant model using this three approaches. The influence of doxorubicin treatment was also evaluated.

The Mammosphere Forming Assay (MFA) is a technique used to identify a population in the cell culture or tissue enriched with CSC (see 'Materials and Methods' section). We performed the MFA in cell lines 231 and in the resistant models 231**DXR** (Figure 24A). 231 and 231**DXR** showed similar Mammosphere Forming Index (MFI), with values of 1.78% ±0.24 and 1.75% ±0.27 respectively. As one of the CSC population characteristic is its intrinsic resistance to chemotherapy[144], we then performed doxorubicin treatments in adherent and mammosphere cell culture, in both sensitive and resistant cell lines. Cell-density, doxorubicin doses, and treatment days were performed equally in both techniques. In adherent condition, cell proliferation inhibition was performed using the MTT assay, while the Mammosphere Forming Inhibition (MFIn) was used for non-adherent culture. Both methods are described in 'Material and Methods' section. Intrinsic resistance to doxorubicin was observed in the CSC enriched population compared to adherent conditions for both sensitive and resistant cell line (Figure 24B). In adherent conditions, cell lines proliferation inhibition (% CPI) ranged from 86.7% (231) to 89.5% (231**DXR**). Otherwise, MFIn values showed significant lower inhibition in both cell lines (*p-values* < 0.001), with values of 60.66% and 51.29% respectively. Furthemore, the cytotoxic effect of doxorubicin was significantly higher in parental than in resistant models (*p- value*: 0.005) .

Another commonly technique used to identify CSC is the evaluation of the cell population with $CD44^{high}/CD24^{low}$ cell surface markers assessed by flow cytometry. As

shown in Figure 25, no differences where observed between parental (99.8% ± 0.12) and resistant model (99.5% ± 0.35), showing both models a high percentage for this population. For that reason, doxorubicin treatment using this methodology was skipped, as no enrichment would be observed.

The last approach used to evaluate if CSC were enriched in our resistant model, was the measurement of ALDH1 activity using the ALDEFLUOR^{TM} assay (Figure 26). Results showed a significant increase (*p-value*=0.048) in the activity of this enzyme in the resistant model 231**DXR** (26,52% ± 1,81) compared with parental (10,81% ± 5,74). Interestingly, doxorubicin treatment also increased the ALDH^{br} cells after 12 and 24 hours in both sensitive and resistant cell line, reaching values of 42.15% ± 10.53 and 38.10% ± 6.71 respectively. Even not significantly, 231**DXR** cells showed increased ALDH1 activity compared to parental after 12h of treatment (36.87% ± 3,56 vs. 17.28% ± 5,68), showing similar levels observed at 24 hours after treatment.

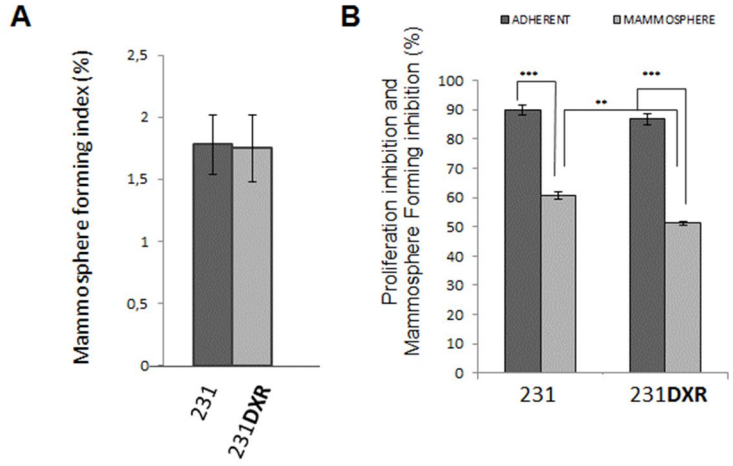

Figure 24. **Mammosphere forming assay (A)** Mammosphere forming index (MFI) for 231 and 231**DXR (B)** Proliferation inhibition and Mammposphere forming inhibition (MFIn) under doxorubicin (70nM) treatment for 5 d**ays** in 231 and 231**DXR**. Experiments were performed at least three times in duplicate. Results are expressed as mean ± SEM. *($p < 0.05$), **($p < 0.01$) and ***($p < 0.001$) indicate levels of statistically significance.

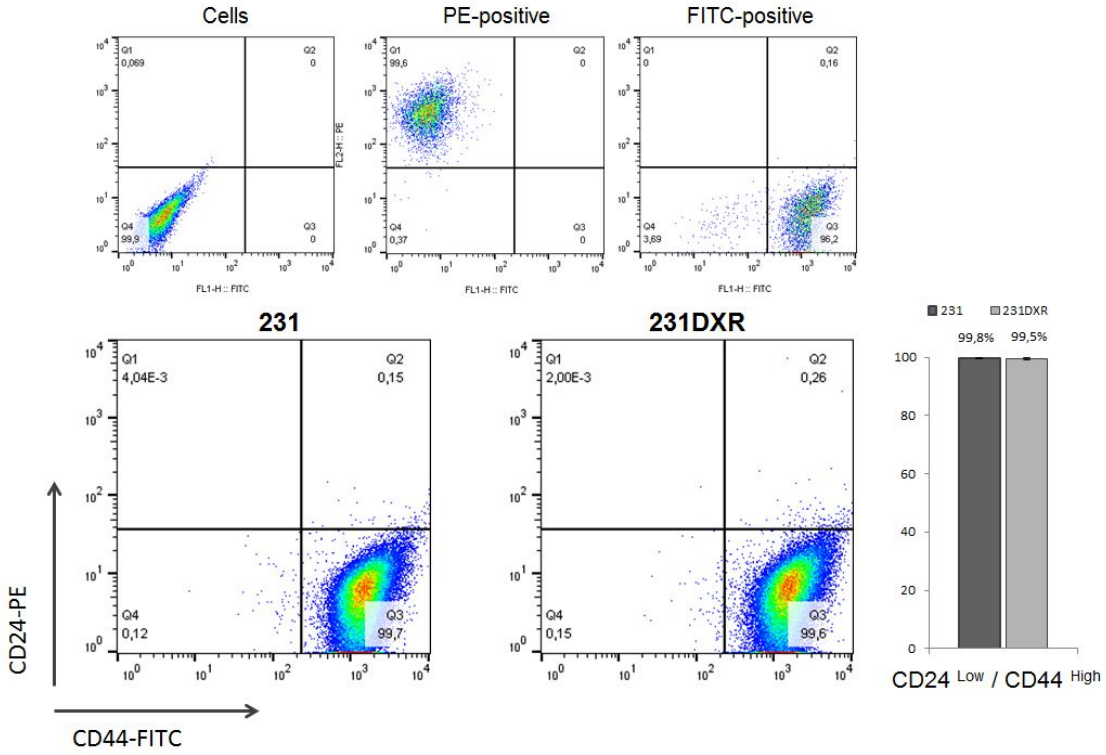

Figure 25. CD44^{high}/CD24^{low} cell surface markers evaluation in 231 and 231DXR cell lines by flow cytometry. Upper panels show control for cells unlabeled, labeled with a PE-positive marker and FITC-positive. Experiments where performed three times.

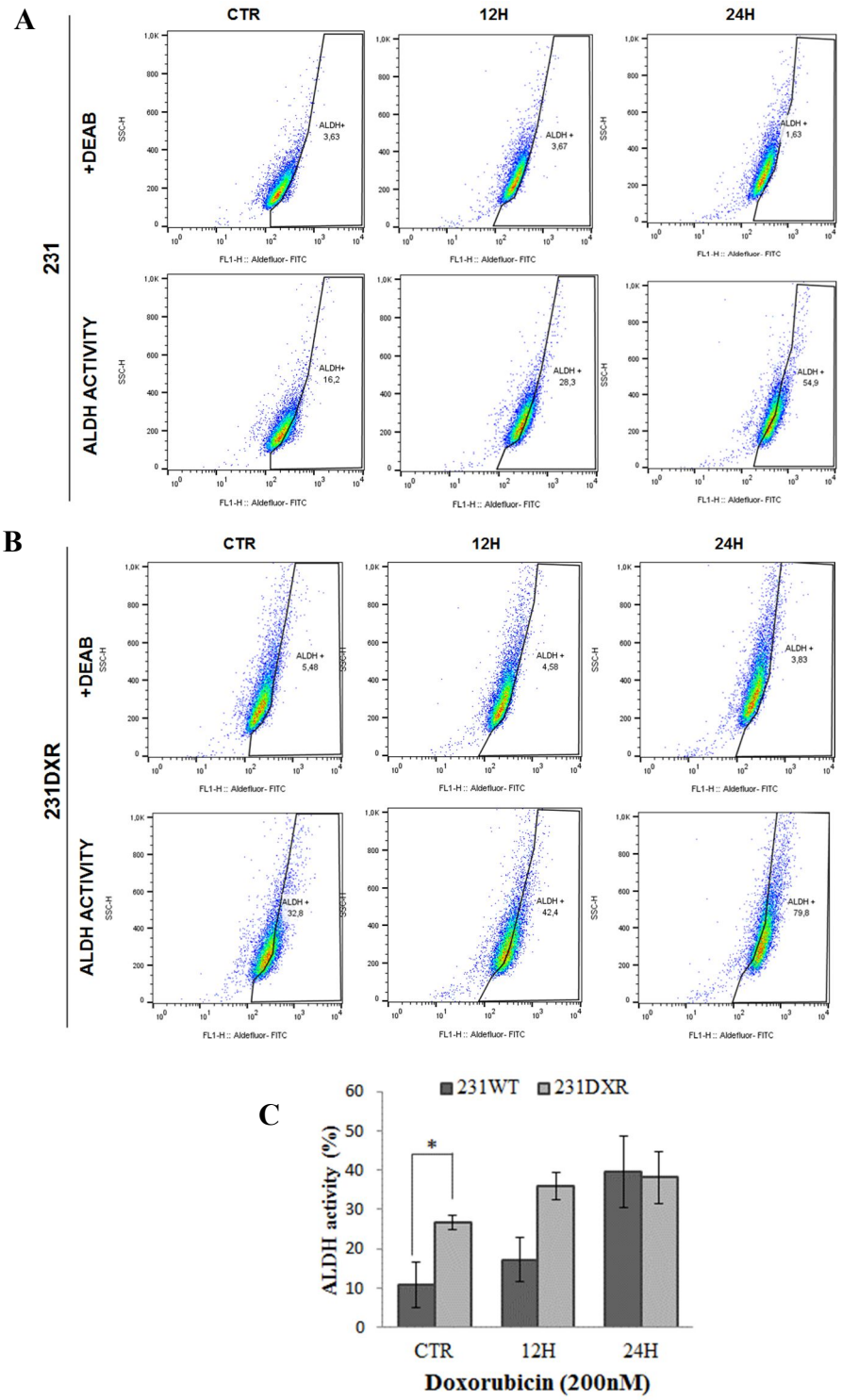

Figure 26. ALDEFLUOR™ assay in 231 and 231DXR after doxorubicin treatment. Representative flow cytometry plots for **(A)** 231 and **(B)** 231**DXR** after doxorubicin treatment (200nM) for 12 and 24 hours. Upper panel shows cells treated with DEAB, an ADLH1 inhibitor (negative control). Low panel, ALDH1^{br} cells compared to negative control for each sample. **(C)** ALDH1^{br} mean results. Experiment was performed at least 3 times. Results are expressed as mean ± SEM. *($p < 0.05$), **($p < 0.01$) and ***($p < 0.001$) indicate levels of statistically significance.

3.3. Doxorubicin triggers EMT and acquired resistance in Mesenchymal-like cell lines

As cell plasticity plays an important role in drug-resistance acquisition[166], we studied the implication of the EMT in resistance acquisition after doxorubicin treatment. Several transcription factors (TF) have been described to induce EMT[169] , consequently inducing cell dedifferentiation and CSC properties, such as chemoresistance[171,172]. For that reason, we evaluated the RNA expression of transcription factors snail, slug, twist, Zeb1 and Zeb2 implicated in EMT under doxorubicin treatment (data not shown). One of the transcription factors, *snai1*, was significantly increased after 12 hours of doxorubicin treatment in both 231 and 231**DXR** cell lines (Figure 27). Furthermore, basal levels of *snai1* gene were increased two times in 231**DXR** compared to 231 (*p-value* <0.05). The expression levels of *vimentin*, an intermediate filament protein related to the mesenchymal phenotype, were also significantly increased in both models after 12h of doxorubicin treatment, with a higher increase in 231**DXR**.

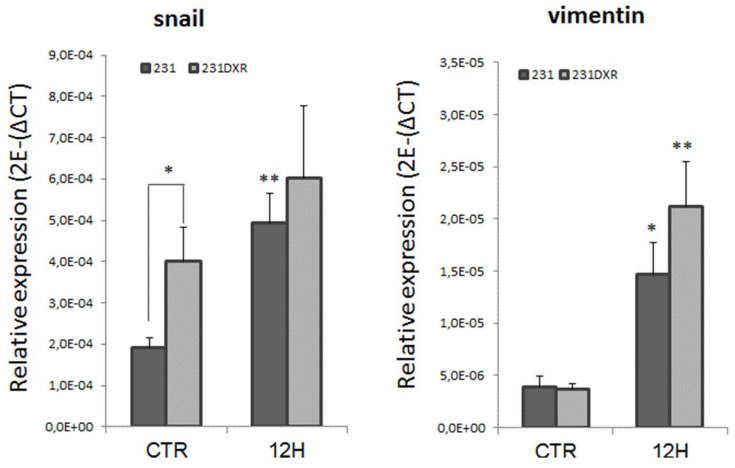

Figure 27. *Snai1* and *vimentin* gene expression after 12h of doxorubicin treatment. (a) MDA-MB-231 and 231**DXR** after 12h of doxorubicin treatment (150nM). Experiments were performed at least three times. *($p < 0.05$), **($p < 0.01$) and ***($p < 0.001$) indicate levels of statistically significance.

3.4. FASN inhibition in CSC enriched population

FASN expression was increased after doxorubicin treatment in 231**DXR** model (Figure 23). To observe the effect of FASN inhibition in the CSC enriched population, the mammosphere forming and ALDEFLUOR™ assays were performed in cell lines 231

and 231**DXR**.

Three different FASN inhibitors, C75, EGCG and G28 were used to calculate the MFI. The concentration that inhibited 30% (IC_{30}) of the cells after 48h for each compound was used. A proliferation inhibition study was performed in parallel with same conditions.

Results showed that C75 had the same effect in adherent and non-adherent conditions in 231 and 231**DXR**, with values of ranging from 45.26% ± 2.94 to 31.43% ± 6.3 (Figure 28). EGCG inhibitory effect was significantly decreased in non-adherent conditions in 231 and 231**DXR.** MFIn values were 25.71% ± 4.42 and 36% ± 14.7, while proliferation inhibition at adherent conditions were of 81.54% ± 3.38 and 85.22% ± 4.97 for 231 (*p-value* <0.001) and 231**DXR** (*p-value*= 0.007) respectively. G28 showed a marked anti-proliferative effect in both adherent and suspension. Even though proliferation inhibition ranged from 78.70% ±2,5 (231) to 72,66% ± 6,76 (231**DXR**) in adherent conditions, the same concentration of G28 showed a significantly more inhibitory effect in suspension, with values of 98.10% ± 0,72 for 231 (p-value<0.001) and 94,70% ± 1,55 for 231**DXR** (p-value<0.001).

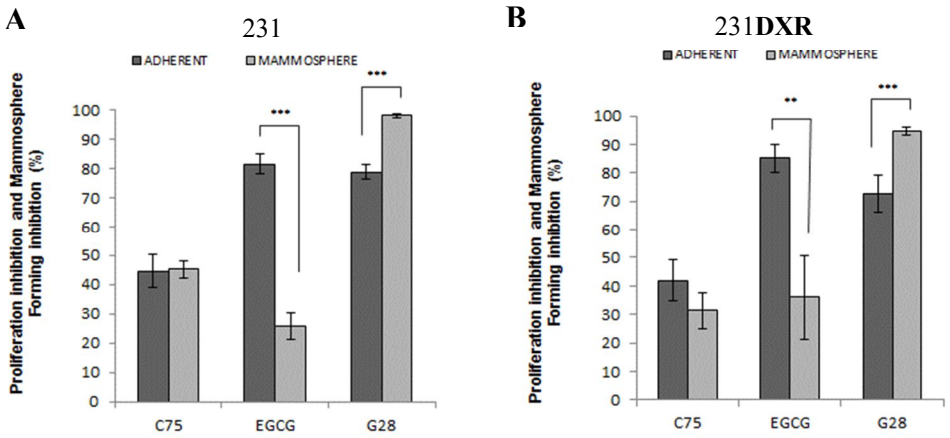

Figure 28. Proliferation inhibition *versus* mammposphere forming inhibition (MFIn) for FASN inhibitor EGCG, C75 and G28. **(A)** 231 and **(B)** 231**DXR** were treated for 5 days with C75 (30µM) and EGCG (120µM) treatment and G28 (50 µM). Experiments were performed at least three times in duplicate. *($p < 0.05$), **($p < 0.01$) and ***($p < 0.001$) indicate levels of statistically significance.

Discussion

1. Pre-Clinical Evaluation of Fatty Acid Synthase and EGFR inhibition in TNBC

Triple-negative breast cancer lacks an approved targeted therapy, and it is mainly treated with a combination of anthracyclines and taxanes[190]. The high rate of relapse after treatment urges for the development of new targeted therapies for these patients. TNBC breast cancer is well known for its heterogeneity[27]. Here we show that FASN, the key enzyme for novo lipogenesis, is not only expressed in all TNBC cell lines included in the study, but also in TNBC patient samples. *In vitro*, basal-like cell lines express more FASN than Mesenchyma-like cell lines (both at gene and protein level) and are more sensitive to the FASN inhibitor C75. Immunostaining of FASN in 29 core-biopsies from TNBC patients shows that FASN is overexpressed in all tumor samples included in the study compared to their non-tumoral, surrounding breast tissues. Recent studies performed in breast and ovarian cancer have demonstrated the overexpression and specificity for FASN staining in neoplastic tissues, and also its relationship with cancer aggressiveness [59,121].

After four decades, doxorubicin is still the most used and effective chemotherapy agent in the clinic for the treatment of breast cancer [191]. For this reason, two doxorubicin-resistant models representative of the two major molecular subtypes in TNBC, 231**DXR** (ML) and HCC**DXR** (BL) were developed in our laboratory. Both models showed significant resistance when exposed to high doses of doxorubicin compared to the parental cell lines. Several mechanisms have been described for doxorubicin resistance in the last few years [191,192], some of them regarding changes in the EGFR pathway. HCC**DXR** showed overexpression of EGFR and overactivation of AKT and ERK1/2 when compared to its parental cell line. Overexpression of EGFR in breast cancer patients after chemotherapy has been already described to be related with higher local recurrence, metastasis and so poor outcome [136,193]. On the other hand, AKT and ERK1/2 have been shown to be overactivated and also linked to chemoresistance in several cancers [194,195]. Interestingly, similar levels of FASN were observed in parental cell lines compared to their resistant derivate (**DXR**). Recent studies pointed out that FASN activity plays an important role in drug resistance because it allows fast synthesis of new phospholipids for membrane remodeling and plasticity[184,186]. Here, we performed combinatorial experiments with doxorubicin and the FASN inhibitors C75, EGCG and G28 in our sensitive and resistant cell lines to determine whether FASN

inhibition may be useful to overcome doxorubicin resistance in TNBC. Although the EGCG antitumor effects may be due to binding probably with other cellular targets than FASN [196], we and others have previously identified EGCG as an inhibitor of FASN activity, able to induce apoptosis in several tumor cell lines and also to reduce the size of mammary tumors in animal models[97,99,112,113,197]. Our results showed that the Interaction index for both combinations was improved in both resistant models (231**DXR** and HCC**DXR**) for C75 and EGCG treatment compared to the parental lines. G28 increased minimally the efficacy in 231**DXR** compared to 231 when combined with doxorubicin, but improved the results obtained with EGCG, as HCC cell line showed additive effect in this settings. Interestingly, C75, EGCG and G28 showed same CPI between parental or **DXR** derivate when treated alone, suggesting FASN activity could play an important role in doxorubicin resistance in TNBC. In addition, FASN inhibition has been described to reverse chemoresistance in ovarian and hepatocellular cancer cells [104,188].

Several studies have shown that EGFR is overexpressed in TNBC [178,183]. Our results showed a high percentage of immunostaining positivity for EGFR in the core biospies from TNBC patients, in concordance with previous findings. The anti-EGFR compound cetuximab showed low levels of CPI *in vitro* in all cell lines except for HCC**DXR,** which showed significantly increased CPI and apoptosis compared to the parental cell line. *In vivo*, while none, low or moderate antitumor effect was observed in 231**DXR**, 231 and HCC xenografts, respectively, cetuximab treatment obtained almost complete tumor shrinkage after two cycles of treatment in HCC**DXR**. These results are consistent with the EGFR overexpression in HCC**DXR** cell line, probably as an adaptation to overcome doxorubicin-induced apoptosis. Paradoxically, this mechanism of chemoresistance could sensitize the cell line to anti-EGFR treatments. This is in agreement with the results of a phase II study combining cetuximab with cisplatin in metastatic TNBC, where the overall response rate was doubled and the progression free survival increased from 1.5 to 3.7 months when compared to cisplatin monotherapy [138].

The common overexpression of EGFR in TNBC and its relationship with cancer progression after therapy, together with FASN expression in all TNBC and in **DXR** models, provided the rationale to test combined FASN inhibitors and EGFR blockade in this these settings. We found that simultaneous treatment of cetuximab and EGCG, C75 and G28 generally resulted in strong synergism in both parental and resistant models. Strong cooperative growth inhibition between FASN and EGFR have been also

observed *in vitro* for ovarian cancer cell lines [198]. The synergism between FASN and EGFR may be due to the mechanisms involving FASN blockade that results in blockage of lipid synthesis, lipid raft destabilization, and further EGFR degradation [198]. Furthermore, EGCG has been described to be closely associated with destabilization and inhibition of EGFR receptor and downstream signaling pathways [199–201]. In addition, Bollu et al. recently found that FASN-dependent palmitoylation of EGFR is required for EGFR dimerization and kinase activation [202]. The same authors, in a previous study, described that FASN-dependent palmitoylation also activates mitochondrial EGFR and promotes cell survival, while its inhibition leads to apoptosis [203]. Furthermore, phosphorylation and activation of FASN by direct interaction with members of the EGFR family have already been described [203].

Together, these *in vitro* results together with TNBC patient sample study, supported evaluation of the antitumor efficacy of cetuximab in combination with the FASN inhibitor EGCG in doxo-sensitive and -resistant TNBC orthoxenograftx *in vivo*. We and others have demonstrated that EGCG displays anti-tumor activity without affecting food intake or weight loss, which are common side effects of other FASN inhibitors [116,197]. We have previously shown that EGCG produces apoptosis *in vitro* and *in vivo* in breast cancer [99,112,197]. Here, EGCG showed strong CPI and high apoptosis *in vitro*, and moderate anti-tumour activity *in vivo*. EGFR inactivation and downregulation is observed in all cell lines after EGCG treatment *in vitro,* consistent with previous studies [199–201,204]. At the same time, slightly decreases in FASN levels were observed in all cell lines, suggesting that the EGFR pathway could be implicated in FASN expression regulation in TNBC [112,117]. Furthermore, p-AKT decreased its activation levels, while p-MAPK increased considerably after EGCG treatment, maybe due to a negative crosstalk between these two proteins [112,195,198].

Here, we clearly validate our *in vitro* results by showing that the combination of EGCG with the EGFR inhibitor cetuximab results in synergistic tumor growth reduction in both doxorubicin-sensitive and resistant xenograft models. Tumor analysis showed decreased EGFR and p-EGFR in the cetuximab and combination settings in all models. However, this event was not observed in the EGCG treatment *in vivo* possibly due to the unstable nature of EGCG in serum [205]. Nevertheless, increased apoptosis was observed in the combination settings in all models compared to the single treatments, even after only one cycle in the HCC and HCC**DXR** xenograft. *In vitro* study interactions also reveal that p-ERK1/2 levels decreased in the combination settings in

the HCC and HCC**DXR** cell lines, and reduced the loop effect in p-ERK1/2 in the combination treatment in 231 and 231**DXR**.

In summary, we found FASN is expressed in all TNBC primary tumor samples tested. We then showed therapeutic benefit of FASN inhibition in sensitive and chemoresistant TNBC preclinical models, as well as strong synergistic anti-tumor effect of FASN inhibitors in combination with cetuximab. Our findings provide a rationale for further investigation of FASN inhibitors in combination with anti-EGFR signaling agents in TNBC and TNBC who progressed after chemotherapy.

2. FASN Expression in TNBC Patients and its Association with Clinical and Histological Characteristics.

Triple-Negative Breast Cancer treatment is mainly restricted to a combination of anthracyclines and taxanes[190]. In spite of several efforts, any effective target therapy has been yet approved for TNBC treatment. Therefore, there is an urge to identify novel molecular targets for this Breast Cancer subtype.

Fatty acid synthase (FASN) has arisen as a potential target in different types of cancer and even currently a FASN inhibitor is being evaluated in a clinical trial[66]. In a recent study with a small cohort of TNBC patients, we have reported a positive FASN staining in all TNBC samples and 31% with high positivity. In the present study we have extended these results using a larger cohort of patients and we have detected a higher percentage of TNBC patients expressing high levels of FASN (45%). Although no significantly, High FASN expressing patients showed lower Overall-Survival (OS) and Disease-Free Survival (DFS) rates than the Low FASN ones. A significant correlation between FASN expression and DFS was earlier observed in early breast carcinomas patients[206]. Recent studies reported a FASN overexpression and specificity in tumoral tissues in breast and ovarian cancer[59,121]. Our results suggest FASN expression may also play a role in TNBC progression and outcomes.

Previous studies concluded that TNBC patients are usually younger and have larger and higher grade tumors with more lymph node involvement than other subtypes of Breast Cancer[19,207,208]. Accordingly, our results showed that our cohort of TNBC patients have large tumors (48.8% stage II and 31.4% stage III) with a high histologic

grade (82,5% grade III). Our cohort also has a high Ki-67 proliferation index (>20%; 97.3%) and a high nodal involvement (46.9% node positive) as was expected in a high risk breast cancer subtype. TNBC tissues have been previously associated with high Ki-67 index (>14; 88%) compared to other breast cancer subtypes[121].

Although breast-conserving therapy is not associated with increased local recurrence and is appropriate for patients with TNBC[209], 50.6% of our patients were treated with mastectomy versus 49.4% with lumpectomy, probably due to the high prevalence of stage II and III tumors. Even though one of the aims of primary chemotherapy is to increase the rate of breast-conserving surgery, most of our TNBC patients received a combination of anthracyclines and taxanes in the adjuvant setting. One must consider that we have included patients diagnosed from 1990 to 2012 and some decades ago the use of primary chemotherapy was less prevalent. Predictors of poor Overall Survival (OS) and Disease-Free Survival (DFS) in the Cox univariate analysis included age, advanced stage and positive node status. The absence or presence of axillary lymph node metastasis is a well-known powerful prognostic factor and a direct relationship exists between the number of lymph nodes and outcome[21,210].

When analyzing FASN association with the aforementioned clinical characteristics, we found that High FASN expression was associated with positive node involvement and negatively associated with tumor grade. On the other hand, no significantly differences were found between Low and High FASN groups regarding age, surgical or adjuvant treatment and stage. As high Ki-67 was observed in most of our TNBC patients, the study of its association with FASN was hampered. However, a relationship between Ki-67 and FASN expression has been described in ovarian cancer[59].

The molecular classification of Breast Cancer provided new insight in the breast cancer biology. The two major subtypes identified comprising Triple-negative breast cancers, basal-like (BL) and mesenchymal-like (ML), showed variations in growth rate, cellular composition of the tumors and presented diverse clinically implications respect to overall survival (OS) and disease-Free survival (DFS)[29,41]. In this work, we have stratified our cohort of TNBC patients in Basal-Like (56.1%), Mesenchymal-Like (31.7%) and Non-Basal/Non-Mesenchymal like (12.2%). Other reports have found similar distributions of TNBC intrinsic subtypes[27,29]. The DFS and OS outcomes

obtained for the two intrinsic subtypes showed similar behaviors as observed in other studies[29,41]. When focusing on FASN expression, we have observed that it was significantly higher in BL patients than in ML ones, in agreement with our previous results *in vitro*[106]. Basal-like breast cancer has been described as a high-proliferative subtype, with specific over-expression of genes for this cluster, while ML was defined as low-proliferative subtype[29]. Consistently, FASN have been associated with high proliferative phenotype and linked to recurrence and poor outcome in several cancers [59,206,211,212].

We also retrospective analyzed the cytokeratins 5/6 and Vimentin used for classify our patients in TNBC intrinsic subtypes. Cytokeratins 5/6 were positively immunostained in 27% of the patients and their expression was significantly associated with poor OS and DFS in concordance with previous studies[39,182]. On the other hand, Vimentin was positive in 72% of the patients. High levels of Vimentin have already been described to be enriched in TNBC[175], and its expression have been correlated with poor outcome[181]. Both ML and BL molecular subtypes are considered to have poor outcome when compared to other molecular subtypes[29]. Here, a negative association between FASN and Vimentin expression was observed. Vimentin is considered a mesenchymal marker[166] and it is highly associated with the ML tumors[29,40,41], a low-proliferative subtype enriched with EMT markers[27,29,40]. Concordantly, FASN expression has been significantly associated with the BL subtype, a more proliferative intrinsic subtype in this study.

EGFR expression is a poor prognosis marker frequently expressed in TNBC [35,183]. In our patients set, EGFR staining was positive in 45% of the samples. In agreement, other authors have shown that between 50-70% of TNBC express EGFR[31,39]. DFS and OS for EGFR expression confirmed the correlation between EGFR positivity and poor survival observed by other authors[135,136], although the differences were not significant in our hands. Interestingly, the univariate analysis showed that high EGFR expression (3+) was significantly associated with poor DFS.

EGFR inhibitors have been evaluated in combination with common chemotherapy, although most of the clinical trials have failed to improve significantly OS or DFS. Interestingly, we have shown in an earlier study a strong synergism between FASN inhibitors and cetuximab (EGFR inhibitor) at low concentrations in

Basal-Like (BL) and Mesenchymal-Like (ML) cell lines and TNBC orthoxenografts, without signs of toxicity[106]. Thus, a combination of FASN and EGFR inhibitors may be a feasible therapeutic approach for the treatment of TNBC patients.

In summary, we found FASN was expressed in most the TNBC tumor samples tested. Although no significantly, High FASN expressing patients showed lower Overall-Survival (OS) or Disease-Free Survival (DFS) rates than the Low FASN ones and were significantly associated with positive node status, one of the most powerful markers for predicting relapse. FASN expression was significantly higher in BL patients than in ML ones, and it was negatively correlated with Vimentin levels. EGFR was found to be expressed in an important subgroup of TNBC patients. We have previously shown than FASN and EGFR co-targeted in a TNBC pre-clinical setting may be an effective therapeutic strategy for TNBC expressing both markers. Altogether, our observations may account for the bases of future therapeutic strategies of TNBC intrinsic subtypes using FASN and EGFR inhibitors.

3. Cancer Stem Cells and FASN Implication in Chemoresitance Acquisition in a Mesenchymal-like Cell Line Sensitive and Resistant to Chemotherapy.

Claudin-low (CL) or Mesenchymal-like (ML) subtype was the last molecular subtype to be identified. Represents 20% of the TNBC (the second in incidence after basal-like in TNBC[29]), is characterized by the enrichment of the EMT features, shows CSC properties, and has a poor prognosis[27,29]. Furthermore, the enrichment of CSC features have been found in tumors who progressed after therapy[32,157]. Here, we used a ML subtype cell line MDA-MB-231 (231) and its resistant derivate 231**DXR**, to evaluate the CSC population in resistance acquisition to chemotherapy.

CSCs represent a rare population within the tumor, and several methodologies have been developed to study the population enriched with this cells *in vitro*. 231 cell line is characterized for developing loose mammospheres structures that can be passaged for several generations[151,152,213,214]. The Mammosphere-forming assay showed no differences in index formation between both cell lines, sensitive or resistant. The same results were obtained using the cell surface signature $CD44^{high}/CD24^{low}$, which represent almost all the population for the 231 cell line[150,189]. The ALDEFLUOR™

assay otherwise, showed that ALDH^{br} cell population was significantly enriched in the 231**DXR** cell line.

Cell plasticity plays an important role in tumor evolution, and the plastic CSCs theory describes that bidirectional conversions may exist between non-CSCs and CSCs, and that this phenotype can be an acquired state, through the activation of the EMT process[170–172]. The addition of the chemo-agent resulted in an increased resistance to this drug in the 231**DXR** cell line compared to 231 in non-adherent conditions. Furthermore, doxorubicin had more inhibitory effect in adherent conditions than in non-adherent, as expected. Interestingly, the addition of doxorubicin increased ALDH1 activity in both sensitive and resistant cell line after 12 and 24 hours of treatment. Furthermore, the expression of snail, an EMT inducer directly linked to tumor progression and recurrence[215–217], increased significantly. Despite its high efficacy as an anti-tumor drug, doxorubicin has already been described to induce stemness in murine cell models[218–220]. Recently, another study showed that intrinsic resistance to doxorubicin of MDA-MB-231 (compared to Hs578T, another Mesenchymal-like cell line) could be due to an increase of stem cell-related signaling pathways under doxorubicin treatment[161].

FASN overexpression not only gives advantages to malignant cells to keep its high proliferation rate, but also plays an important role in drug resistance[104,184,186]. In our hands, FASN inhibition re-sensitized doxorubicin-resistant cell lines to the chemo-agent and FASN protein levels increased significantly in the resistant model after doxorubicin treatment. A recently published study from Gonzalez-Guerrico and Espinoza *et al.*, revealed that suppression of FASN restored a non-malignant phenotype, reversing Mesenchyma-like to a more differentiate phenotype by down-regulating EMT markers in a model of breast cancer progression[118]. Furthermore, pharmacological inhibition of lipogenesis by the FASN inhibitor Metformin was sufficient to promote a switch from basal- to luminal-like sphere morphologies[118]. Another FASN inhibitor, resveratrol, suppressed the growth of cancer stem-like cells by down-regulating FASN expression both *in vitro* and in a xenograft model of breast cancer[221]. FASN expression also have been shown to play a role in stemness maintenance in glioma[222]. Here, we evaluated FASN inhibitor effect in CSCs population through their ability to inhibit mammosphere formation compared to adherent conditions. C75 showed the same inhibitory effect in adherent and non-adherent conditions and, interestingly, G28 showed markedly increased inhibitory effect in non-adherent conditions in both cell

lines sensitive and resistance, contrary to the results obtained with doxorubicin.

In summary, our results suggest that chemoresitance in a ML cell line 231**DXR** is not only a static drug-selected profile, but and acquired reversible phenotype that can be activated by the drug itself. The CSCs phenotype was enriched in 231**DXR** compared with its parental cell line, and activated in the presence of doxorubicin through the EMT process. Even thought our results are preliminary, and more approaches should be performed to evaluate FASN inhibition in a CSC enriched population, several studies already have found that FASN suppression not only can be a feasible target for high proliferative neoplasia's such as TNBC, but also seems to invert the CSCs acquired phenotype and thou avoiding acquired resistance to chemotherapy.

4. General Discussion

The main objective of this work was the evaluation of FASN expression and inhibition in Triple-negative breast cancer sensitive and resistant to current therapies. This work has been performed using pre-clinical models (both *in vitro* and *in vivo*) and a large cohort of TNBC tumor samples.

In the first part of this thesis, we evaluated the expression of FASN in pre-clinical models of TNBC. We showed that all cell lines expressed FASN, and its expression levels correlated with IC_{50} values resulting from its inhibition using the specific FASN inhibitor C75 or G28. Then, FASN expression was analyzed by IHC in TNBC tumor patients. FASN expression was evaluated first in 29 biopsy cores, showing positive staining in all samples and 31% of them with high positivity. The study of FASN expression in a large cohort of patients (n=100), showed that FASN expression was positive in almost all TNBC samples (92%), and that 45% of them showed High FASN expression.

In vitro, two different expression levels of FASN were observed between Mesenchymal-like and Basal-like cell lines. In order to validate these results in patient, we stratified the tumor samples by IHC (using EGFR, CK5/6, and Vimentin) in BL, ML or NonBLML. High FASN expression was significantly higher in BL (52.5%) than in ML (19.2%). FASN have been associated with high proliferative phenotypes, recurrence and poor outcome in several cancer[59,206,211,212]. Consistently, Basal-like breast cancer has been described as a high-proliferative subtype, while ML show lower proliferative features[29].

When analyzing FASN association with clinical and histopathological characteristics, we found that high FASN expressing patients showed lower OS and DFS, and were significantly associated with positive node status, one of the most powerful markers to predict relapse[223,224]. FASN expression was also found to be negatively correlated with Vimentin levels, a mesenchymal marker highly associate with ML subtype, an intrinsic subtype that we found to be associated with Low FASN expression group.

EGFR is commonly expressed in TNBC[35,183], and its over-expression has been linked to tumor initiation and progression in cancer[126]. *In vitro*, almost all cell lines showed constitutive activation of this receptor. The IHC in TNBC tumor samples showed positive staining for 75.9% of the core biopsies analyzed (n=29) and 45% of the TMAs (n=100). Similar studies showed that EGFR expression is positive in 50-70% of TNBC samples[39,49]. The differences in EGFR positive staining between the two patients' samples cohorts might be due to study size, sample antiquity, or sample inclusion protocol to paraffin. For instance, the diagnosis date of the patient cohort used in the biopsy-core study ranged from 2007 to 2012, while the TMA range starts in 1990 until 2012. Furthermore, core biopsy inclusion protocol is very strict and controlled compared to lumpectomy samples, which also can diverge in size, shape and volume.

The correlation between EGFR expression and poor survival has been observed in other studies of breast cancer, including TNBC[135,136]. In our hands, EGFR positive expression showed poor OS and DSF compared to EGFR-negative patients, although the differences observed were not significant. On the other hand, high EGFR expression (3+) was significantly associated with poor DFS.

Triple-negative breast cancer patients are mainly restricted to a treatment based on a combination of anthracyclines and taxanes, as they lack an approved target therapy. Although TNBC have a higher sensitivity to chemotherapy[42], this subtype of cancer show the highest relapse rates compared to other subtypes[19,20].

Overexpression of EGFR in breast cancer patients after chemotherapy has been already described to be correlated with higher local recurrence, metastasis and so poor outcome[135,136,193]. Here we showed that basal-like doxorubicin-resistant cell line HCC**DXR** increased total EGFR protein level, and thus sensitized this cell line to the EGFR inhibitor cetuximab, both *in vitro* and *in vivo*.

FASN overexpression give cancer cells the essential building blocks to keep its high proliferation rate, but also, plays an important role in drug resistance. Recent studies pointed out that FASN activity allows fast synthesis of new phospholipids for membrane remodeling and plasticity[184,186], and that FASN blockade, can reverse chemoresistance in ovarian and hepatocellular models[104,188].

Our results showed that FASN inhibition re-sensitized resistant cell lines to doxorubicin when treated in combination, while FASN inhibition alone showed no differences between parental and resistant cell lines. The evaluation of FASN expression after doxorubicin treatment in the Mesenchymal-like subtype cell line (231) and its resistant derivate (231**DXR**), showed increased expression in both models after 24h, but interestingly increased significantly in the resistant cell line.

The urge for the development of new targeted therapies to treat TNBC patients is in the spotlight of many studies. The common expression of EGFR in TNBC (and its relationship with progression after therapy) and the findings that FASN enzyme is overexpressed in TNBC (both tumor samples and pre-clinical models), provided the rational to test combined FASN inhibitors (C75, EGCG and G28) and the EGFR inhibitor cetuximab.

The simultaneous treatment of cetuximab with C75, EGCG or G28 resulted in strong synergism in all cell lines, both sensitive and resistant to doxorubicin. *In vivo*, the combination of cetuximab and EGCG improved the mono treatments in all cell lines, in spite of the HCC**DXR** cell line, where EGFR overexpression sensitized this cell line to cetuximab treatment and the combination effect could not be evaluated. Western blot results showed that the combination enhanced EGFR downstream inhibition in both cell lines and lead to apoptosis activation.

EGFR localization in the plasma membrane is confined to lipid raft, which are dynamic micro domains enriched in phospholipids. FASN inhibition in cancer cells, lead to a lack of phospholipids, disrupting lipid raft stability and therefore delocalizing the proteins anchored in this micro domains, such as EGFR[64,66,198]. Furthermore, protein correct localization through the addition of palmitate (a post-translational modification) is also disrupted after FASN inhibition. For instance, Bollu *et al.* found that FASN-dependent palmitoylation of EGFR is required for EGFR dimerization and kinase activation [202], event also observed in mitochondrial EGFR[203].

We and others have previously identified EGCG as an inhibitor of FASN activity, able to induce apoptosis in several tumor cell lines and also to reduce the size of mammary tumors in animal models[97,99,112,113,197]. EGCG antitumor effects might be not be only due to FASN inhibition activity, but probably by binding with other cellular targets[196]. Interestingly EGCG has been described to be closely associated with destabilization and inhibition of EGFR receptor and downstream signaling pathways [199–201].

The theory of Cancer Stem Cells had arisen in the last years, with evidences that cells within the tumor having stem cell features might be responsible for drug resistance and relapse[32,157,225]. The molecular classification of breast cancer identified an intrinsic subtype within the TNBC group, called claudin-low (also known as Mesenchymal-like, ML), enriched with stem cells features[29]. The evaluation of the CSC enriched population in a ML cell line and its resistance derivate showed increased CSC features in the resistant cell line and in both sensible and resistant cell lines after doxorubicin treatment.

We have identified here FASN as possible co-target to overcome drug resistance in two doxorubicin models, and therefore we checked FASN expression during drug treatment. Interestingly, we observed that FASN increased significantly after doxorubicin treatment in the resistant cell line. FASN increased expression after drug resistance acquisition is a mechanism already described in breast cancer[226]. Considering this both facts, we decided to evaluate FASN inhibition effect in the CSC enriched population using the mammosphere forming assay approach.

Our results showed that both C75 and the novel FASN inhibitor G28 inhibited at the same or increased level respectively the mammosphere forming ability compared to adherent conditions. Even these results are still preliminary and more approaches should be perform, some recently published studies support the fact that FASN not also plays a role in highly proliferative neoplasia, but also in drug resistance and in maintaining malignancy in cancer[118,221,222].

In summary, the results of this thesis showed that FASN is expressed in both pre-clinical models and in in almost all TNBC patients. Furthermore, different expression levels of FASN between molecular subtypes observed *in vitro* correlate with those obtained in tumor patients, showing that pre-clinical models might reflect the features of

those observed in TNBC patients. In addition, Patients with tumors that express high levels of FASN seemed to have poor prognosis (positive node association, lower DFS and OS but not significantly) compared to those with lower or none expression, although this results should be validated in a larger cohort of patients. Furthermore, we have shown that EGFR is commonly expressed in our patient cohort, with similar results obtained by other authors, and that EGFR positivity correlates with poor outcome.

Our results suggested that fatty acid synthesis through FASN activity increasing might play a crucial role in drug resistance and therefore, the inhibition of its activity could also provide a new strategy to overcome drug resistance. Interestingly, FASN and EGFR inhibition lead to a synergic effect in triple-negative cell lines *in vitro* and *in vivo.* In addition, several studies pointed out that a direct link between palmitate and EGFR correct function might be disturbed after FASN inhibition and therefore this combination might be feasible for the treatment of cancer that express both markers, such as TNBC.

Conclusions

1. FASN is expressed in cellular models and tumor samples of TNBC and its expression is associated with positive lymph node status, one of the most powerful markers to predict relapse.

2. Basal-like tumor samples and Basal-like cell lines express higher FASN levels than Mesenchymal-like ones, being Basal-like cell lines more sensitive to specific FASN inhibitors. Furthermore, FASN is negatively correlated with Vimentin expression, a mesenchymal marker highly associate to the low proliferative intrinsic subgroup Mesenchymal-like.

3. Doxorubicin-resistant cell lines express FASN and are sensitive to FASN inhibitors at same levels as parental cell lines, but the addition of these inhibitors to doxorubicin treatment re-sensitize resistant cell lines to common chemotherapy. Furthermore, our preliminary results showed FASN inhibitors may be efficient to inhibit CSC enriched population, suggesting that FASN might not also play a role in highly proliferative neoplasia, but also in drug resistance and malignancy in cancer.

4. EGFR is expressed in TNBC cell lines and patient samples (92% in core-biopsy studies and 45% in TMA) and high EGFR expression (3+) was significantly associated with poor DSF. Furthermore, patients with EGFR positivity showed poor DFS and OS compared to the negative ones.

5. FASN inhibitors (EGCG, C75 or G28) synergized with cetuximab *in vitro* with both Mesenchymal-like and Basal-like cell lines, and the FASN inhibitor EGCG showed marked anti-tumor activity *in vivo* compared to the mono-treatments.

6. Molecular interaction showed that the addition of EGCG to cetuximab treatment resulted in enhanced EGFR downstream inhibition, suggesting (and supported by other studies) that a direct link between palmitate and EGFR correct function might be disturbed after FASN activity blocking.

7. Mesenchymal-like cell line 231**DXR** might be a useful *in vitro* model to study CSC evolution during chemotherapy resistance acquisition and to help treatment development as several features observed by other studies using tumor patients or in vivo studies were reflected in this model.

The general conclusion of this thesis is that Fatty Acid Synthase (FASN) is expressed in pre-clinical models and in tumor samples of triple-negative breast cancer, and additionally, high FASN expression is associated with several poor prognosis factors such as positive-node involvement. The inhibition of its activity in combination with doxorubicin re-sensitizes resistant cell lines to the primary treatment, and interestingly, its inhibition in combination with an EGFR inhibitor synergizes in both cellular and animal models. Our findings encourage us to think that FASN has a role not only in cancer progression but in resistance-acquisition to general chemotherapy, and that its inhibition in combination with EGFR could be a potential therapeutic target in primary TNBC and in those patients who progressed after therapy. However, further preclinical and clinical studies should be performed to elucidate the potential of FASN inhibition for the treatment of TNBC.

Bibliography

1. DeSantis CE, Lin CC, Mariotto AB, Siegel RL, Stein KD, Kramer JL, Alteri R, Robbins AS, J. A. Cancer treatment and survivorship statistics, 2014. *CA Cancer J Clin* **64,** 252–71 (2014).
2. Siegel, R. L., Miller, K. D. & Jemal, A. Cancer statistics. **66,** 7–30 (2016).
3. La Vecchia, C., Rota, M., Malvezzi, M. & Negri, E. Potential for improvement in cancer management: reducing mortality in the European union. *Oncologist* **20,** 495–8 (2015).
4. World Health Organization. Cancer data and statistics. (2016). Available at: http://www.euro.who.int/en/health-topics/noncommunicable-diseases/cancer/data-and-statistics.
5. NIH. National Institute of Health (NIH). Available at: http://www.cancer.gov/about-cancer/understanding/what-is-cancer.
6. Hanahan, D. & Weinberg, R. A. The Hallmarks of Cancer. in *Cell* **100,** 57–70 (2000).
7. Hanahan, D. & Weinberg, R. A. Hallmarks of cancer: The next generation. *Cell* **144,** 646–674 (2011).
8. World Health Organization. *World Cancer Report 2014*. (2014).
9. Carey, L. A. *et al.* Race , Breast Cancer Subtypes , and Survival in the Carolina Breast Cancer Study. *JAMA* **295,** 2492–2502 (2006).
10. Sorlie, T. *et al.* Repeated observation of breast tumor subtypes in independent gene expression data sets. *Proc. Natl. Acad. Sci. U. S. A.* **100,** 8418–23 (2003).
11. Swaby, R. F., Sharma, C. G. N. & Jordan, V. C. SERMs for the treatment and prevention of breast cancer. *Rev. Endocr. Metab. Disord.* **8,** 229–239 (2007).
12. Lumachi, F., Santeufemia, D. A. & Basso, S. M. Current medical treatment of estrogen receptor-positive breast cancer. *World J. Biol. Chem.* **6,** 231–9 (2015).
13. Holbro, T. *et al.* The ErbB2/ErbB3 heterodimer functions as an oncogenic unit: ErbB2 requires ErbB3 to drive breast tumor cell proliferation. *Proc. Natl. Acad. Sci. U. S. A.* **100,** 8933–8 (2003).
14. Slamon, D. J. *et al.* Human breast cancer: correlation of relapse and survival with amplification of the HER-2/neu oncogene. *Science (80-.).* **235,** 177–182 (1987).
15. Witton, C. J., Reeves, J. R., Going, J. J., Cooke, T. G. & Barlett, J. M. S. Expression of the HER1-4 family of receptor tyrosine kinases in breast cancer. *Journal of Pathology* **200,** 290–297 (2003).
16. Yarden, Y. The EGFR family and its ligands in human cancer. signalling mechanisms and therapeutic opportunities. *Eur. J. Cancer* **37 Suppl 4,** S3–S8 (2001).
17. Barros, F. F. T. F. T., Powe, D. G., Ellis, I. O. & Green, A. R. Understanding the HER family in breast cancer: Interaction with ligands, dimerization and treatments. *Histopathology* **56,** 560–572 (2010).
18. Bauer, K. R., Brown, M., Cress, R. D., Parise, C. A. & Caggiano, V. Descriptive analysis of estrogen receptor (ER)-negative, progesterone receptor (PR)-negative, and HER2-negative invasive breast cancer, the so-called triple-negative phenotype: a population-based study from the California cancer Registry. *Cancer* **109,** 1721–8 (2007).
19. Dent, R. *et al.* Triple-negative breast cancer: clinical features and patterns of recurrence. *Clin. Cancer Res.* **13,** 4429–34 (2007).
20. Carey, L. A. *et al.* The triple negative paradox: primary tumor chemosensitivity of breast cancer subtypes. *Clin. Cancer Res.* **13,** 2329–34 (2007).
21. DeVita, V., Lawrence, T. & Rosenber, S. *Cancer: Principles & Practice of Oncology*. (Wolters Kluber / Lippincott Wiliams & Wilkins, 2008).
22. Tuttle, T. M. *et al.* A Review of Technical Aspects of Sentinel Lymph Node Identification for Breast Cancer. *J Am Coll Surg* **7515,** 261–268 (2002).
23. Urruticoechea, A., Smith, I. E. & Dowsett, M. Proliferation marker Ki-67 in early breast cancer. *J. Clin. Oncol.* **23,** 7212–7220 (2005).
24. Hammond, M. E. H. *et al.* American Society of Clinical Oncology/College Of American Pathologists guideline recommendations for immunohistochemical testing of estrogen and progesterone receptors in breast cancer. *J. Clin. Oncol.* **28,** 2784–95 (2010).
25. Sørlie, T. *et al.* Gene expression patterns of breast carcinomas distinguish tumor subclasses with clinical implications. *PNAS* **98,** (2001).
26. Hynes, N. E. & Lane, H. a. ERBB receptors and cancer: the complexity of targeted inhibitors. *Nat. Rev. Cancer* **5,** 341–54 (2005).
27. Prat, A. & Perou, C. M. Deconstructing the molecular portraits of breast cancer. *Mol. Oncol.* **5,** 5–23 (2011).
28. Perou, C. M. *et al.* Molecular portraits of human breast tumours. *Nature* **406,** 747–752 (2000).
29. Prat, A. *et al.* Phenotypic and molecular characterization of the claudin-low intrinsic subtype of breast cancer. (2010).
30. Herschkowitz, J. *et al.* Identification of conserved gene expression features between murine mammary carcinoma models and human breast tumors. *Genome Biol* **8,** R76 (2007).
31. Lehmann, B. D. *et al.* Identification of human triple-negative breast cancer subtypes and preclinical models for selection of targeted therapies. *J. Clin. Invest.* **121,** (2011).
32. Creighton, C. J. *et al.* Residual breast cancers after conventional therapy display mesenchymal as well as tumor-initiating features. *Proc. Natl. Acad. Sci. U. S. A.* **106,** 13820–13825 (2009).
33. Bernard, P. S. *et al.* Supervised risk predictor of breast cancer based on intrinsic subtypes. *J. Clin. Oncol.* **27,** 1160–1167 (2009).

34. Perou, C. & Borresen, A. Systems Biology and Genomics of Breast Cancer. *Cold spring Harb Perspect Biol* 1–18 (2011). doi:10.1101/cshperspect.a003293
35. Bertucci, F., Finetti, P. & Birnbaum, D. Basal Breast Cancer: A Complex and Deadly Molecular Subtype. *Curr. Mol. Med.* **12,** 96–110 (2012).
36. Perou, C. M. Comprehensive molecular portraits of human breast tumors. *Nature* **490,** 61–70 (2012).
37. Yamamoto, Y. *et al.* Clinical significance of basal-like subtype in triple-negative breast cancer. *Breast Cancer* **16,** 260–267 (2009).
38. Cheang, M. C. U. *et al.* Basal-like breast cancer defined by five biomarkers has superior prognostic value than triple-negative phenotype. *Clin. Cancer Res.* **14,** 1368–1376 (2008).
39. Nielsen, T. O. *et al.* Immunohistochemical and Clinical Characterization of the Basal-Like Subtype of Invasive Breast Carcinoma. *Clin. Cancer Res.* **10,** 5367–5374 (2004).
40. Gerhard, R. *et al.* Immunohistochemical features of claudin-low intrinsic subtype in metaplastic breast carcinomas. *Breast* **21,** 354–360 (2012).
41. Choi, J., Jung, W.-H. & Koo, J. S. Clinicopathologic features of molecular subtypes of triple negative breast cancer based on immunohistochemical markers. *Histol. Histopathol.* **27,** 1481–1493 (2012).
42. Liedtke, C. *et al.* Response to neoadjuvant therapy and long-term survival in patients with triple-negative breast cancer. *J. Clin. Oncol.* **26,** 1275–81 (2008).
43. Metzger-Filho, O. *et al.* Dissecting the heterogeneity of triple-negative breast cancer. *J. Clin. Oncol.* **30,** 1879–1887 (2012).
44. O'Shaughnessy, J. *et al.* Iniparib plus Chemotherapy in Metastatic Triple-Negative Breast Cancer. *N. Engl. J. Med.* **364,** 205–214 (2011).
45. Gibson, J. Anti-PD-L1 for metastatic triple-negative breast cancer. *Lancet Oncol.* **16,** e264 (2015).
46. García-Teijido, P., Cabal, M. L., Fernández, I. P. & Pérez, Y. F. Tumor-Infiltrating Lymphocytes in Triple Negative Breast Cancer: The Future of Immune Targeting. *Clin. Med. Insights. Oncol.* **10,** 31–9 (2016).
47. Rose, A. A. N. *et al.* Glycoprotein nonmetastatic b is an independent prognostic indicator of recurrence and a novel therapeutic target in breast cancer. *Clin. Cancer Res.* **16,** 2147–2156 (2010).
48. Yardley, D. A. *et al.* EMERGE: A randomized phase II study of the antibody-drug conjugate glembatumumab vedotin in advanced glycoprotein NMB - Expressing breast cancer. *J. Clin. Oncol.* **33,** 1609–1619 (2015).
49. Lehmann, B. D. & Pietenpol, J. A. Identification and use of biomarkers in treatment strategies for triple-negative breast cancer subtypes. *J. Pathol.* **232,** 142–150 (2014).
50. Warburg, O. On the origin of cancer Cells. *Science (80-.).* **123,** 309–314 (1956).
51. Devic, S. Warburg Effect - a Consequence or the Cause of Carcinogenesis? *J. Cancer* **7,** 817–22 (2016).
52. Ward, P. S. & Thompson, C. B. Metabolic Reprogramming: A Cancer Hallmark Even Warburg Did Not Anticipate. *Cancer Cell* **21,** 297–308 (2012).
53. Currie, E., Schulze, A., Zechner, R., Walther, T. C. & Farese, R. V. Cellular fatty acid metabolism and cancer. *Cell Metab.* **18,** 153–161 (2013).
54. Kuhajda, F. P. Fatty-acid synthase and human cancer: new perspectives on its role in tumor biology. *Nutrition* **16,** 202–208 (2000).
55. Wakil, S. J. Fatty Acid Synthase, A Proficient Multifunctional Enzyme. *Biochemestry* **28,** 4523–4530 (1989).
56. Zaytseva, Y. Y. *et al.* Increased expression of fatty acid synthase provides a survival advantage to colorectal cancer cells via upregulation of cellular respiration. *Oncotarget* **6,** 18891–18904 (2015).
57. Witkiewicz, A. K. *et al.* Co-expression of fatty acid synthase and caveolin-1 in pancreatic ductal adenocarcinoma: Implications for tumor progression and clinical outcome. *Cell Cycle* **7,** 3021–3025 (2008).
58. Shah, U. S. *et al.* Fatty acid synthase gene overexpression and copy number gain in prostate adenocarcinoma. *Hum. Pathol.* **37,** 401–409 (2006).
59. Veigel, D. *et al.* Fatty acid synthase is a metabolic marker of cell proliferation rather than malignancy in ovarian cancer and its precursor cells. *Int. J. Cancer* **136,** 2078–2090 (2015).
60. Sul, H. S. & Wang, D. Nutritional and hormonal regulation of enzymes in fat synthesis: studies of fatty acid synthase and mitochondrial glycerol-3-phosphate acyltransferase gene transcription. *Annu. Rev. Nutr.* **18,** 331–351 (1998).
61. Katsurada, a *et al.* Effects of nutrients and hormones on transcriptional and post-transcriptional regulation of fatty acid synthase in rat liver. *Eur. J. Biochem.* **190,** 427–433 (1990).
62. Macias, H. & Hinck, L. Mammary gland development. *Wiley Interdisciplinary Reviews: Developmental Biology* **1,** 533–557 (2012).
63. Anderson, S. M., Rudolph, M. C., McManaman, J. L. & Neville, M. C. Key stages in mammary gland development. Secretory activation in the mammary gland: it's not just about milk protein synthesis! *Breast Cancer Res.* **9,** 204 (2007).
64. Menendez, J. a & Lupu, R. Fatty acid synthase and the lipogenic phenotype in cancer pathogenesis. *Nat. Rev. Cancer* **7,** 763–77 (2007).
65. Ventura, R. *et al.* Inhibition of de novo Palmitate Synthesis by Fatty Acid Synthase Induces Apoptosis in Tumor Cells by Remodeling Cell Membranes, Inhibiting Signaling Pathways, and Reprogramming Gene Expression. *EBioMedicine* **2,** 806–22 (2015).
66. Jones, S. F. & Infante, J. R. Molecular Pathways: Fatty Acid Synthase. *Clin. Cancer Res.* 1–16 (2015).

doi:10.1158/1078-0432.CCR-15-0126
67. Weiss, L. *et al.* Fatty-Acid Biosynthesis in Man, a Pathway of Minor Importance Purification, Optimal Assay Conditions, and Organ Distribution of Fatty-Acid Synthase. *Biol. Chem. Hoppe. Seyler.* **367,** 905–912 (1986).
68. Pizer, E. S., Kurman, R. J., Pasternack, G. R. & Kuhajda, F. P. Expression of fatty acid synthase is closely linked to proliferation and stromal decidualization in cycling endometrium. *Int. J. Gynecol. Pathol.* **16,** 45–51 (1997).
69. Schweizer, M., Roder, K., Zhang, L. & Wolf, S. S. Transcription factors acting on the promoter of the rat fatty acid synthase gene. *Biochem. Soc. Trans.* **30,** 1070–1072 (2002).
70. Swierczynski, J. Leptin and age-related down-regulation of lipogenic enzymes genes expression in rat white adipose tissue. in *Journal of Physiology and Pharmacology* **57,** 85–102 (2006).
71. Swinnen, J. V. *et al.* Overexpression of fatty acid synthase is an early and common event in the development of prostate cancer. *Int. J. Cancer* **98,** 19–22 (2002).
72. Kumar-Sinha, C., Ignatoski, K., Lippman, M., Ethier, S. & Chinnaiyan, A. Transcriptome analysis of HER2 reveals a molecular connection to fatty acid synthesis. *Cancer Res* **63,** 132–9 (2003).
73. Menendez, J. A., Mehmi, I., Verma, V. A., Teng, P. K. & Lupu, R. Pharmacological inhibition of fatty acid synthase (FAS): A novel therapeutic approach for breast cancer chemoprevention through its ability to suppress Her-2/neu (erbB-2) oncogene-induced malignant transformation. *Mol. Carcinog.* **41,** 164–178 (2004).
74. Sande, T. Van De, Schrijver, E. De, Heyns, W., Verhoeven, G. & Swinnen, J. V. Advances in Brief Role of the Phosphatidylinositol 3 -Kinase / PTEN / Akt Kinase Pathway in the Overexpression of Fatty Acid Synthase in LNCaP Prostate Cancer Cells 1. 642–646 (2002).
75. Wang, H. Q. *et al.* Positive feedback regulation between AKT activation and fatty acid synthase expression in ovarian carcinoma cells. *Oncogene* **24,** 3574–82 (2005).
76. Heemers, H. *et al.* Androgens stimulate lipogenic gene expression in prostate cancer cells by activation of the sterol regulatory element-binding protein cleavage activating protein/sterol regulatory element-binding protein pathway. *Mol. Endocrinol.* **15,** 1817–28 (2001).
77. Graner, E. *et al.* The isopeptidase USP2a regulates the stability of fatty acid synthase in prostate cancer. *Cancer Cell* **5,** 253–261 (2004).
78. Maier, T., Jenni, S. & Ban, N. Architecture of Mammalian Fatty Acid Synthase at 4.5 A ˚ Resolution. **311,** 1258–1263 (2006).
79. Asturias, F. J. *et al.* Structure and molecular organization of mammalian fatty acid synthase. *Nat. Struct. Mol. Biol.* **12,** 225–232 (2005).
80. Flavin, R., Peluso, S., Nguyen, P. L. & Loda, M. Fatty acid synthase as a potential therapeutic target in cancer. *Futur. Oncol.* **6,** 551–562 (2010).
81. Funabashi, H. *et al.* Binding site of cerulenin in fatty acid synthetase. *J. Biochem.* **105,** 751–755 (1989).
82. Kuhajda, F. P. *et al.* Synthesis and antitumor activity of an inhibitor of fatty acid synthase. *Proc. Natl. Acad. Sci.* **97,** 3450–3454 (2000).
83. Rendina, A. R. & Cheng, D. Characterization of the inactivation of rat fatty acid synthase by C75: inhibition of partial reactions and protection by substrates. *Biochem. J.* **388,** 895–903 (2005).
84. McFadden, J. M. *et al.* Application of a flexible synthesis of (5R)-thiolactomycin to develop new inhibitors of type I fatty acid synthase. *J. Med. Chem.* **48,** 946–961 (2005).
85. Kridel, S. J. Orlistat Is a Novel Inhibitor of Fatty Acid Synthase with Antitumor Activity. *Cancer Res.* **64,** 2070–2075 (2004).
86. Sadowski, M. C. *et al.* The fatty acid synthase inhibitor triclosan : repurposing an anti- microbial agent for targeting prostate cancer. **5,** (2014).
87. Wang, X. & Tian, W. Green tea epigallocatechin gallate: a natural inhibitor of fatty-acid synthase. *Biochem. Biophys. Res. Commun.* **288,** 1200–1206 (2001).
88. Oliveras, G. *et al.* Novel anti-fatty acid synthase compounds with anti-cancer activity in HER2+ breast cancer. *Ann. N. Y. Acad. Sci.* **1210,** 86–92 (2010).
89. Puig, T. *et al.* A novel inhibitor of fatty acid synthase shows activity against HER2+ breast cancer xenografts and is active in anti-HER2 drug-resistant cell lines. *Breast Cancer Res.* **13,** R131 (2011).
90. Hardwicke, M. A. *et al.* A human fatty acid synthase inhibitor binds β-ketoacyl reductase in the keto-substrate site. *Nat Chem Biol* **10,** 774–779 (2014).
91. Shaw, G. *et al.* 509 THERAPEUTIC FATTY ACID SYNTHASE INHIBITION IN PROSTATE CANCER AND THE USE OF 11C-ACETATE TO MONITOR THERAPEUTIC EFFECTS. *J. Urol.* **189,** e208–e209 (2016).
92. Lu, T. *et al.* Abstract 4747: Design and synthesis of a series highly potent and bioavailable FASN KR domain inhibitors for cancer. *Cancer Res.* **74,** 4747 (2014).
93. Brophy, E. *et al.* Abstract 1891: Pharmacological target validation studies of fatty acid synthase in carcinoma using the potent, selective and orally bioavailable inhibitor IPI-9119. *Cancer Res.* **73,** 1891 (2014).
94. Brenner, A. J. *et al.* First-in-human investigation of the oral first-in-class fatty acid synthase (FASN) inhibitor, TVB-2640. *J Clin Oncol (Meeting Abstr.* **33,** (2015).
95. Pizer, E. S. *et al.* Inhibition of Fatty Acid Synthesis Delays Disease Progression in a Xenograft Model of

Ovarian Cancer Advances in Brief Inhibition of Fatty Acid Synthesis Delays Disease Progression in a Xenograft Model of Ovarian Cancer1. 1189–1193 (1996).
96. Li, J. N. *et al.* Pharmacological inhibition of fatty acid synthase activity produces both cytostatic and cytotoxic effects modulated by p53. *Cancer Res.* **61,** 1493–1499 (2001).
97. Puig, T. *et al.* Fatty acid metabolism in breast cancer cells: differential inhibitory effects of epigallocatechin gallate (EGCG) and C75. *Breast Cancer Res. Treat.* **109,** 471–9 (2008).
98. Puig, T., Porta, R. & Colomer, R. Fatty acid synthase: a new anti-tumor target. *Med. Clin. (Barc).* **132,** 359–63 (2009).
99. Blancafort, A. *et al.* Dual Fatty Acid Synthase and HER2 Signaling Blockade Shows Marked Antitumor Activity against Breast Cancer Models Resistant to Anti-HER2 Drugs. *PLoS One* **10,** e0131241 (2015).
100. Bandyopadhyay, S. *et al.* Mechanism of apoptosis induced by the inhibition of fatty acid synthase in breast cancer cells. *Cancer Res.* **66,** 5934–40 (2006).
101. Seguin, F. *et al.* The fatty acid synthase inhibitor orlistat reduces experimental metastases and angiogenesis in B16-F10 melanomas. *Br. J. Cancer* **107,** 977–987 (2012).
102. Browne, C. D., Hindmarsh, E. J. & Smith, J. W. Inhibition of endothelial cell proliferation and angiogenesis by orlistat, a fatty acid synthase inhibitor. *FASEB J.* **20,** 2027–2035 (2006).
103. Meena, A. S. *et al.* Inherent and acquired resistance to paclitaxel in hepatocellular carcinoma: molecular events involved. *PLoS One* **8,** e61524 (2013).
104. Rysman, E. *et al.* De novo lipogenesis protects cancer cells from free radicals and chemotherapeutics by promoting membrane lipid saturation. *Cancer Res.* **70,** 8117–26 (2010).
105. Menendez, J. a, Vellon, L., Colomer, R. & Lupu, R. Pharmacological and small interference RNA-mediated inhibition of breast cancer-associated fatty acid synthase (oncogenic antigen-519) synergistically enhances Taxol (paclitaxel)-induced cytotoxicity. *Int. J. Cancer* **115,** 19–35 (2005).
106. Giró-Perafita, A. *et al. Preclinical Evaluation of Fatty Acid Synthase and EGFR Inhibition in Triple Negative Breast Cancer*. *Clinical cancer research : an official journal of the American Association for Cancer Research* (2016). doi:10.1158/1078-0432.CCR-15-3133
107. Kuhajda, F. P. *et al.* Fatty acid synthesis: a potential selective target for antineoplastic therapy. *Proc. Natl. Acad. Sci. U. S. A.* **91,** 6379–83 (1994).
108. Menendez, J. a & Lupu, R. Fatty acid synthase-catalyzed de novo fatty acid biosynthesis: from anabolic-energy-storage pathway in normal tissues to jack-of-all-trades in cancer cells. *Arch. Immunol. Ther. Exp. (Warsz).* **52,** 414–26 (2004).
109. Mollinedo, F. & Gajate, C. Lipid rafts as major platforms for signaling regulation in cancer. *Adv. Biol. Regul.* **57,** 130–146 (2015).
110. Simons, K. & Sampaio, J. L. Membrane organization and lipid rafts. *Perspect Biol* **3,** a004697 (2011).
111. Pizer, E. S. *et al.* Malonyl-coenzyme-A is a potential mediator of cytotoxicity induced by fatty-acid synthase inhibition in human breast cancer cells and xenografts. *Cancer Res.* **60,** 213–218 (2000).
112. Relat, J. *et al.* Different fatty acid metabolism effects of (-)-epigallocatechin-3-gallate and C75 in adenocarcinoma lung cancer. *BMC Cancer* **12,** 280 (2012).
113. Puig, T. *et al.* Novel Inhibitors of Fatty Acid Synthase with Anticancer Activity. *Clin. Cancer Res.* **15,** 7608–7615 (2009).
114. Vance, D. *et al.* Inhibition of fatty acid synthetases by the antibiotic cerulenin. *Biochem. Biophys. Res. Commun.* **48,** 649–656 (1972).
115. Alli, P. M., Pinn, M. L., Jaffee, E. M., McFadden, J. M. & Kuhajda, F. P. Fatty acid synthase inhibitors are chemopreventive for mammary cancer in neu-N transgenic mice. *Oncogene* **24,** 39–46 (2005).
116. Loftus, T. M. Reduced Food Intake and Body Weight in Mice Treated with Fatty Acid Synthase Inhibitors. *Science (80-.).* **288,** 2379–2381 (2000).
117. Swinnen, J. V *et al.* Stimulation of tumor-associated fatty acid synthase expression by growth factor activation of the sterol regulatory element-binding protein pathway. *Oncogene* **19,** 5173–81 (2000).
118. Gonzalez-Guerrico, A. M. *et al.* Suppression of endogenous lipogenesis induces reversion of the malignant phenotype and normalized differentiation in breast cancer. *Oncotarget* (2016). doi:10.18632/oncotarget.9463
119. Lee, K. H. *et al.* Targeting energy metabolic and oncogenic signaling pathways in triple-negative breast cancer by a novel adenosine monophosphate-activated protein kinase (AMPK) activator. *J. Biol. Chem.* **286,** 39247–39258 (2011).
120. Liu, B. *et al.* Metformin induces unique biological and molecular responses in triple negative breast cancer cells. *Cell Cycle* **8,** 2031–2040 (2009).
121. Kim, S., Lee, Y. & Koo, J. S. Differential expression of lipid metabolism-related proteins in different breast cancer subtypes. *PLoS One* **10,** e0119473 (2015).
122. Braicu, C. & Gherman, C. Epigallocatechin gallate induce cell death and apoptosis in triple negative breast cancer cells Hs578T. *J. Drug Target.* **21,** 250–256 (2012).
123. Wahdan-Alaswad, R. S. *et al.* Metformin-induced killing of triple-negative breast cancer cells is mediated by reduction in fatty acid synthase via miRNA-193b. *Horm. Cancer* **5,** 374–89 (2014).
124. van der Geer, P., Hunter, T. & Lindberg, R. A. Receptor protein-tyrosine kinases and their signal transduction pathways. *Annu. Rev. Cell Biol.* **10,** 251–337 (1994).

125. Prenzel, N., Fischer, O. M., Streit, S., Hart, S. & Ullrich, A. The epidermal growth factor receptor family as a central element for cellular signal transduction and diversification. in *Endocrine-Related Cancer* **8,** 11–31 (2001).
126. Porter, A. C. & Vaillancourt, R. R. Tyrosine kinase receptor-activated signal transduction pathways which lead to oncogenesis. *Oncogene* **17,** 1343–52 (1998).
127. Roskoski, R. ErbB/HER protein-tyrosine kinases: Structures and small molecule inhibitors. *Pharmacol. Res.* **87,** 42–59 (2014).
128. Yarden, Y. & Pines, G. The ERBB network: at last, cancer therapy meets systems biology. *Nat. Rev. Cancer* **12,** 553–563 (2012).
129. Flynn, J. F., Wong, C. & Wu, J. M. Anti-EGFR therapy: Mechanism and advances in clinical efficacy in breast cancer. *J. Oncol.* **2009,** (2009).
130. Wang, Z. *et al.* Mechanistic insights into the activation of oncogenic forms of EGF receptor. *Nat Struct Mol Biol* **18,** 1388–1393 (2011).
131. Baselga, J. The EGFR as a target for anticancer therapy-focus on cetuximab. *Eur. J. Cancer* **37,** S16–S22 (2001).
132. Vincenzi, B., Zoccoli, A., Pantano, F., Venditti, O. & Galluzzo, S. CETUXIMAB: From Bench to Bedside. *Curr. Cancer Drug Targets* **10,** 80–95 (2010).
133. Nelson, M. H. & Dolder, C. R. Lapatinib: a novel dual tyrosine kinase inhibitor with activity in solid tumors. *Ann. Pharmacother.* **40,** 261–9 (2006).
134. Herbst, R. S., Heymach, J. V & Lippman, S. M. Lung Cancer. *N. Engl. J. Med.* **359,** 1367–1380 (2008).
135. Park, H. S. *et al.* High EGFR gene copy number predicts poor outcome in triple-negative breast cancer. *Mod. Pathol.* **27,** 1–11 (2014).
136. Buchholz, T. a. *et al.* Epidermal growth factor receptor expression correlates with poor survival in patients who have breast carcinoma treated with doxorubicin-based neoadjuvant chemotherapy. *Cancer* **104,** 676–681 (2005).
137. Carey, L. a. *et al.* TBCRC 001: Randomized phase II study of cetuximab in combination with carboplatin in stage IV triple-negative breast cancer. *J. Clin. Oncol.* **30,** 2615–2623 (2012).
138. Baselga, J. M. *et al.* Randomized Phase II Study of the Anti-Epidermal Growth Factor Receptor Monoclonal Antibody Cetuximab With Cisplatin Versus Cisplatin Alone in Patients With Metastatic Triple-Negative Breast Cancer. *J. Clin. Oncol.* **31,** 1–8 (2013).
139. Reya, T., Morrison, S. J., Clarke, M. F. & Weissman, I. L. Stem cells, cancer, and cancer stem cells. **414,** 105–111 (2001).
140. Al-Hajj, M., Wicha, M. S., Benito-Hernandez, A., Morrison, S. J. & Clarke, M. F. Prospective identification of tumorigenic breast cancer cells. *Proc. Natl. Acad. Sci. U. S. A.* **100,** 3983–8 (2003).
141. Dontu, G. *et al.* In vitro propagation and transcriptional profiling of human mammary stem / progenitor cells. *genes Dev.* **17,** 1253–1270 (2003).
142. Huang, E. H. *et al.* NIH Public Access. **69,** 3382–3389 (2010).
143. Ginestier, C. *et al.* ALDH1 Is a Marker of Normal and Malignant Human Mammary Stem Cells and a Predictor of Poor Clinical Outcome. *Cell Stem Cell* **1,** 555–567 (2007).
144. Dean, M., Fojo, T. & Bates, S. Tumour stem cells and drug resistance. *Nat Rev Cancer* **5,** 275–284 (2005).
145. Eyler, C. & Rich, J. Survival of the fittest: cancer stem cells in therapeutic resistance and angiogenesis. *J. Clin. Oncol.* **26,** 2839–2845 (2008).
146. Bonnefoix, T., Bonnefoix, P., Verdiel, P. & Sotto, J. J. Fitting limiting dilution experiments with generalized linear models results in a test of the single-hit Poisson assumption. *J. Immunol. Methods* **194,** 113–119 (1996).
147. Dick, J. E., Bhatia, M., Gan, O., Kapp, U. & Wang, J. C. Assay of human stem cells by repopulation of NOD/SCID mice. *Stem Cells* **15 Suppl 1,** 199-203–7 (1997).
148. Charafe-Jauffret, E., Ginestier, C. & Birnbaum, D. Breast cancer stem cells: tools and models to rely on. *BMC Cancer* **9,** 202 (2009).
149. Jaggupilli, A. & Elkord, E. Significance of CD44 and CD24 as cancer stem cell markers: An enduring ambiguity. *Clin. Dev. Immunol.* **2012,** (2012).
150. Stuelten, C. H. *et al.* Complex display of putative tumor stem cell markers in the NCI60 tumor cell line panel. *Stem Cells* **28,** 649–660 (2010).
151. Wang, R. *et al.* Comparison of mammosphere formation from breast cancer cell lines and primary breast tumors. *J. Thorac. Dis.* **6,** 829–837 (2014).
152. Shaw, F. L. *et al.* A detailed mammosphere assay protocol for the quantification of breast stem cell activity. *J. Mammary Gland Biol. Neoplasia* **17,** 111–7 (2012).
153. Manuel Iglesias, J. *et al.* Mammosphere formation in breast carcinoma cell lines depends upon expression of E-cadherin. *PLoS One* **8,** e77281 (2013).
154. Armstrong, L. *et al.* Phenotypic characterization of murine primitive hematopoietic progenitor cells isolated on basis of aldehyde dehydrogenase activity. *Stem Cells* **22,** 1142–1151 (2004).
155. Mieog, J. S. D. *et al.* Age determines the prognostic role of the cancer stem cell marker aldehyde dehydrogenase-1 in breast cancer. *BMC Cancer* **12,** 42 (2012).

156. Domingo-Domenech, J. *et al.* Suppression of Acquired Docetaxel Resistance in Prostate Cancer through Depletion of Notch- and Hedgehog-Dependent Tumor-Initiating Cells. *Cancer Cell* **22,** 373–388 (2012).
157. Vidal, S. J., Rodriguez-Bravo, V., Galsky, M., Cordon-Cardo, C. & Domingo-Domenech, J. Targeting cancer stem cells to suppress acquired chemotherapy resistance. *Oncogene* 1–13 (2013). doi:10.1038/onc.2013.411
158. Li, X. *et al.* Intrinsic resistance of tumorigenic breast cancer cells to chemotherapy. *J. Natl. Cancer Inst.* **100,** 672–679 (2008).
159. Yu, F. *et al.* let-7 Regulates Self Renewal and Tumorigenicity of Breast Cancer Cells. *Cell* **131,** 1109–1123 (2007).
160. Sakakibara, M. *et al.* Aldehyde dehydrogenase 1-positive cells in axillary lymph node metastases after chemotherapy as a prognostic factor in patients with lymph node-positive breast cancer. *Cancer* **118,** 3899–3910 (2012).
161. Tudoran, O. *et al.* Regulation of stem cells-related signaling pathways in response to doxorubicin treatment in Hs578T triple-negative breast cancer cells. *Mol. Cell. Biochem.* **409,** 163–176 (2015).
162. Hoey, T. *et al.* DLL4 blockade inhibits tumor growth and reduces tumor-initiating cell frequency. *Cell Stem Cell* **5,** 168–177 (2009).
163. Muñoz, P., Iliou, M. S. & Esteller, M. Epigenetic alterations involved in cancer stem cell reprogramming. *Mol. Oncol.* **6,** 620–36 (2012).
164. Thiery, J. P. Epithelial-mesenchymal transitions in development and pathologies. *Curr. Opin. Cell Biol.* **15,** 740–746 (2003).
165. Singh, A. & Settleman, J. EMT cancer stem cells and drug resistance. *Oncogene* **29,** 4741–4751 (2010).
166. Thiery, J. P. Epithelial-mesenchymal transitions in tumour progression. *Nat. Rev. Cancer* **2,** 442–54 (2002).
167. Scheel, C. & Weinberg, R. a. Cancer stem cells and epithelial-mesenchymal transition: Concepts and molecular links. *Semin. Cancer Biol.* **22,** 396–403 (2012).
168. Huber, M. A., Kraut, N. & Beug, H. Molecular requirements for epithelial-mesenchymal transition during tumor progression. *Current Opinion in Cell Biology* **17,** 548–558 (2005).
169. Tomaskovic-Crook, E., Thompson, E. W. & Thiery, J. P. Epithelial to mesenchymal transition and breast cancer. *Breast Cancer Res.* **11,** 213 (2009).
170. Marjanovic, N. D., Weinberg, R. a. & Chaffer, C. L. Cell plasticity and heterogeneity in cancer. *Clin. Chem.* **59,** 168–179 (2013).
171. Mani, S. A. *et al.* The epithelial-mesenchymal transition generetes cell with properties of stem cells. *Cell* **133,** 704–715 (2008).
172. Morel, A.-P. *et al.* Generation of breast cancer stem cells through epithelial-mesenchymal transition. *PLoS One* **3,** e2888 (2008).
173. Polyak, K. & Weinberg, R. A. Transitions between epithelial and mesenchymal states: acquisition of malignant and stem cell traits. *Nat. Rev. Cancer* **9,** 265–273 (2009).
174. Edge, S. B. & American Joint Committee on Cancer. *AJCC cancer staging manual.* (Springer, 2010).
175. Sarrió, D. *et al.* Epithelial-mesenchymal transition in breast cancer relates to the basal-like phenotype. *Cancer Res.* **68,** 989–997 (2008).
176. IBM Corp. Released 2015. IBM SPSS Statistics for Windows, Version 23.0. Armonk, NY: IBM Corp.
177. R Core Team (2016). R: A language and environment for statistical computing. R Foundation for Statistical Computing, Vienna, Austria. URL http://www.R-project.org/.
178. Corkery, B., Crown, J., Clynes, M. & O'Donovan, N. Epidermal growth factor receptor as a potential therapeutic target in triple-negative breast cancer. *Ann. Oncol.* **20,** 862–867 (2009).
179. Martin, V. *et al.* Molecular characterization of EGFR and EGFR-downstream pathways in triple negative breast carcinomas with basal like features. *Histol. Histopathol.* **27,** 785–792 (2012).
180. Ferraro, D. a *et al.* Inhibition of triple-negative breast cancer models by combinations of antibodies to EGFR. *Proc. Natl. Acad. Sci. U. S. A.* **110,** 1815–20 (2013).
181. Yamashita, N. *et al.* Vimentin as a poor prognostic factor for triple-negative breast cancer. *J. Cancer Res. Clin. Oncol.* **139,** 739–746 (2013).
182. Rijn, M. Van De *et al.* Expression of Cytokeratins 17 and 5 Identifies a Group of Breast Carcinomas with Poor Clinical Outcome. **161,** 1991–1996 (2002).
183. Hoadley, K. a *et al.* EGFR associated expression profiles vary with breast tumor subtype. *BMC Genomics* **8,** 258 (2007).
184. Liu, H. *et al.* Fatty acid synthase causes drug resistance by inhibiting TNF-α and ceramide production. *J. Lipid Res.* **54,** 776–85 (2013).
185. Zeng, L. *et al.* Saturated fatty acids modulate cell response to DNA damage: implication for their role in tumorigenesis. *PLoS One* **3,** e2329 (2008).
186. Wu, X., Qin, L., Fako, V. & Zhang, J.-T. Molecular mechanisms of fatty acid synthase (FASN)-mediated resistance to anti-cancer treatments. *Adv. Biol. Regul.* **54,** 214–21 (2014).
187. Talebi, A., Dehairs, J. & Swinnen, J. V. De novo lipogenesis and membrane remodeling in cancer . **23,** 49–53 (2012).
188. Bauerschlag, D. O. *et al.* Fatty acid synthase overexpression: target for therapy and reversal of chemoresistance in ovarian cancer. *J. Transl. Med.* **13,** 1–12 (2015).

189. Ricardo, S. *et al.* Breast cancer stem cell markers CD44, CD24 and ALDH1: expression distribution within intrinsic molecular subtype. *J. Clin. Pathol.* **64,** 937–946 (2011).
190. Griffiths, C. L. & Olin, J. L. Triple Negative Breast Cancer: A Brief Review of its Characteristics and Treatment Options. *J. Pharm. Pract.* **25,** 319–323 (2012).
191. Broxterman, H. J., Gotink, K. J. & Verheul, H. M. W. Understanding the causes of multidrug resistance in cancer: a comparison of doxorubicin and sunitinib. *Drug Resist. Updat.* **12,** 114–126 (2009).
192. Nielsen, D., Maare, C. & Skovsgaard, T. Cellular resistance to anthracyclines. *Gen. Pharmacol.* **27,** 251–255 (1996).
193. Tzaida, O. *et al.* Evaluation of the prognostic and predictive value of HER-1/EGFR in breast cancer patients participating in a randomized study with dose-dense sequential adjuvant chemotherapy. *Oncology* **72,** 388–396 (2008).
194. McCubrey, J. a. *et al.* Roles of the RAF/MEK/ERK and PI3K/PTEN/AKT pathways in malignant transformation and drug resistance. *Adv. Enzyme Regul.* **46,** 249–279 (2006).
195. Hennessy, B. T., Smith, D. L., Ram, P. T., Lu, Y. & Mills, G. B. Exploiting the PI3K/AKT pathway for cancer drug discovery. *Nat. Rev. Drug Discov.* **4,** 988–1004 (2005).
196. Colomer, R., Sarrats, A. & Puig, R. L. and T. Natural Polyphenols and their Synthetic Analogs as Emerging Anticancer Agents. *Current Drug Targets* **17,** 1 (2016).
197. Puig Miquel, T. *et al.* Green tea catechin inhibits fatty acid synthase without stimulating carnitine palmitoyltransferase-1 or inducing weight loss in experimental animals. *Anticancer Res.* **28,** 3671–3676 (2008).
198. Grunt, T. W. *et al.* Interaction between fatty acid synthase- and ErbB-systems in ovarian cancer cells. *Biochem. Biophys. Res. Commun.* **385,** 454–459 (2009).
199. Adachi, S. *et al.* (-)-Epigallocatechin gallate causes internalization of the epidermal growth factor receptor in human colon cancer cells. *Carcinogenesis* **29,** 1986–1993 (2008).
200. Adachi, S. *et al.* The inhibitory effect of (-)-epigallocatechin gallate on activation of the epidermal growth factor receptor is associated with altered lipid order in HT29 colon cancer cells. *Cancer Res.* **67,** 6493–6501 (2007).
201. Fujimura, Y., Yamada, K. & Tachibana, H. A lipid raft-associated 67 kDa laminin receptor mediates suppressive effect of epigallocatechin-3-O-gallate on Fc??RI expression. *Biochem. Biophys. Res. Commun.* **336,** 674–681 (2005).
202. Bollu, L. R., Katreddy, R. R. & Blessing, A. M. Intracellular activation of EGFR by fatty acid synthase dependent palmitoylation. **6,** (2015).
203. Bollu, L. R. *et al.* Involvement of de novo synthesized palmitate and mitochondrial EGFR in EGF induced mitochondrial fusion of cancer cells. *Cell Cycle* **13,** 2415–30 (2014).
204. Tachibana, H., Koga, K., Fujimura, Y. & Yamada, K. A receptor for green tea polyphenol EGCG. *Nat. Struct. Mol. Biol.* **11,** 380–381 (2004).
205. Van Amelsvoort, J. M. *et al.* Plasma concentrations of individual tea catechins after a single oral dose in humans. *Xenobiotica* **31,** 891–901 (2001).
206. Alò, P. L. *et al.* Fatty acid synthase (FAS) predictive strength in poorly differentiated early breast carcinomas. *Tumori* **85,** 35–40
207. Dawson, S. J., Provenzano, E. & Caldas, C. Triple negative breast cancers: clinical and prognostic implications. *Eur. J. Cancer* **45 Suppl 1,** 27–40 (2009).
208. Rakha, E. A. *et al.* Prognostic markers in triple-negative breast cancer. *Cancer* **109,** 25–32 (2007).
209. Gangi, A. *et al.* Breast-conserving therapy for triple-negative breast cancer. *JAMA Surg.* **149,** 252–8 (2014).
210. Lakhani, S., Ellis, I., Schnitt, S., Tan, P. & van de Vijver, M. *WHO Classification of Tumours of the Breast*. (World Health Organization. International Agency for Research on Cancer, 2012).
211. Gansler, T. S., Hardman, W., Hunt, D. A., Schaffel, S. & Hennigar, R. A. Increased expression of fatty acid synthase (OA-519) in ovarian neoplasms predicts shorter survival. *Hum. Pathol.* **28,** 686–92 (1997).
212. Visca, P. *et al.* Fatty Acid Synthase (FAS) is a Marker of Increased Risk of Recurrence in Lung Carcinoma. **4174,** 4169–4173 (2004).
213. Prud'Homme, G. J. *et al.* Breast cancer stem-like cells are inhibited by a non-toxic aryl hydrocarbon receptor agonist. *PLoS One* **5,** (2010).
214. Grimshaw, M. J. *et al.* Mammosphere culture of metastatic breast cancer cells enriches for tumorigenic breast cancer cells. *Breast Cancer Res.* **10,** R52 (2008).
215. Moody, S. E. *et al.* The transcriptional repressor Snail promotes mammary tumor recurrence. *Cancer Cell* **8,** 197–209 (2005).
216. Tran, H. D. *et al.* Transient SNAIL1 expression is necessary for metastatic competence in breast cancer. *Cancer Res.* **74,** 6330–6340 (2014).
217. Ye, X. *et al.* Distinct EMT programs control normal mammary stem cells and tumour-initiating cells. *Nature* **525,** 256–260 (2015).
218. Zhuang, X. *et al.* Doxorubicin-enriched, ALDH(br) mouse breast cancer stem cells are treatable to oncolytic herpes simplex virus type 1. *BMC Cancer* **12,** 549 (2012).
219. Kruger, J. A. *et al.* mice Characterization of stem cell – like cancer cells in immune-competent mice. **108,**

3906–3912 (2012).
220. Bandyopadhyay, A. *et al.* Doxorubicin in combination with a small TGFβ inhibitor: A potential novel therapy for metastatic breast cancer in mouse models. *PLoS One* **5,** (2010).
221. Pandey, P. R. *et al.* Resveratrol suppresses growth of cancer stem-like cells by inhibiting fatty acid synthase. *Breast Cancer Res Treat* **130,** 387–398 (2011).
222. Yasumoto, Y. *et al.* Inhibition of fatty acid synthase decreases expression of stemness markers in glioma stem cells. *PLoS One* **11,** 1–14 (2016).
223. Borgstein MD, P. J. *et al.* Sentinel Lymph Node Biopsy in Breast Cancer: Guidelines and Pitfalls of Lymphoscintigraphy and Gamma Probe Detection. *J. Am. Coll. Surg.* **186,** 275–283 (1998).
224. Wong, S. L. *et al.* Sentinel lymph node biopsy for breast cancer: Impact of the number of sentinel nodes removed on the false-negative rate. *J. Am. Coll. Surg.* **192,** 684–691 (2001).
225. Lee, H. E. *et al.* An increase in cancer stem cell population after primary systemic therapy is a poor prognostic factor in breast cancer. *Br. J. Cancer* **104,** 1730–8 (2011).
226. Liu, H., Liu, Y. & Zhang, J.-T. A new mechanism of drug resistance in breast cancer cells: fatty acid synthase overexpression-mediated palmitate overproduction. *Mol. Cancer Ther.* **7,** 263–70 (2008).

Annex

Ariadna Giró-Perafita, Sonia Palomeras, David Lum, Adriana Blancafort, Gemma Viñas, Glòria Oliveras, Ferran Pérez-Bueno, Ariadna Sarrats, Alana L Welm and Teresa Puig. “Preclinical Evaluation of Fatty Acid Synthase and EGFR Inhibition in Triple Negative Breast Cancer”. *Clinical cancer research* (2016) : p.: 1-11

- Received January 7, 2016.
- Revision received March 18, 2016.
- Accepted March 23, 2016.

DOI: http://dx.doi.org/10.1158/1078-0432.CCR-15-3133

http://clincancerres.aacrjournals.org/content/early/2016/04/22/1078-0432.CCR-15-3133

Abstract

Abstract Purpose: Triple Negative Breast Cancer (TNBC) lacks an approved targeted therapy. Despite initial good response to chemotherapy, 30% of the patients relapse within 5 years after treatment. EGFR overexpression is a common marker in TNBC, and its expression has been correlated with poor outcome. Inhibition of Fatty Acid Synthase (FASN) activity leads to apoptosis of human carcinoma cells overexpressing FASN. We tested the hypothesis that blocking FASN in combination with anti-EGFR signaling agents would be an effective antitumor strategy in sensitive and chemoresistant TNBC. Experimental Design: Several TNBC cell lines and 29 primary tumors were included to determine whether FASN is a potential target in TNBC. Doxorubicin-resistant TNBC cell lines (231DXR and HCCDXR) have been developed and characterized in our laboratory. Cellular and molecular interactions of anti-FASN compounds (EGCG and C75) with cetuximab were analyzed. In vivo tumor growth inhibition was evaluated after cetuximab, EGCG or the combination in TNBC orthoxenograft models. Results: TNBC cell lines showed overexpression of FASN enzyme and its inhibiton correlated to FASN levels. FASN staining was observed in all of the 29 TNBC tumor samples. In vitro, EGCG and C75 plus cetuximab showed strong synergism in sensitive and chemoresistant cells. In vivo, the combination of EGCG with cetuximab displayed strong antitumor activity against the sensitive and chemoresistant TNBC orthoxenografts, without signs of toxicity. Conclusions: Our results show that the simultaneous blockade of FASN and EGFR is effective in preclinical models of sensitive and chemoresistant TNBC.

Fatty Acid Synthase and EGFR Expression in Association with Clinical Outcomes in Triple-Negative Breast Cancer Patients

Authors

Giró-Perafita A[1,*] and Sarrats A[1,*], Pérez-Bueno F[1,2], Oliveras G[1,3], Buxó M[4], Brunet J[1,3], Viñas G[1,3**] and Puig T[1**]

Affiliations

[1] New Terapeutics Targets Lab (TargetsLab), Department of Medical Sciences, University of Girona, Spain; [2] Pathology Department, Dr. Josep Trueta Hospital and Catalan Institute of Health (ICS), Girona; [3] Medical Oncology Department, Catalan Institute of Oncology (ICO), Girona, Spain; [4]Girona Biomedical Research Institute (IDIBGI), Girona, Spain.

*** The Authors contributed equally to this work.**

****Corresponding Authors**: Teresa Puig, TargetsLab, Department of Medical Sciences, Emili Grahit 77, University of Girona, 17071 Girona. Phone: +34-972-419628; Fax: +34-972-419617. E-mail: teresa.puig@udg.edu

Gemma Viñas, Medical Oncology Department, Catalan Institute of Oncology (ICO), Hospital Josep Trueta, Avinguda de França, S/N, 17007 Girona. Phone: +34-972-225834 ext. 4034. E-mail: G.vinyes@iconcologia.net.

ABSTRACT

Background: The uncontrolled cell proliferation of neoplastic disease involves not only deregulated control of cell growth but also altered metabolic pathways. Lipogenic enzymes, such as fatty acid synthase (FASN), are commonly overexpressed in cancer. Patients with Triple-Negative Breast Cancer (TNBC) have poor prognosis, and they lack of an approved targeted therapy. We previously showed that all TNBC samples from a small cohort expressed high levels of FASN and its inhibition synergized with the EGFR inhibitor cetuximab *in vitro* and in animal models of TNBC. The purpose of the present study was to evaluate FASN expression in a large cohort of TNBC samples and study its association with clinico-pathological characteristics, intrinsic subtypes and its potential as a

prognosis marker.

Methods: FASN, EGFR, CK5/6 and Vimentin expression were retrospective evaluated in a tissue microarray of 100 primary TNBC by Immunohistochemistry. FASN expression was classified in High FASN and Low FASN expressing groups. EGFR, CK5/6 and Vimentin expression were used to classify TNBC intrinsic subtypes. Overall Survival (OS) and Disease Free Survival (DFS) were evaluated in Low and High FASN expressing groups, EGFR positive and negative tumor samples and TNBC intrinsic subtypes. Clinical and histopathological features were obtained for each patient.

Results: FASN was expressed 92% of the TNBC tumor samples tested. Although no significantly, High FASN expressing patients showed lower Overall Survival (OS) and Disease-Free Survival (DFS) rates than the Low FASN ones. Interestingly, High FASN expressing group was significantly associated with positive node status. FASN expression was significantly higher in Basal-like patients than in Mesenchymal-like ones, and it was negatively associated with Vimentin levels. EGFR expression was positive in 50% of the tumors, and those patients showed poorer DFS.

Conclusions: FASN is overexpressed in TNBC and its expression may be related with poorer outcomes. These results may account for the bases of future therapeutic strategies of TNBC using FASN inhibitors in combination with other agents, such as EGFR inhibitors.

KEYWORDS

Triple-Negative Breast Cancer (TNBC), Tissue Microarrays (TMA), Fatty Acid Synthase (FASN), EGFR, molecular subtypes, Vimentin, Cytokeratin 5/6, Overall-Survival (OS), Disease Free Survival (DFS).

Available online at www.sciencedirect.com

ScienceDirect

Procedia CIRP 49 (2016) 61 – 66

www.elsevier.com/locate/procedia

The Second CIRP Conference on Biomanufacturing

Optimization of Poli(ε-caprolactone) scaffolds suitable for 3D cancer cell culture

Giró-Perafita Ariadna[a], Rabionet Marc[a], Puig Teresa[a]* and Ciurana Joaquim[b]*

a Oncology Unit (TargetsLab), Department of Medical Sciences - Faculty of Medicine - University of Girona, Emili Grahit 77, 17077 Girona, Spain
b Department of Mechanical Engineering and Industrial Construction - University of Girona, Maria Aurèlia Capmany 61, 17071 Girona, Spain

* Corresponding authors. Tel.: +34-972-41-8265 ; fax: +34-972-41-9098. *E-mail address:* quim.ciurana@udg.edu
Tel.: +34-972-41-9628 *E-mail address:* teresa.puig@udg.edu

Abstract

Fused Deposition Model (FDM) as Additive manufacturing (AM) technologies may offer a viable and simpler alternative to manufacture scaffolds for different purposes such as tissue engineering and cells culture. Existing commercial FDM machines are currently being modified to improve their accuracy, capabilities and use. However, for biocompatible and/or bioimplantable materials such as Poli (ε -caprolactone) PCL there is still a lot of work to do to set up process parameters. Cells culture had been carried on 2D without being a proper and real midst. In fact cells do not grow only in two flat directions but in all directions making strong net. Since cells responses to proteins or drugs is important for knowing proliferation or enrichment more real culture in 3D is needed. This work focuses on the study and optimization of open-source 3D printer machine, called RepRap, employed to manufacture biocompatible scaffolds for 3D cells culture of Triple-Negative Breast Cancer (TNBC). It has been shown that scaffolds culture can enhance the Cancer Stem Cell (CSC) population, responsible in part for tumour recurrence after chemotherapy. Mammosphere Forming Index (MFI) was defined in all cell lines to evaluate this population in TNBC cell lines sensible and resistant to chemotherapy. Enriching TNBC cells with CSC after scaffold culture will help to study new therapeutic treatments directed to this population. Several process parameters are tested to manufacture scaffolds and cells culture had been carried out in order to validate the results. Results show that porosity plays an important role in scaffolds manufacture having low cells adhesion and growth. Lower porosity values should be tested to further evaluate MFI index after scaffold culture as cell growth and enrichment indication.

Peer-review under responsibility of the scientific committee of The Second CIRP Conference on Biomanufacturing

Keywords: PCL; Scaffold; Additive Manufacturing; Fused deposition model; Cancer Cells; 3D Cell-Culture; Stem Cells

1. Introduction

Cell culture is a technique widely used in cancer research laboratories, for instance to the study of cancer biology and the development of new therapeutic strategies. Nowadays, 2D cell culture is the most frequent technique used. Although interest for 3D cell culture is emerging because cell architecture and interactions simulates better the biology of a tissue compared to the flat-growing 2D systems [1].

The development of accurate constructs made of a matrix or scaffold and living cells to repair and regenerate damaged tissue is a current challenge in the tissue engineering field [2]. Taking advantage of this, scaffold fabrication for 3D cell-culture has emerged using technologies already developed for this purpose. One of these techniques is the additive manufacturing technology, which enables the fabrication of customized scaffolds directly from the patient. For this purpose, existing additive manufacturing machines are currently being modified to improve their accuracy and capabilities. The optimization of process parameters is a major challenge to obtain adequate scaffold morphology and biomechanical behavior, which are to improve cell adhesion and proliferation. Indeed, appropriate porosity, pore size, pore shape, and mechanical strength are required to achieve cell growth and matrix formation [3]. Open source extruders, like the RepRap machine, allow a thorough study of several process parameters involved in the fabrication of scaffolds such as deposition speed, layer thickness, filament distance, deposition pattern, extrusion and bed temperatures and speed movement. Therefore, a precise control over this manufacturing process is required.

Peer-review under responsibility of the scientific committee of The Second CIRP Conference on Biomanufacturing
doi:10.1016/j.procir.2015.07.031

Triple-Negative Breast Cancer (TNBC) is a type of breast cancer which runs an aggressive course and has a poor prognosis. It shows the highest recurrence rate compared to other breast cancer types [4]. TNBC lacks of validated directed therapy, and patients are treated mainly with chemotherapy (anthracyclines and taxans). Even though TNBC shows a good response to these therapies, recurrence at 5 years following diagnosis is about 30% of the cases [5,6].

Recent studies showed that chemoresistance can be achieved by a unique and rare cell niche with stemness features, the so-called Cancer Stem Cells (CSC) [7,8]. These cells, capable of tumor initiation, are not only responsible for tumor recurrence, but also metastasis [9]. Interestingly, scaffolds not only allow cells to interact in a 3D way improving the in-vitro 2D system, but also it has been described that 3D cultures can enhance the CSC population [10,11].

In this study it had been investigated the optimization of the open source and low-cost 3D extruder machine RepRap, employed to fabricate PCL scaffolds suitable for 3D cell culture. Design and manufacturing parameters were determined to ensure the best performance. In addition, this work focuses in 3D scaffolds ability to enrich the CSC population for developing new therapeutic strategies to target this population.

2. Materials and Methods

2.1. Material

A 3mm Poli(ε-caprolactone) (PCL) wire (Perstorp, Malmö, Sweden) was used to manufacture the scaffolds. PCL is biodegradable polyester proven to be biocompatible and free of toxic dye.

2.2. 3D printer machine and software

Printer machine RepRap BCN 3D+ was used to produce three-dimensional scaffolds. It is an open source and modular 3D printer designed by RepRap BCN. This printer uses the Fused Filament Fabrication (FFF) technology so called Fused Depostion Model (FDM). The filament unwound from a coil is supplied to the extruder. Then, at certain temperature and pressure, exerted by a gear, causes the extrusion of the material through the nozzle, which is finally deposited onto a heated computer-controlled Cartesian platform.

The scaffold's design was carry out with the computer-aided design (CAD) software SolidWorks. The designs were saved in STL file formats, which are transferred to a computer-aided manufacturing (CAM) software called Slic3r. This program was used for establishing the printing parameters. It generates G-code files able to command and control the machine in order to obtain the scaffolds printed.

Table 1 shows the process parameters utilized for the experimental set up. Design parameters, such as shape, layer thickness, diameter of filament and distance between filaments, were studied and analysed. Deposition angle between layers was fixed at 0-90º. Shape refers to the basic feature of the scaffold produced. Thickness is the total height of the scaffold and the distance between filaments is the shortest distance between two filaments located within the same layer.

Table 1. Scaffold parameters and levels tested in order to obtain the optimal printing

	Parameters	Levels
DESIGN PARAMETERS	Deposition angle (º)	0-90
	Shape	square, round
	Thickness (mm)	1.8, 3.6
	Diameter of filament (mm)	0.175, 0.30, 0.50
	Distance between filaments (mm)	0.5, 0.7, 1
MANUFACTURING PARAMETERS	Deposition speed (mm/s)	10, 20, 30, 50
	Layer height (mm)	0.15, 0.20, 0.25, 0.28, 0.30, 0.35
	Extrusion temperature (ºC)	65, 75, 80, 85, 90, 95, 105, 110, 115, 120, 130, 150, 155, 160, 180, 200
	Bed temperature (ºC)	25, 30, 33, 35, 37

Other parameters were set, like deposition speed, layer height and temperatures. The deposition speed was defined as the speed for printing movements of the extruder. Layer height is the distance between two connected layers along the Z axis. Finally, temperatures of the extruder and the glass platform were set up as well.

2.3. Cell Culture

MCF-7, MDA-MB-231 and HCC1806 breast carcinoma cells were obtained from the American Type Culture Collection (ATCC, Rockville, MD, USA). MDA-MB-231 and HCC1806 are cell lines established from patients with TNBC. MCF-7 are a HER2 positive cell line, (a type of breast cancer that overexpresses the Human Epidermal Growth Factor Receptor 2), used for scaffold validation. Doxorubicin (chemotherapeutic drug) was used to create resistant models from MDA-MB-231 (231**DXR**) and HCC1806 (HCC**DXR**) in our laboratory by treating cells at increasing doses of doxorubicin for 48 hours periods until 6 months.

MCF-7, and MDA-MB-231 and 231**DXR** cells were cultured in DMEM (Dulbecco's Modified Eagle's Medium) (Gibco, Walthman, MA, USA) supplemented with 10% fetal bovine serum, 1% L-glutamine, 1% sodium pyruvate, 50U/mL penicillin and 50µg/mL streptomycin (HyClone, Logan, UT, USA). HCC1806 and HCC**DXR** cells were cultured in RPMI (Roswell Park Memorial Institute) (Gibco, Walthman, MA, USA) and supplemented as above. All cells were maintained at 37ºC and 5% CO_2 atmosphere.

2.4. Mammosphere-forming assay

In order to evaluate CSC population, the mammosphere-forming technique was performed (Figure 1). Cells from 2D or PCL scaffolds were removed by trypsinitzation. Then cells were counted, and seeded into a 6-well cell culture microplate coated with pHEMA using DMEM/F12 medium supplemented with B27, EGF and FGF (20ng/mL), 1% L-glutamine, 1% sodium pyruvate and 25U/mL penicillin and

25µg/mL streptomycin . Finally, cells were incubated for 5 or 7 days and mammospheres bigger than 50µm were counted using an inverted opical microscope. Mammosphere Forming Index (MFI) was calculated using the formula described below:

$$MFI = \frac{Nº\ mammosphere}{Nº\ cells\ plated} \cdot 100$$

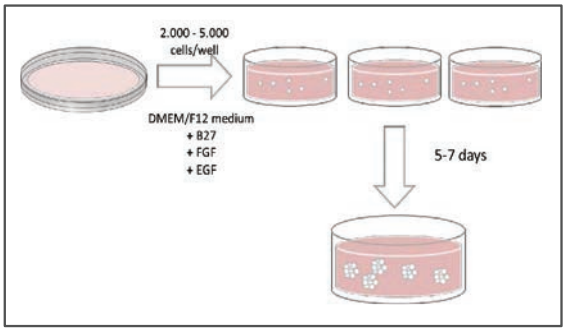

Figure 1. Mammosphere-forming assay protocol

For the mammosphere treatment experiments, doxorubicin was added in the seeding process. Mammosphere Forming Inhibition (MFIn) was calculated, as shown in the formula below:

$$MFIn = 100 - \frac{Nº\ mammospheres_{treatment}}{Nº\ mammospheres_{control}} \cdot 100$$

2.5. Growth inhibition assay

MDA-MB-231, HCC1806, 231**DXR** and HCC**DXR** were plated out at a density of $5x10^3$ cells/2mL/well in 6-well plates. Posterior overnight cell adherence, fresh medium along with the corresponding doxorubicin concentration was added to the cultures. Following treatment, media was replaced by drug-free medium (1mL/well) containing MTT (3,4,5-dimetylthiazol-2-yl-2,5-diphenyltetraolim bromide, Sigma) solution, and incubation was prolonged for 2 hours at 37ºC. Formazan crystals formed by metabolically viable cells were dissolved in DMSO (300µL/well) and absorbance was determined at 570nm in a multi-well plate reader (Model Anthos Labtec 2010 1.7). Using control OD values (*C*) and test OD values (*T*), % of Cell Proliferation Inhibition (CPI) was calculated from the equation below:

$$CPI = 100 - \frac{T}{C} \cdot 100$$

Data presented are from two separate wells per assay and the assay was performed at least three times.

2.6. Scaffold sterilization

Scaffolds were sterilized with 70% ethanol/water solution overnight, washed with PBS (Gibco, Walthman, MA, USA) and finally exposed to UV light for 90 minutes.

2.7. Cell culture in scaffolds

Scaffolds were placed into a 12-well cell culture microplate. First, 250µL of cell suspension (10.000-100.000 cells) were placed onto the centre of its surface to allow cells attach on the scaffold. After 1 hour incubation period, 1.5mL of fresh medium was added to cover the scaffold. Cells were incubated for 72 hours and then counted. (Figure 2).

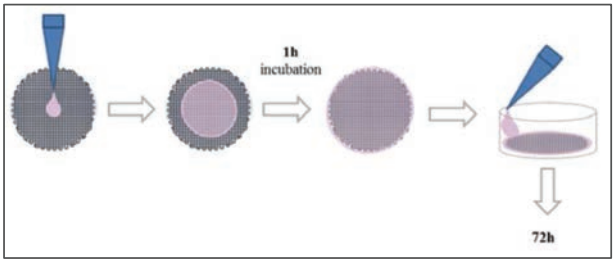

Figure 2. Cell seeding protocol on PCL scaffolds.

To quantify the cells attached, the scaffold was placed in a new well, washed with PBS and 1mL of trypsin was added. After incubation, 2.5mL of fresh medium were added and the cell suspension was collected and centrifuged at 1500rpm for 5 min. Finally, the supernatant was discarded and cells were counted using a Neubauer Chamber and an inverted optical microscope. The same procedure was done to obtain the cells attached at the well where the scaffold was placed.

2.8. Statistical analysis

All data are expressed as mean ± standard error (SE). Data were analyzed by Student *t* test. Statistical significant levels were $p < 0.05$ (denoted as *), $p < 0.01$ (denoted as **) and $p < 0.001$ (denoted as ***). *p-value* is shown in results when significance is reached ($p < 0.05$).

3. Results

3.1. Scaffolds design and manufacturing

Scaffolds were designed with a round shape, with the size of 19mm diameter to allow their use in regular cell culture plate-dishes of 12 wells. The final designs had 1.8mm of thickness, composed of 6 different layers of polymeric material, being 0.3mm of thickness each layer. The distance between filaments was 0.7mm and the deposition angle was established at 0-90º (Table 2).

Scaffolds manufacturing parameters were optimized by screening experiments to print the scaffolds efficiently and properly for cells culture (Table 3).

The deposition speed took a small value to optimize the material's deposition. The nozzle tip size was fixed at 0.35mm. The printed filaments had a diameter of 0.30mm. With visual screening, it was proved that the optimal extrusion temperature was 85ºC (Figure 3). Finally, scaffolds were fabricated with a bed temperature of 35ºC, to guarantee their adhesion to the printing platform.

Table 2. Scaffold desig parameters.

Parameters	
Diameter	19mm
Shape	Round
Thickness	1.8mm
Number of layers	6
Distance between filaments	0.7mm
Deposition angle	0-90º
Diameter of filament	0.30mm

Table 3. Scaffold manufacturing parameters

Parameters	
Deposition velocity	10mm/s
Layer height	0.30mm
Nozzle tip size	0.35mm
Extrusion temperature	85ºC
Bed temperature	35ºC

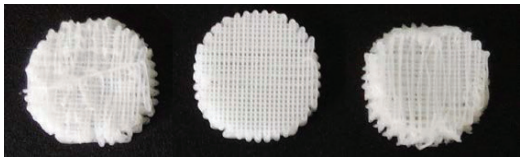

(a) (b) (c)

Figure 3. Scaffold manufacturing at different extrusion temperature (a) 80ºC, (b) 85ºC, (c) 90ºC.

3.2. Cancer Stem Cells population characterization

Cancer Stem Cells are a very rare population within the tumor. These cells have been demonstrated to have the ability to survive and propagate in a non-adherent way, forming spheres called mammospheres [7,12,13].

To determine CSC population, the mammosphere-forming assay was performed in cell lines MCF-7, MDA-MB-231, HCC1806, and resistant models 231DXR and HCCDXR (Figure 4). MFI was then calculated (Table 4).

CSC represents a small population in all cell lines, with values ranging from 0.67% to 2.47% of MFI. When comparing the ability to form mammosphere between parental and resistant cells to doxorubucin, no increase of MFI was observed in the two models.

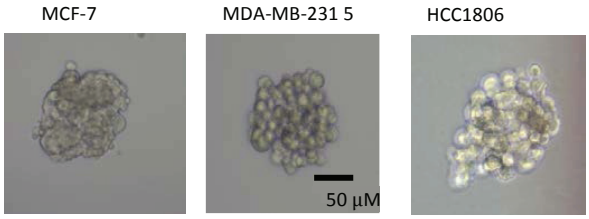

Figure 4. Mammospheres under optic microscope for MCF-7, MDA-MB-231 and HCC1806.

Table 4. Mammosphere Forming Index (MFI).

Cell Line	**Cells seeded (cells/well)**	**Days**	**MFI (%)**
MCF-7	2.000	7	2.47±0.26
MDA-MB-231	5.000	5	1.78±0.24
HCC1806	5.000	5	0.92±0.17
231**DXR**	5.000	5	1.75±0.27
HCC**DXR**	5.000	5	0.67±0.04

Data are shown as mean ±SEM.

As cell plasticity plays an important role in tumor biology and drug resistance, it was checked the ability to form mammospheres under doxorubicin pressure [14-16]. To do so, the experiments were repeated in presence of doxorubicin in both sensible and resistant cell lines and MFIn was calculated for each model. The same experiment was performed in adherent conditions using the MTT assay as described in Material and Methods section. Intrinsic resistance of CSC to doxorubicin was observed in all models (Figure 4). In adherent conditions, cell lines proliferation inhibition (% CPI) ranged from 84.2% to 89.5%. Otherwise, MFIn values showed significant lower inhibition in all cell lines, ranging from 20.6% to 60.7% (*p-values* < 0.001).

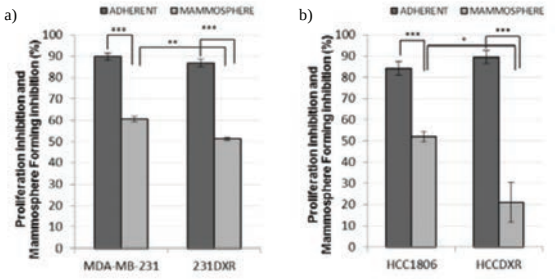

Figure 5. Proliferation inhibition and Mammposphere forming inhibition (MFIn) under doxorubicin treatment for 5 days. (a) MDA-MB-231 and 231**DXR** with doxorubicin (70nM). (b) HCC1806 and HCC**DXR** with doxorubicin (140nM). Experiments were performed at least three times in duplicate. *($p < 0.05$), **($p < 0.01$) and ***($p < 0.001$) indicate levels of statistically significance.

The cytotoxic effect of doxorubicin was then evaluated in CSC population comparing parental and resistant models (Figure 4). MDA-MB-231 and 231**DXR** showed an MFIn of 60.66% and 51.29% (*p value*: 0.005) respectively. HCC1806 MFIn was 51.97% and 20.61% for HCC**DXR** (*p value*: 0.036). CSC population from resistant models HCC**DXR** and 231**DXR** showed significance resistant to doxorubicin, maybe due to an enrichment of this population in this models [8].

3.3. Scaffolds and cell culture

The scaffold with deposition angles of 0-90º (Figure 2a) was printed and tested for cell culture (Figure 5).

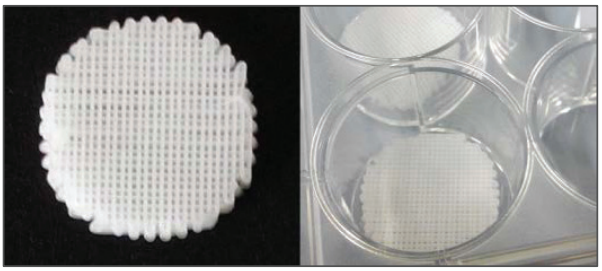

Figure 5. Scaffold fabricated with RepRap Machine a) 19mm diameter, 1.8mm thick, and deposition angles of 0-90º b) the scaffold plated in a 12 well-plate.

Before its use, scaffolds were sterilized as mentioned in Material and Methods section. Then MCF-7 cells were seeded at different densities (10.000, 50.000 and 100.000 cells/well) during 72 hours. Attached and non-attached cells were counted.

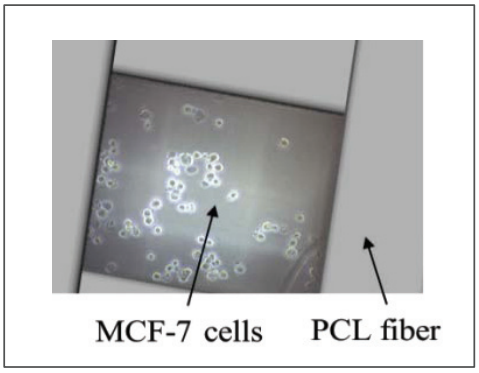

Figure 6. Optical microscope images of MCF-7 cells attached at the bottom of the well. Scaffold fiber has been drawn on the top.

In this first attempt, no cells were attached to the scaffold. As it was described and then observed under the microscope, this scaffold has large pores. The fibers of the different layers have the same disposition angle and, for that reason, cells can easily fall to the bottom of the well before they can get attached to PCL fibers (Figure 6).

As PCL fibers have already been tested in cell culture [10], new goal is set up focusing on designing and testing new scaffolds with different deposition angles between layers to achieve different and smaller pore sizes.

Two more designs have been performed, where the deposition angles were variable, taking the values of 0-60-120º and 0-45-90-135º (Figure 7). The variation of the angle deposition between layers results in a different pore size and shapes between the scaffolds (Table 5).

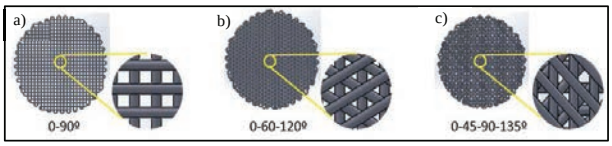

Figure 7. Scaffolds designs with different deposition angles: (a) 0-90º, (b) 0-60-120º, (c) 0-45-90-135º.

Table 5. Pore characteristics depending on the deposition angle

Deposition angles	Pores shape	Area
0-90º	Square	0.15mm^2
0-60-120º	Equilateral triangle	0.1256mm^2
0-45-90-135º	6 variable forms (triangles and irregular polygons)	1.98x10^{-4} to 0.13mm^2

4. Conclusions

In this study, the parameters of the open source RepRap 3D printer have been optimized to fabricate scaffolds of PCL suitable for cell culture.

Parameters, like deposition speed, diameter of the filament and extrusion and bed temperatures have been determined to obtain an optimal manufacture.

Design parameters, such are round shape, diameter and thickness were thought to allow its use in regular 12 well-cell culture plates. Three different designs have been performed, with different angles between layers, obtaining different pores sizes in all designs.

MCF-7 and TNBC cell lines had the ability to form mammospheres with low values of MFI, showing that CSC represents a very small population in these cell lines. CSC enriched population showed also intrinsic resistance to chemotherapy when compared to adherent culture. On the other hand, CSC population in resistant cell models developed in our lab (HCC**DXR** and 231**DXR**) showed increased ability to form mammospheres compared to the parental models under doxorubicin treatment.

MCF-7 cell line was used to test the scaffolds printed with deposition angles of 0-90º. Because of the same distribution of the fibers between layers and the large pores size of this design, cells drifted at the bottom of the well without attaching the scaffold. The other two designs, with smallest pore size will be tested in further studies.

Acknowledgements

This work was supported in part by Spanish Grants: Fundación Ramón Areces (TP), Instituto de Salud Carlos III (PI1400329, TP), Ministerio de Economía i Competitividad

(DPI2013-45201-P), and the support of Catalonian Government (2014SGR00868).
Marc Rabionet is the recipient of a Departmental Collaboration Grant from the Ministerio de Educación Cultura y Deportes of Spain for the academic years 2014-2015.

References

[1] D. Antoni, H. Burckel, E. Josset, G. Noel, Three-Dimensional Cell Culture: A Breakthrough in Vivo, Int. J. Mol. Sci. 16 (2015) 5517–5527. doi:10.3390/ijms16035517.

[2] B. Bártolo, P.J., Almeida, H.A., Rezende, R.A., Laoui, T., Bidanda, Advanced Processes to Fabricate Scaffolds for Tissue Engineering, in: P.B. Bopaya Bidanda (Ed.), Virtual Prototyp. Bio Manuf. Med. Appl., Springer, 2008: pp. 149–170.

[3] T.J. Hollister SJ., Maddox RD., Optimal Design and Fabrication of Scaffolds to Mimic Tissue Properties and Satisfy Biological Constraints, Biomaterials. (2002) 4095–4103.

[4] L.A. Carey, C.M. Perou, C.A. Livasy, L.G. Dressler, D. Cowan, K. Conway, et al., Race , Breast Cancer Subtypes , and Survival in the Carolina Breast Cancer Study, JAMA. 295 (2006) 2492–2502.

[5] O. Metzger-Filho, A. Tutt, E. De Azambuja, K.S. Saini, G. Viale, S. Loi, et al., Dissecting the heterogeneity of triple-negative breast cancer, J. Clin. Oncol. 30 (2012) 1879–1887. doi:10.1200/JCO.2011.38.2010.

[6] R. Dent, M. Trudeau, K.I. Pritchard, W.M. Hanna, H.K. Kahn, C. a Sawka, et al., Triple-negative breast cancer: clinical features and patterns of recurrence., Clin. Cancer Res. 13 (2007) 4429–34. doi:10.1158/1078-0432.CCR-06-3045.

[7] G. Dontu, W.M. Abdallah, J.M. Foley, K.W. Jackson, M.F. Clarke, M.J. Kawamura, et al., In vitro propagation and transcriptional profiling of human mammary stem / progenitor cells, Genes Dev. 17 (2003) 1253–1270. doi:10.1101/gad.1061803.potential.

[8] C.J. Creighton, X. Li, M. Landis, J.M. Dixon, V.M. Neumeister, A. Sjolund, et al., Residual breast cancers after conventional therapy display mesenchymal as well as tumor-initiating features., Proc. Natl. Acad. Sci. U. S. A. 106 (2009) 13820–13825.

[9] B.K. Abraham, P. Fritz, M. Mcclellan, P. Hauptvogel, M. Athelogou, H. Brauch, Prevalence of CD44 + / CD24 − / low Cells in Breast Cancer May Not Be Associated with Clinical Outcome but May Favor Distant Metastasis, Clin. Cancer Res. (2005) 1154–1159.

[10] S. Feng, X. Duan, P.-K. Lo, S. Liu, X. Liu, H. Chen, et al., Expansion of breast cancer stem cells with fibrous scaffolds., Integr. Biol. (Camb). 5 (2013) 768–77. doi:10.1039/c3ib20255k.

[11] S. Saha, P.-K. Lo, X. Duan, H. Chen, Q. Wang, Breast tumour initiating cell fate is regulated by microenvironmental cues from an extracellular matrix, Integr. Biol. 4 (2012) 897. doi:10.1039/c2ib20034a.

[12] F.L. Shaw, H. Harrison, K. Spence, M.P. Ablett, B.M. Simões, G. Farnie, et al., A detailed mammosphere assay protocol for the quantification of breast stem cell activity., J. Mammary Gland Biol. Neoplasia. 17 (2012) 111–7. doi:10.1007/s10911-012-9255-3.

[13] T. Pereira, G. Ivanova, A.R. Caseiro, P.P. Barbosa, P.J. Bartolo, J.D. Santos, A.L. Luis, A.C. Mauricio. MSCs conditioned media and umbilical cord blood plasma metabolomics and composition. PLOS ONE. 9 (2014) (11): e113769

[14] N.D. Marjanovic, R. a. Weinberg, C.L. Chaffer, Cell plasticity and heterogeneity in cancer, Clin. Chem. 59 (2013) 168–179. doi:10.1373/clinchem.2012.184655

[15] T. Pereira, P.A.S Armanda-da-Silva, I. Amorim, A. Rema, A.R. Caseiro, A. Gartner, M. Rodrigues, M. Lopes, P.J. Bartolo, J.D. Santos, A.L. Luís, A.C. Mauricio. Effects of human mesenchymal stem cells (HMSCs) isolated from the Whorton's jelly of the umbilical cord and condinioned media (CM) on skeletal muscle regeneration using myectomy model. Stem Cells International, (2014) Article ID 376918

[16] T. Pereira, A. Gartner, I. Amorim, A. Almeida, A.R. Caseiro, P.A. Armanda-da-Silva, S. Amado, F. Fregnan, A.S. Varejão, J.D. Santos, P.J. Bartolo, S. Geuna, A.L. Luís, A.C Mauricio. Promoting nerve regeneration in a neurotmesis rat model using poly(DL-lactide-e-caprolactone) membranes and mesenchimal stem cells from the Wharton's jelly: in vitro and in vivo analysis. BioMed Research International. (2014) Article ID 302659, 2014

.